38e jaargang 2016 nummer 4 issn 1381 - 4842

TIJDSCHRIFT VOOR NUCLEAIRE GENEESKUNDE

Special issue
Advances in Nuclear Therapy

Rapiscan® regadenoson

Now this won't take a minute...

Rapiscan is the only standard dose, infusion pump-free, selective coronary vasodilator for use as a pharmacological stress agent for radionuclide myocardial perfusion imaging.

- **Administer Rapiscan as a full 10 sec IV injection**
- **Flush immediately with 5 ml saline**
- **Deliver radiotracer 10-20 seconds after saline flush**
- **EU/1/10/643/001**

Nano-scan®

Human Serum Albumin nano sized colloid 500 µg

Kit for radiopharmaceutical Preparation

- Up to 5.5 GBq (150 mCi) of 99mTc per vial
- Particle size ≤ 80 nm (min. 95%)
- 8 hours stability post reconstitution
- 20 minutes incubation time
- 6 vials per kit
- RVG 112760

IDB Holland bv
From Atom to Image
An Advanced Accelerator Applications company

Weverstraat 17
5111 PV Baarle-Nassau
The Netherlands

Tel.: +31(0)13 507 95 58
Fax: +31(0)13 507 99 12
E-mail: sales@idb-holland.com

www.idb-holland.com

Beste lezers,

Nucleaire behandelingen zijn een belangrijk onderdeel van ons vak. Elk jaar wordt in Nederland een toenemend aantal patiënten op afdelingen Nucleaire geneeskunde behandeld. Was dit vroeger vaak beperkt tot behandelingen van benigne en maligne schildklieraandoeningen, inmiddels is er een scala aan therapeutische mogelijkheden. Diagnostiek en behandeling zijn daarbij vaak nauw met elkaar verbonden. Dat is bij uitstek een kenmerk van de Nucleaire Geneeskunde.

Door de voortschrijdende integratie met Radiologie ontstaan nieuwe mogelijkheden, ook wat betreft therapeutische mogelijkheden. Niet alleen is de radiologische diagnostiek vaak complementair met de nucleaire diagnostiek, de radiologische diagnostiek is door de integratie ook gemakkelijker beschikbaar voor onze eigen patiënten, en vice versa. Aanvullende echografie bij een schildklierpatiënt is tegenwoordig snel gemaakt, maar echografie kan bijvoorbeeld ook gebruikt worden voor het vaststellen van ascites na behandeling. Daarnaast zijn ook de kennis en vaardigheden van onze radiologisch geschoolde collega's vaak complementair. De opkomst van radioembolisatie als behandeling tegen leverkanker heeft bijvoorbeeld gezorgd voor een intensivering van de samenwerking tussen interventieradiologen en nucleair geneeskundigen. De voortgaande integratie van de afdelingen zal dit verder faciliteren. Samenwerking tussen radiologen en nucleair geneeskundigen enerzijds en nucleair geneeskundigen en andere specialismen anderzijds creëert mogelijkheden voor een belangrijke verbreding van ons specialisme. Alleen door voldoende kennis op te bouwen van samenwerkende specialismen kunnen we excelleren in ons eigen vak. De combinatie van verbreding enerzijds en verdieping anderzijds is een noodzakelijke voedingsbodem voor de ontwikkeling van innovatieve nucleaire behandelingen. Bovendien creëert deze samenwerking draagvlak voor Nucleaire Geneeskunde als klinisch specialisme.
Bij voorkeur treedt de nucleair geneeskundige bij verwijzing op als hoofdbehandelaar. Volgens de meest gebruikte definitie stelt de hoofdbehandelaar de indicatie voor de behandeling, informeert de patiënt over de behandeling, voert de behandeling uit, en verzorgt tevens de noodzakelijke nazorg en follow-up. Daarmee is de hoofdbehandelaar het aanspreekpunt voor de patiënt.
Voor wat betreft nucleaire behandelingen kunnen deze taken alleen uitgevoerd worden door een nucleair geneeskundige.
De nucleair geneeskundige moet mijns inziens dan ook die verantwoordelijkheid nemen en na verwijzing de taak van hoofdbehandelaar (tijdelijk) op zich nemen. Dat betekent ook dat patiënten voor, tijdens en na de behandeling (poli)klinisch op de afdeling Nucleaire Geneeskunde gezien moeten worden. Alleen dan kunnen de nucleaire behandelingen zich verder ontwikkelen en tot volle wasdom komen, inclusief gezonde financieringsstructuur.

De reeds genoemde integratie met de Radiologie heeft de technische ontwikkeling van de nucleaire behandelingen in een stroomversnelling gebracht. Van oudsher waren nucleaire behandelingen systemische behandelingen, oraal of intraveneus toegediend. Meer recentelijk heeft de ontwikkeling van beeldgestuurde behandelingen de weg geplaveid voor lokale nucleaire behandeling. Enerzijds door toediening van nucleaire behandelingen via een katheter in de vasculatuur van een orgaan, anderzijds via rechtstreekse injectie van radioactieve bronnen op de plek van de pathologie, onder begeleiding van beeldvorming (zoals echografie of CT).

Systemische nucleaire behandelingen hebben de laatste jaren een enorme vlucht genomen. Radium-223 (^{223}Ra) chloride wordt sinds enkele jaren dagelijks gebruikt tegen symptomatisch ossaal uitgezaaide prostaatkanker, nadat in een gerandomiseerde placebo gecontroleerde fase 3 studie aangetoond werd dat deze nucleaire behandeling tot overlevingswinst leidt. Dit jaar werd tevens bekend gemaakt dat de nucleaire behandeling lutetium-177 (^{177}Lu) dotataat leidt tot overlevingswinst bij patiënten met neuroendocriene tumoren, eveneens in een gerandomiseerde placebo gecontroleerde fase 3 studie. De verwachting is dat dit geneesmiddel net als ^{223}Ra snel voor vergoeding in aanmerking zal komen. Daarnaast zijn er veelbelovende ontwikkelingen op het gebied van andere radioactief gelabelde peptiden, zoals bijvoorbeeld ^{177}Lu-PSMA tegen prostaatkanker. Het is interessant om te constateren dat al deze behandelingen gefractioneerd gegeven worden. Wellicht hebben zij juist daardoor een goede effectiviteit en acceptabele toxiciteit, analoog aan uitwendige radiotherapie en systemische chemotherapie. Dit in tegenstelling tot sommige andere nucleaire behandelingen, zoals samarium-153 (^{153}Sm) EDTMP voor de bestrijding van botpijn en jodium-131 (^{131}I) jodide tegen schildklierkanker, die meestal als eenmalige monotherapie gegeven worden. Om die reden zijn er verschillende studies gaande naar gefractioneerde / herhaalde nucleaire behandelingen, al dan niet in combinatie met andere systemische behandelingen.

Sinds kort staan ook lokale nucleaire behandelingen volop in de belangstelling. Zo hoort vanaf dit jaar de lokale behandeling van colorectale levermetastasen middels yttrium-90 (^{90}Y) radioembolisatie tot de vergoede zorg. Onder voorwaarde dat er een goede indicatie gesteld wordt (dat wil zeggen refractaire inoperabele ziekte, lever-dominant), patiënten geregistreerd worden ter evaluatie van effectiviteit en toxiciteit, en het aantal behandelcentra beperkt blijft tot expertise centra, heeft het zorginstituut een positief oordeel gegeven. De lokale behandeling van HCC middels ^{90}Y-radioembolisatie werd al enkele jaren vergoed. De gebruikte ^{90}Y geladen microsferen zijn geregistreerd als medisch hulpmiddel en niet als geneesmiddel. Dat heeft als voordeel dat deze nucleaire behandeling door de beperktere wet- en regelgeving relatief snel beschikbaar kwam voor patiënten wereldwijd. Verschillende fase 3 studies bij patiënten met colorectale levermetastasen en HCC zijn momenteel gaande om uiteindelijk de positie van deze nucleaire behandeling in de behandelstrategie goed te kunnen definiëren. Daarnaast is er onderzoek gaande naar nieuwe medische hulpmiddelen en radiofarmaca, intra-arteriële toediening van bestaande radiofarmaca (bijvoorbeeld ^{177}Lu-dotataat), en nieuwe indicaties, zoals bijvoorbeeld niertumoren.

Tot slot krijgt ook de directe injectie van radioactieve bronnen in het pathologische focus de laatste jaren meer aandacht. Op beperkte schaal wordt al vele jaren radiosynoviorthesis toegepast tegen artritis, en werd tot voor kort peritonitis carcinomatosa bestreden met fosfor-32 (^{32}P) colloïd. Inmiddels is er ook aandacht voor directe intratumorale behandeling met radioactiviteit. Onder echo, CT, of MRI geleiding kan steeds nauwkeuriger de positie van de naald bepaald worden en daarmee het behandelplan geoptimaliseerd worden. Naar verwachting zullen deze technieken de komende jaren verder ontwikkeld worden.

Dosimetrie is voor al deze nucleaire behandelingen van groot belang. Omdat het aantal nucleaire behandelingen toeneemt, in eerdere fasen van ziekten, in combinatie met andere behandelingen, en gefractioneerd, neemt de druk op verbetering toe. Dosimetrie op basis van kwantitatieve beeldvorming moet leiden tot een goede selectie van patiënten, een individueel behandelplan naar analogie van de uitwendige radiotherapie, en een accurate analyse van de therapie tijdens of na de nucleaire behandeling. Vanwege het veelal ontbreken van farmacokinetiek bij lokale nucleaire behandelingen zijn deze in het voordeel ten opzichte van systemische behandelingen.

Nucleaire behandelingen zijn booming. Nucleaire geneeskunde heeft een trackrecord op het gebied van snelle translatie van innovatieve diagnostische en therapeutische modaliteiten. Behalve snelle translatie naar de patiënt en goede effectiviteit worden de nucleaire behandelingen gekenmerkt door beperkte bijwerkingen met behoud van kwaliteit van leven. Daarnaast is er een nauwe relatie tussen nucleaire behandelingen en begeleidende diagnostiek voor selectie van patiënten, het maken van een individueel behandelplan, begeleiding van de behandeling zelf, en adequate follow-up. Nucleair geneeskundigen moeten samenwerken met radiologen en andere specialismen om de innovatie van nucleaire behandelingen verder te stimuleren.

Prof. dr. Marnix G.E.H. Lam
Gast-hoofdredacteur,
Hoogleraar Nucleaire Geneeskunde
UMC Utrecht

Voorplaat: Yttrium-90 glas radioembolisatie (met dank aan afdeling Radiologie en Nucleaire Geneeskunde, UMC Utrecht)

Radioembolisatie met yttrium-90 bij colorectale levermetastasen: de huidige status

B.J. de Wit-van der Veen, PhD[1]; D.M.V. Huizing, MSc[1]; M.L. Donswijk, MD, MSc[1]; M. Meier, MD, MSc[2]; M.P.M. Stokkel,MD, PhD[1]

Afdelingen [1]Nucleaire Geneeskunde en [2]Radiologie, Antoni van Leeuwenhoek – Nederlands Kanker Instituut, Amsterdam

Abstract

De Wit-van der Veen BJ, Huizing DMV, Donswijk ML, Meier M, Stokkel MPM. Radioembolisation with yttrium-90 in colorectal liver metastases – current status in the Netherlands. Yttrium-90 (^{90}Y) radioembolisation has recently been approved in the Netherlands as treatment for chemorefractory metastatic liver-dominant colorectal cancer. The safety and clinical effects of this therapy, which is based on local transarterial administration of ^{90}Y-loaded microspheres, have been evaluated in a number of recent studies. Even in heavily pre-treated patients, radioembolisation is well tolerated and results in an overall survival benefit in comparison to best supportive care. The current article provides an update of the literature that has led to this Dutch approval. Additionally, the clinical procedures will be briefly discussed, with a special focus on activity dosage and post-treatment dosimetry. In the Netherlands, nine specialized centres perform radioembolisation as salvage therapy in metastatic colorectal cancer.
Tijdschr Nucl Geneesk 2016; 38(4):1613-1621

Introductie

Sinds enkele jaren behoort radioembolisatie, ook wel selectieve interne radiotherapie (SIRT) genoemd, tot een van de behandelopties bij niet-reseceerbare levermaligniteiten. Bij deze behandeling wordt gebruik gemaakt van de dubbele vasculatuur van de lever. De tumoren worden door neovascularisatie voornamelijk van bloed voorzien door de arteria hepatica, terwijl het gezonde parenchym voornamelijk bloed ontvangt van de vena porta. Via de arteria hepatica worden radioactieve microsferen ingespoten die vastlopen in het vaatbed in en rond de tumoren, en zo de tumor intern bestralen. Patiënten die slecht reageren op systemische therapie of moeten stoppen vanwege bijwerkingen komen voor radioembolisatie in aanmerking.
In Nederland wordt deze behandeling bij colorectale metastasen in beperkte mate ingezet, en vaak alleen in studieverband. In 2011 concludeerde Zorginstituut Nederland (ZINL, voorheen College voor Zorgverzekeringen, CVZ) nog dat de toepassing radioembolisatie alleen voor hepatocellulair carcinoom (HCC) vergoed zou worden. Het bewijs voor toepassing van radioembolisatie voor secundaire levermaligniteiten als eerste/tweedelijns of als salvage therapie was destijds onvoldoende. De laatste drie jaar zijn echter enkele grootschalige studies uitgevoerd naar radioembolisatie als eerste/tweedelijns behandeling, al dan niet in combinatie met systemische therapieën. Deze stijging is duidelijk te zien in figuur 1, waar het aantal gepubliceerde artikelen over de jaren op een rij gezet zijn. Gezien deze ontwikkelingen heeft recent een herbeoordeling plaatsgevonden door ZINL waardoor radioembolisatie met yttrium-90 (^{90}Y) nu als salvage therapie bij niet-reseceerbare colorectale levermetastasen wordt vergoed. Op dit moment zijn er een beperkt aantal specialistische centra in Nederland die de therapie aanbieden voor deze indicatie. Binnen dit overzichtsartikel zal dieper ingegaan worden op de ontwikkelingen rond radioembolisatie bij niet-reseceerbare colorectale levermetastasen.

Radioembolisatie

De procedure rond radioembolisatie van levermaligniteiten bestaat grofweg uit vier stappen: 1) selectie van de patiënten, 2) voorbereiding op de behandeling, 3) dosisbepaling,

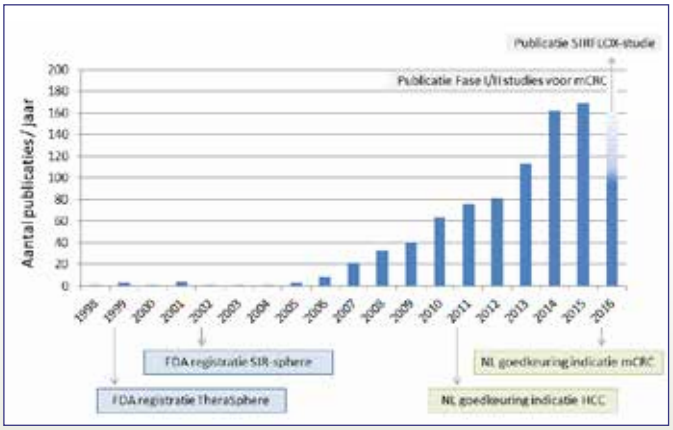

Figuur 1. Sinds de registratie van ^{90}Y-geladen microsferen als medisch hulpmiddel in 1999 zijn er al meer dan 900 studies gepubliceerd. De laatste vijf jaren worden er in toenemende mate studies gepubliceerd naar de veiligheid en effectiviteit van radioembolisatie in de salvage setting bij colorectale levermetastasen.

en 4) de daadwerkelijke radioembolisatie. Deze stappen zijn reeds uitgebreid beschreven door Lam et al. in een eerdere editie, daarom volgt hieronder alleen een korte beschrijving van deze stappen (1).

1. Selectie patiënten

Binnen een multidisciplinair overleg (waarbij onder andere aanwezig zijn: oncoloog, chirurg, interventieradioloog, nucleair geneeskundige) worden patiënten geselecteerd. De belangrijkste selectie criteria zijn leverdominante ziekte, ≤70% aangedaan levervolume, goede algehele conditie (WHO 1-2) en acceptabele lever- en nierfunctie (ALAT, ASAT en AF ≤5x ULN, bilirubine en creatinine ≤1,5x ULN). Als voorbereiding op de angiografie ondergaat de patiënt doorgaans een diagnostische CT om de levermaligniteit en de arteriële levervascularisatie in kaart te brengen, en een fluor-18 (^{18}F) FDG PET/CT om de uitgebreidheid van extrahepatische ziekte te beoordelen. Bij voorkeur wordt de beeldvorming kort (1-2 weken) voorafgaand aan de angiografie verricht. Op basis van deze beeldvorming wordt een behandelplan voorgesteld: gehele leverbehandeling met centrale katheterpositie in arteria hepatica propria, meerdere toedieningen selectief in de arteria hepatica dextra en sinistra, of eventueel een behandeling van de leverhelften in twee tempi. Bij zeer lokale ziekte kan gekozen worden voor een super-selectieve benadering, waarbij de katheter in het aanvoerende vat van een segment gelegd wordt, om vervolgens een zeer hoge dosis in een enkel segment te geven. Deze benadering wordt bijna alleen bij HCC toegepast.

2. Voorbereiding behandeling

Voordat de behandeling wordt uitgevoerd ondergaat de patiënt een angiografische procedure om de arteriële viscerale vascularisatie nauwkeurig in kaart te brengen. Hierbij wordt vaak de arteria gastrica dextra dan wel gastroduodenalis of andere relevante extrahepatische collateralen gecoild zodat tijdens de daadwerkelijke ^{90}Y-toediening deposities van activiteit in de maag, duodenum en pancreas voorkomen worden. Daarna wordt de katheter onder doorlichting op de voorgestelde behandelposities gelegd om een testdosis van 75-150 MBq ^{99m}Tc-macro-albumine aggregaat (^{99m}Tc-MAA) toe te dienen. De MAA eiwitten zijn van vergelijkbare grootte als de microsferen die worden gebruikt bij de behandeling, dus er wordt aangenomen dat deze deeltjes op dezelfde manier vastlopen in het arteriële vaatbed rond de tumor. Vervolgens gaat de patiënt direct door naar de afdeling Nucleaire Geneeskunde voor een planaire total body en SPECT-opnamen van het abdomen (figuur 2). Er wordt gecontroleerd of het percentage toegediende dosis dat naar de longen gaat (zogenaamde longshunt) niet te hoog is. Een shunt meer dan 20% is een contra-indicatie voor therapie, bij een shunt van 10-20% kan de ^{90}Y-dosis aangepast worden om de stralenbelasting op de longen te verkleinen. Een alternatieve benadering is om de longdosis te berekenen en een maximale dosis van 30 Gy op het longweefsel te tolereren. De aanwezigheid van duidelijke gastro-intestinale deposities is ook een contra-indicatie voor therapie indien deze niet gecoild kan worden. Aan het einde van de dag mag de patiënt naar huis.

Figuur 2. Longshuntbepaling bij een patiënt met HCC die in aanmerking komt voor radioembolisatie. Op de planaire beelden links is een duidelijke longshunt te zien van 26%, wat een contra-indicatie is voor radioembolisatie. Een jaar later wordt wederom een work-up voor radioembolisatie gestart, waarbij de patiënt een longshunt had van 4%. Tussen deze twee procedures in is transarteriële chemo-embolisatie (TACE) gegeven met doxorubicine geladen sferen als behandeling voor HCC waardoor de shunt dichtgezet is.

3. Dosisbepaling

De methodologie om de therapeutische ^{90}Y-dosis te bepalen is verschillend per leverancier van de ^{90}Y-microsferen. Tabel 1 geeft een overzicht van de twee geregistreerde producten (^{90}Y-microsferen) in Nederland. Opvallend is het grote verschil in specifieke activiteit en de geadviseerde benadering voor het berekenen van de therapeutische dosis. Bij de SIR-spheres (Sirtex, Australië) zal de geadviseerde dosis altijd uitkomen onder de 3 GBq, terwijl de geadviseerde dosis voor Theraspheres (BTG International Ltd, United Kingdom) op kan lopen tot boven 6 GBq. Deze mathematische methoden worden voornamelijk uitgevoerd bij therapie van de gehele lever of een enkele leverkwab. In specifieke gevallen kan de meer accurate partitie- of image-based dosimetrie gebruikt worden, waarbij de accumulatie op de SPECT-beelden in het aangedane en normale parenchym meegenomen worden in de dosisberekening. Aanname voor deze vorm van dosimetrie is dat de ^{90}Y-verdeling accuraat geschat wordt door de ^{99m}Tc-MAA afbeeldingen. In de sectie over dosisbepaling wordt hier dieper op ingegaan (voor meer informatie zie ook de richtlijnen van EANM en AAPM (2,3)). Veelal worden de berekeningen uitgevoerd in samenspraak met een klinisch fysicus of technisch geneeskundige.

Tabel 1. Overzicht van de ^{90}Y-microsferen.*

	SIR-Spheres®	TheraSpheres®
leverancier	Sirtex Medical, Australia	BTG International Ltd, United Kingdom
materiaal	acrylpolymeer (hars) waar ^{90}Y aan gebonden wordt	yttrium is ingebouwd in een glasmatrix (wordt daarna geactiveerd in de reactor)
diameter	20-60 µ	20-40 µ
dichtheid	1,6 g/cm3	3,29 g/cm3
activiteit per bolletje	40-70 Bq	1250-2700 Bq
1 Gbq bestaat uit	± 20 miljoen microsferen	± 0,5 miljoen microsferen
geadviseerde dosisberekening (in GBq)	BSA-methode: $+x\frac{tumor\ volume}{totaal\ lever\ volume}$	non-compartimenten MIRD: $\frac{gewenste\ dosis\ (Gy)\times levermassa}{50}$
leverbare dosering	3 GBq	3-20 GBq
hanteren	specifieke dosering(en) worden opgetrokken in het lokale lab	aanpassingen in de bestelde dosering zijn niet mogelijk
houdbaarheid	tot 24 uur na kalibratietijd	tot 12 dagen na kalibratietijd
^{90}Y halfwaardetijd	2,67 dagen	
^{90}Y energie van β-	0,935 MeV per desintegratie (max. 2.27 MeV)	
dracht in weefsel	2,5 mm (max. 11 mm)	

BSA = body surface area (m^2)

* Gebaseerd op de productinformatie van SIR-Spheres en TheraSpheres

4. Radioembolisatie

Een tot twee weken na de planningsangiografie komt de patiënt terug voor de therapeutische procedure. Afhankelijk van het behandelplan (segment, enkele leverkwab of gehele lever) wordt de katheter onder doorlichting op dezelfde positie(s) gelegd als tijdens de ^{99m}Tc-MAA toediening. Na toediening van de ^{90}Y-microsferen gaat de patiënt terug naar de afdeling. In de loop van de dag wordt wederom de verdeling van de microsferen gecontroleerd met een remstraling SPECT/CT of een ^{90}Y-PET/CT. Uit eerdere studies blijkt dat ^{90}Y-PET/CT superieur is voor de beoordeling van de dosisverdeling. Doorgaans wordt de patiënt een nacht opgenomen op klinische gronden om mogelijke bijwerkingen te monitoren.

Direct na de toediening van ^{90}Y treedt in ongeveer een derde van de patiënten lokale abdominale pijn op. Daarnaast voelen patiënten zich frequent misselijk, als reactie van de maag op de ioniserende straling, of ontwikkelen soms koorts. Deze bijwerkingen kunnen enkele dagen aanhouden, maar zijn doorgaans zeer goed te beheersen met pijnmedicatie en anti-emetica. Ook ondervindt een groot deel van alle patiënten moeheid tot drie weken na de behandeling. Ernstige bijwerkingen zoals gastro-intestinale ulceraties, portale hypertensie, radioembolisatie-geïnduceerde leverziekte, ascites, cholecystitis en leverfalen zijn zeldzaam (4,5).

Effectiviteit in de salvage setting

Van de patiënten met colorectale levermetastasen komt ongeveer een derde in aanmerking voor partiële leverresectie met curatieve opzet. De overwegingen en het beleid rondom het uitvoeren van een dergelijke resectie verschillen sterk per centrum. Als chirurgie geen optie is door comorbiditeiten of een ongunstige locatie van de laesies, kunnen lokale therapieën zoals radiofrequente ablatie of stereotactische radiotherapie ingezet worden naast systemische therapie. Chemotherapeutica die in de Nederlandse richtlijn colorectaal carcinoom (CRC) geadviseerd worden zijn fluoropyrimidines (5FU, capecitabine), oxaliplatin, en/of irinotecan; geadviseerde targeted therapieën zijn anti-VEGF (bevacizumab en aflibercept), anti-EGFR (cetuximab en panitumumab) en tyrosine kinase remmers (regorafenib). Combinaties van chemotherapie plus targeted therapie vormen de eerste/tweedelijns behandeling voor irresectabele levermetastasen. Deze systematische therapieën worden doorgaans gecontinueerd tot aan progressie of het optreden van onaanvaardbare toxiciteit. Tweedelijns schema's met FOLFOX + bevacizumab hebben een mediane overleving van ongeveer 12,9 maanden, versus 10,8 maanden met alleen FOLFOX (6); een schema met FOLFIRI + aflibercept heeft een overleving van 13,5 maanden, versus 12,1 maanden met FOLFIRI + placebo (7). Bij het falen van deze tweedelijns therapieën

hangt de vervolgbehandeling af van de voorgaande therapie en de uitgebreidheid van de ziekte.
Binnen de salvage setting wordt radioembolisatie sinds begin dit jaar ook aangeboden als standaard zorg in enkele specialistische centra in Nederland. Voorheen werd radioembolisatie alleen uitgevoerd in het kader van studies, of werd de vergoeding door het centrum zelf verzorgd. De effectiviteit en veiligheid van deze behandeling is reeds in verschillende studies geëvalueerd (tabel 2). Ondanks dat al deze studies verschillen vertonen in opzet en follow-up van de patiënten, is de mediane overleving na radioembolisatie in de salvage setting ongeveer 10,1 maanden (gecorrigeerd voor aantal geïncludeerde patiënten). Recentelijk zijn er twee grote retrospectieve cohort studies verschenen van Kennedy et al. en Hickey et al. die de effectiviteit van respectievelijk de glazen en de hars microsferen hebben beschreven (5,8). Binnen de studie van Kennedy et al. was de mediane overleving 9,6 maanden (95% CI 9,0-11,1), echter deze studie includeerde een zeer heterogene populatie waarbij radioembolisatie ook als tweedelijns therapie gegeven werd. Hickey et al. vonden bij de behandeling met glazen microsferen een mediane overleving van 10,6 maanden (95% CI 8,8-12,4). Ondanks het grote verschil in de gemiddelde toegediende dosis voor hars en glas microsferen (1,5 GBq versus 2,4 GBq, respectievelijk), is dit niet direct terug te zien in de mediane overleving.
Studies die de waarde van radioembolisatie ten opzichte van standaard klinische zorg beschrijven zijn zeer beperkt. Bester et al. vergelijkt retrospectief 224 patiënten met CRC-metastasen, met de beste standaard zorg in 29 patiënten (9). Hierbij moet opgemerkt worden dat deze 29 patiënten eerder ongeschikt bevonden waren voor radioembolisatie vanwege afwijkende arteriële leveranatomie, gastro-intestinale activiteitstapeling, te hoge longshunt of door afzegging van de patiënt zelf. De incidentie van extrahepatische ziekte of het percentage aangedane lever was echter vergelijkbaar tussen

Tabel 2. Radioembolisatie binnen de salvage setting (2010-2016).

eerste auteur	type studie	behandeling		n*	^{90}Y dosis (in GBq)	mediane TTLP (range in mnd)	mediane OS (range in mnd)
Cosimelli (2010) (26)	fase II	SIRT	Sirtex	50	1,7 (0,9 – 2.2)		12,6 (7,0 – 18,3) **
Hendlisz (2010) (10)	fase II	fluorouracil vs. fluorouracil + SIRT	Sirtex	23 21	0 1,8 (1,3 – 2,2)	2,1 (NB) 5,5 (NB)	7,3 (NB) 10,0 (NB)
Evans (2010) (34)	RS	SIRT	Sirtex	140	1,8 (0,4 – 2,6)		7,9 (6,3 – 10,1)
Chua (2011) (12)	RS	chemo + SIRT	Sirtex	140	1,8 (0,4 – 2,6)		9,0 (1,0 – 43)
Bester (2012) (9)	RS	SIRT vs. standaard zorg	Sirtex	224 29	1,8 (0,4 – 2,6) 0		11,9 (10,1 – 14,9) 6,6 (NB)
Turkman (2013) (27)	fase II	SIRT		23	2,0 (1,0 – 2,5)		14,0 (NB)
Benson (2013) (23)	fase II	SIRT	Thera	61	2,3 (2,0 – 2,7)	3,0 (2,0 – 5,8) **	8,8 (6,6 – 11,9) **
Sofocleous (2014) (28)	fase I	SIRT	Sirtex	19	1,2 (0,4 – 2,0) 0,7 (0,3 – 1,6)	5,2 (3,3 – 6,4) **	14,9 (6,4 – 25,6) **
Lewandowski (2014)*** (29)	RS	SIRT	Thera	214	2,4 (0,6 – 10)		10,6 (8,5 – 15,0)
Hickey (2014) (5)	fase I	capecitabine + SIRT	Thera	9	2,2 (0,4 – 5,0)		14,0 (7,8 – 20,3)
Cohen (2014) (24)	fase I	capecitabine + SIRT	Sirtex	24	1,0 (0,2 – 1,6)		8,1 (15,3 – 43,3)
Kennedy (2015) (4)	RS	SIRT	Sirtex	606	1,5 (0,1 – 5,5)		9,6 (9,0 – 11,1) **
Saxena (2015) (30)	RS	SIRT	Sirtex	302	1,7 (0,4 – 2,6)		10,5 (NB)
Golfieri (2015) (31)	CS	SIRT	Sirtex	52	1,7 (NB)		7,0 (1,3 – 72,3)
Abbott (2015) (32)	RS	SIRT	Thera	68	2,7 (2,0 – 7,8)		11,6 (9,7 – 24,7)
Hickey (2016)*** (33)	RS	SIRT	Thera	531	2,4 (0,7 – 7,8)	.	10,6 (8,8 – 12,4) **
Jakobs (2016) (13)	RS	SIRT	Sirtex	104	1,6 (NB)		10,2 (7,8 – 13,0)

RS = retrospectief, CS = casus serie, TTLP = tijd tot lever progressie, OS = algehele overleving, NB = data niet beschikbaar, mnd = maanden
** alleen de cohorten binnen publicaties met gemetastaseerd colorectaal carcinoom zijn geselecteerd*
*** weergave van het 95% betrouwbaarheidsinterval in plaats van de range*
**** forse overlap in de patiëntenpopulaties*

de cohorten. Voor de radioembolisatiegroep was de mediane overleving 11,9 maanden, versus 6,6 maanden voor de groep met standaard zorg (Hazard ratio 0,49; 95% CI 0,30-0,77). Een jaar na therapie was de overleving 36% na radioembolisatie versus 24% met standaard zorg. Natuurlijk was dit een niet-gerandomiseerde studie waarbinnen enige selectie bias aanwezig is door de manier waarop patiënten geïncludeerd zijn.
Hendlisz et al. heeft in een gerandomiseerde fase III studie de waarden van radioembolisatie naast fluorouracil onderzocht in een cross-over design (10). Patiënten kregen radioembolisatie + fluorouracil (n = 21) of alleen fluorouracil (n = 23), bij progressie ontvingen deze patiënten alsnog radioembolisatie of alternatieve palliatieve therapie. De tijd van behandeling tot progressie van de levermaligniteiten was 5,6 maanden versus 2,1 maanden, respectievelijk (Hazard ratio 0,35; 95% CI 0,18-0,69). De mediane overleving tussen de groepen was 7,3 versus 10,0 maanden, waarbij er geen significant verschil aangetoond werd door het te lage patiëntenaantal voor deze vraagstelling (Hazard ratio 0,92; 95% CI 0,47-1,78).

Resultaten van de SIRFLOX-studie

SIRFLOX is de eerste grote gerandomiseerde multicenter studie die is opgezet om de meerwaarde van radioembolisatie bij eerstelijns oxaliplatin-gebaseerd chemotherapie regimes aan te tonen. Tussen 2006 en 2013 zijn in totaal 530 patiënten in centra over de hele wereld geïncludeerd. De studie bestaat uit twee armen; FOLFOX ± bevacizumab (controle arm, n = 267) of FOLFOX ± bevacizumab + radioembolisatie (interventie arm, n = 246). De gemiddelde toegediende ^{90}Y-dosis was 1,4 GBq (range 0,4 – 3,1 GBq). De progressievrije overleving voor de twee groepen bleek niet te verschillen (10,2 versus 10,7 maanden). De tijd tot progressie van levermaligniteiten was in de interventiegroep behandeld met radioembolisatie langer dan in de controlegroep (20,5 versus 12,6) (11). Er werd gesteld dat deze lokale remming van hepatische metastasen mogelijk een substantiële impact kan hebben op de algehele overleving van patiënten. Echter, deze hypothese zal pas geëvalueerd kunnen worden zodra de data van drie grote gerandomiseerde multicenter studies (SIRFLOX, FOXFIRE en FOXFIRE Global) samengevoegd worden. De FOXFIRE en FOXFIRE Global studies hebben ook als doel de toegevoegde waarde van radioembolisatie bij eerstelijns chemotherapie te bepalen. De verwachting is dat deze data pas mid-2017 gepubliceerd zullen worden. Echter, door het gebrek aan voldoende wetenschappelijk bewijs heeft ZINL geadviseerd om radioembo¬lisatie nog niet goed te keuren als eerste/tweedelijns behandeling bij secundaire levermaligniteiten.

Selectie van salvage patiënten

Radioembolisatie wordt, zelfs in patiënten die meerdere lijnen van behandelingen gehad hebben, over het algemeen goed verdragen, mits voldaan wordt aan de eisen van longdosis <30 Gy en geen extrahepatische deposities op de pre-therapeutische MAA scan. Daarnaast kan de therapie veilig gecombineerd worden met aanvullende systemische behandelingen. Gemiddeld wordt een overlevingswinst van ongeveer 3-4 maanden behaald in vergelijking met het geven van alleen standaard zorg (9). Echter, zoals bij elke behandeling, zijn er groepen patiënten die meer baat hebben bij deze therapie.
Een betere overleving wordt vooral gezien in patiënten met een totaal tumorvolume in de lever <25%, die geen extrahepatische ziekte hebben, een ECOG status 0-1 en waarbij radioembolisatie gecombineerd wordt met chemotherapie (5,12,13).
Afgeleiden van deze factoren zoals de CEA-status en de leverbiomarkers die voorafgaand aan de radioembolisatie bepaald zijn o.a. albumine en bilirubine concentraties), worden in statistische modellen ook vaak als voorspellers aangemerkt. Elk van deze karakteristieken beschrijft vanzelfsprekend al een groep patiënten die ook zonder therapie waarschijnlijk een betere overleving zouden hebben. Binnen het advies van ZINL wordt acceptabele extrahepatische ziekte gedefinieerd als enkele locoregionale kliermetastasen (maximale doorsnede 2cm) en/of longmetastasen (maximaal 5, met doorsnede van 1cm), waarbij de primaire tumor nog in situ mag zitten. Onacceptabel is onder meer peritonitis carcinomatosa, ossale metastasen en metastasen in het centraal zenuwstelsel. Daarnaast moet de levensverwachting van de patiënt nog minimaal drie maanden zijn.

Dosisberekening op basis van ^{99m}Tc-MAA SPECT

Eerder is al kort genoemd dat er verschillende methoden zijn om de therapeutische dosering microsferen voor een individuele patiënt te bepalen. Zowel SIRSpheres als TheraSpheres, de merknamen voor ^{90}Y-microsferen van de twee grootste fabrikanten, hanteren elk hun eigen voorgestelde berekening (tabel 1). Opvallend is dat er bij deze benaderingen geen sprake is van 'echte' dosimetrie, aangezien het verschil in verdeling van sferen over de tumor en het gezonde leverparenchym niet meegenomen wordt. Op basis van de ^{99m}Tc-MAA SPECT (met attenuatiecorrectie) kan de tumor-tot-normaal (T/N) ratio geschat worden; het volume van de tumor en de gehele lever wordt bepaald op anatomische beeldvorming. Voor beide typen sferen kan vervolgens voorafgaand aan de toediening de geabsorbeerde dosis (D) op de verschillende doelgebieden geschat worden.

Deze benadering wordt het partitiemodel genoemd omdat er drie relevante doelgebieden gedefinieerd zijn, waarbij aangenomen wordt dat de activiteit binnen deze gebieden homogeen verdeeld is. De conversiefactor van 50 Gy/(MBq/cm^3) wordt onder andere bepaald door de halfwaardetijd en afgegeven bèta-energie. Een homogene dosis van 1 GBq/kg ^{90}Y zal een geabsorbeerde dosis geven van ongeveer 50 Gy. In elke berekening wordt de stralingsdosis gecorrigeerd voor de fractie van de microsferen die in de longen terecht komt als gevolg van shunting. Let wel, het feitelijke therapeutische

$$Longshunt = \frac{Cts_{longen}}{Cts_{lever} + Cts_{longen}} \quad (1)$$

$$T/N\ ratio = \frac{A_{tumor}/m_{tumor}}{A_{normaalLever}/m_{normaalLever}} \quad (2)$$

$$D_{longen} = \frac{50 \times A_{toegediend} \times Longshunt}{m_{longen}} \quad (3)$$

$$D_{normaalLever} = \frac{50 \times A_{toegediend} \times (1 - Longshunt)}{m_{normaalLever} + T/N\ ratio \times m_{tumor}} \quad (4)$$

$$D_{tumor} = \frac{50 \times A_{toegediend} \times (1 - Longshunt)}{\frac{1}{T/N\ ratio}(m_{normaalLever} + T/N\ ratio \times m_{tumor})} \quad (5)$$

$$= T/N\ ratio \times D_{normaalLever}$$

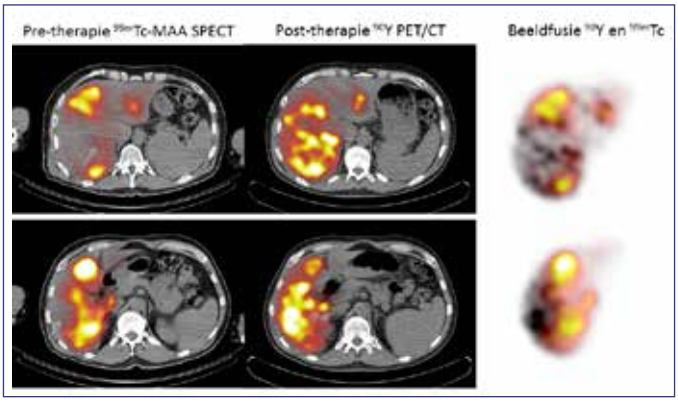

Figuur 3. Vergelijking van de ^{99m}Tc-MAA en ^{90}Y-verdeling. Ondanks de goede ^{99m}Tc-MAA accumulatie in het merendeel van de laesies zijn er ook enkele gebieden die geen of weinig stapeling vertonen (zie pijlen). Op de post-therapiescans is te zien dat laesies in deze gebieden wel degelijk een intense ^{90}Y-accumulatie vertonen. De mismatch tussen ^{99m}Tc en ^{90}Y is nog duidelijker te zien in de beeldfusie van deze twee acquisities.

effect van 50 Gy (0,5 miljoen) glassferen is anders dan 50 Gy (20 miljoen) harssferen, doordat de spatiële verdeling op microniveau sterk zal verschillen.
Het grootste nadeel van pre-therapeutische dosimetrische benadering is dat hierbij aangenomen wordt dat de verdeling van MAA eiwitten op de SPECT overeenkomt met de verdeling van de ^{90}Y-micorsferen, terwijl dit zeker niet altijd opgaat. Wondergem et al. bestudeerde in 39 procedures de verdeling over de acht leversegmenten tussen ^{99m}Tc-MAA en ^{90}Y-remstraling SPECT (14). Beide scans werden genormaliseerd naar ^{90}Y-activiteit. In ongeveer een derde van alle procedures was er een suboptimale overeenkomst in katheterpositie tussen beide procedures. In de procedures met een goede overeenkomst in katheterpositie was het gemiddelde verschil -0,03 ± 0,56 MBq/cm^3. Dit betekent voor een lever van 1200ml slechts een klein verschil in totale ^{90}Y-dosering van ongeveer 40 MBq. Toch leert de ervaring dat op segment- en laesie-basis er frequent een mismatch is, wat in het uiterste geval kan leiden tot een verkeerde inschatting van het mogelijke therapeutisch effect en onterechte toe/afwijzing van patiënten voor therapie (figuur 3). Op basis van de ^{99m}Tc-MAA beeldvorming kunnen dus de relevante extrahepatische deposities en longshunt goed bepaald worden, maar de intrahepatische dosisverdeling zal hooguit een benadering zijn van de therapeutische situatie.

De introductie van Yttrium-PET

Na toediening van ^{90}Y-microsferen lopen deze vast in het levervaatbed. Aansluitend worden afbeeldingen gemaakt van de daadwerkelijke dosisverdeling. Oorspronkelijk werd aangenomen dat ^{90}Y een zuivere bèta-emitter was. Naast remstraling ontstaan er echter bij het verval van ^{90}Y als gevolg van paarproductie ook in zeer beperkte mate positronen (branching ratio is ongeveer 32 x 10^{-6}). Een van de eerste studies naar het gebruik van PET scans na injectie van ^{90}Y werd gepubliceerd in 2009. Tegenwoordig wordt de traditionele ^{90}Y-SPECT steeds vaker vervangen door een ^{90}Y-PET/CT.
Enkele studies hebben beeldkarakteristieken zoals contrast, ruis, resolutie en nauwkeurigheid van ^{90}Y-SPECT en ^{90}Y-PET vergeleken in fantoom- en patiëntenstudies (15,16). De acquisitieduur van beide typen scans is vergelijkbaar; ±30 minuten voor een SPECT versus ±40 minuten voor een PET. Echter, moderne time-of-flight PET/CT systemen hebben een betere resolutie en detecteerbaarheid van laesies in verhouding tot remstraling SPECT, daarnaast is de kwantificatie met deze PET systemen nauwkeuriger. Voor dus zowel de visuele evaluatie van de verdeling van intra- en extrahepatische deposities, als de dosimetrische berekeningen, is PET de modaliteit van eerste keuze.
Er zijn een aantal factoren die het PET signaal beïnvloeden, zoals de hoge flux aan remstraling in verhouding tot de lage fractie annihilatiefotonen, de random- en scattercorrectie algoritmen, of de gamma emissie door detectorkristallen (LSO/LYSO) in bepaalde PET scanners. Daarnaast is ^{90}Y niet altijd beschikbaar als isotoop preset binnen PET systemen. Er kan worden gescand onder natrium-22, yttrium-86 of germanium-68, maar dan moet gecorrigeerd worden voor halfwaardetijd en branching ratio. De scanner respons voor klinische activiteitconcentraties (0,5 – 3 GBq) is lineair gebleken, waarbij resoluties van 5-10 mm gehaald worden (17). De studie van Willowson et al.(18) laat duidelijk zien dat time-of-flight scanners (GE, Philips en Siemens) in variërende mate de activiteitconcentraties in zowel de laesies als achtergrond onderschatten. Door middel van een scanner-specifieke correctiefactor is accurate kwantificatie van ^{90}Y-PET binnen een instituut mogelijk.

Voor de verslaglegging van post-therapiebeelden is het aan te raden dat de beelden verslagen worden door de specialist die ook betrokken was bij de therapieplanning. De ^{90}Y-beelden worden visueel vergeleken met de ^{99m}Tc-MAA scan en diagnostische scans. Er kan van een succesvolle procedure gesproken worden indien ^{90}Y-accumulatie gezien wordt in de grotere target laesies (>1cm) en geen significante accumulatie aanwezig is in het normale leverparenchym of overige non-target gebieden. Deze bevindingen dienen beschreven te worden in het licht van de initiële verwachtingen naar aanleiding van de therapieplanning (19). Er kan bijvoorbeeld bewust gekozen worden voor een partiële leverbehandeling als het risico van een volledige bestraling te hoog is; deze beslissing moet dan genoemd worden in het post-therapieverslag.

Post-therapie dosimetrie

Bij de bepaling van de daadwerkelijk geabsorbeerde stralingsdosis op basis van post-therapie beelden wordt aangenomen dat na toediening de verdeling van de radioactieve sferen niet meer verandert. Hierdoor is beeldvorming op één tijdstip voldoende om de totale stralingsdosis over de tijd te bepalen. Verder kunnen er nog twee belangrijke aannamen gedaan worden die de berekeningen aanzienlijk vereenvoudigen; 1) de bijdrage van de remstraling aan de totale stralingsdosis is verwaarloosbaar, en 2) de bèta-energie wordt binnen een gebied met de grootte van één voxel afgegeven. Afhankelijk van het gekozen isotoop preset waarmee gescand is, wordt een specifieke conversie factor (K), vervalconstante (λ) en de tijd tussen injectie en PET (t) gebruikt om de dosis te bepalen:

$$D_{90Y}\,(Gy) = A_{PET} \times K \times e^{(\lambda_{90Y} - \lambda_{isotoop}) \times t} \qquad (6)$$

isotoop	branching ratio	verval λ (h-1)	factor K* (Gy ∘ ml/Bq)
^{90}Y	32 x 10-6	1,083 x 10-2	4,782 x 10-5
^{22}Na	0,905	3,038 x 10-5	1,353
^{86}Y	0,319	4,702 x 10-2	0,477
^{68}Ge	0,890	1,066 x 10-4	1,330

* $K = K_{90Y} * \beta_{isotoop} / \beta_{90Y}$

De resultaten van deze zogenaamde 'local deposition' methode (LD) lijken voor de toepassing van ^{90}Y-radioembolisatie overeen te komen met meer complexe dosimetrische modellen zoals 'dose-point kernel convolution' (20). Binnen deze meer complexe dosimetrische modellen worden ook de interacties tussen de voxels en de bijdragen van remstraling gesimuleerd. Echter, het grote voordeel van LD-dosimetrie is de relatief gemakkelijke implementatie in een klinische workflow, waardoor de geabsorbeerde dosis in 3D gevisualiseerd kan worden. Evaluatie van deze 3D-dosisverdeling maakt het mogelijk om voorzichtige uitspraken te doen over het te verwachten lokale therapeutische effect (21). Echter, het therapeutische effect van glazen en hars ^{90}Y-microsferen verschilt sterk bij eenzelfde geabsorbeerde dosis. Dit verschil in uiteindelijk therapeutisch effect wordt zeer waarschijnlijk verklaard door het aantal sferen, en dus de spatiële verdeling van de dosis in en rond de tumor. Op dit moment is er slechts beperkte data beschikbaar over de optimale therapeutische dosis voor colorectale metastasen, de meerwaarde van fractioneren en het effect van combinaties tussen systemische therapie en radioembolisatie.

Responsevaluatie

Het primaire doel van radioembolisatie binnen de salvage setting is het verlengen van de duur tot progressie van de levermetastasen, en uiteindelijk het verlengen van de algehele overleving. Doordat ook patiënten met leverdominante ziekte in aanmerking komen voor de behandeling, zijn er drie aspecten die beschreven moeten worden na behandeling: 1) respons van behandelde hepatische laesies, 2) het al dan niet ontstaan van nieuwe hepatische laesies, en 3) eventuele progressie van extrahepatische laesies. Voor de beoordeling van het therapeutische effect van de radioembolisatie is het belangrijk om dit onderscheid te maken, ook in de verslaglegging. In figuur 4 en 5 zijn voorbeelden te zien van een patiënt met goede en slechte respons drie maanden na therapie.
Binnen de landelijke richtlijn *Colorectaalcarcinoom versie 3.0* wordt voor metastatische ziekte van de lever geadviseerd om CT of MRI te vervaardigen. FDG PET heeft klinische meerwaarde voor het aantonen van extrahepatische ziekte, en hierom wordt FDG PET bij voorkeur uitgevoerd binnen de standaard work-up voorafgaand aan radioembolisatie bij levermetastasen (22). Follow-up beeldvorming bestaat uit CT eventueel aangevuld met FDG PET. In enkele studies (tabel 2) wordt het lokale therapeutisch effect 2-3 maanden na behandeling geëvalueerd op basis van de RECIST criteria (10, 23, 24). Binnen deze studies varieert de tijd tot intra-hepatische progressie tussen de 2-6 maanden. In dat opzicht is evaluatie binnen twee maanden na radioembolisatie aan te raden voor een objectieve registratie van mogelijke respons. De vroege moleculaire respons is mogelijkerwijs met FDG PET binnen een maand na therapie te visualiseren en kwantificeren, waardoor risicostratificatie van patiënten mogelijk wordt (25). De waarde van vroege FDG PET voor deze indicatie moet nog verder uitgekristalliseerd worden.

Toekomstvisie

De goedkeuring van radioembolisatie als behandeling voor HCC en leverdominante colorectale metastasen in een salvage setting door ZINL is een grote stap vooruit voor deze innovatieve nucleaire therapie. De behandeling vergt een zeer goede samenwerking tussen de interventieradioloog, nucleair geneeskundige en klinisch fysicus of technisch geneeskundige.

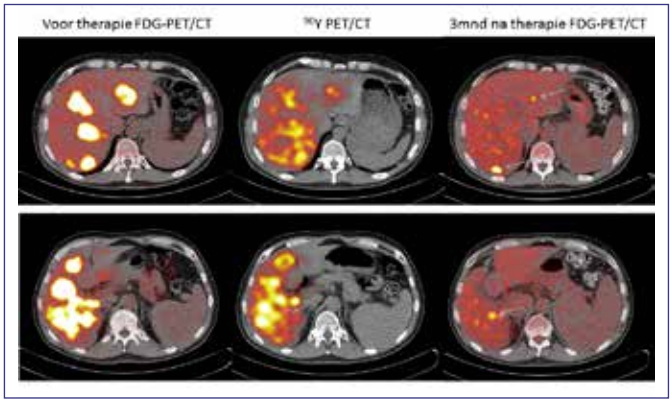

Figuur 4. Voorbeeld van een goede lokale respons op radioembolisatie. Patiënt is bekend met gemetastaseerd sigmoïdcarcinoom en status na meerdere lijnen chemotherapie. Na radioembolisatie is een goede accumulatie te zien ter plaatse van alle leverlaesies op de ^{90}Y-PET/CT (^{90}Y-dosis 2,0 GBq, totale levervolume 1600 ml, geschat tumorvolume 620ml). Drie maanden na therapie wordt op de FDG PET/CT een zeer goede partiële respons gezien (dezelfde patiënt als in figuur 3).

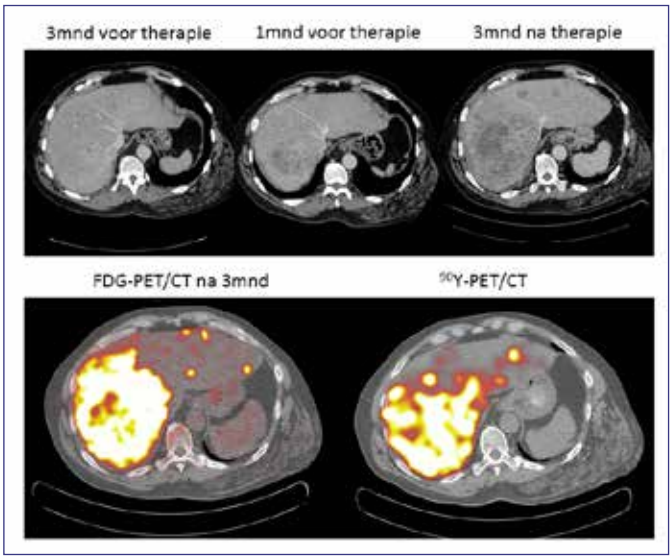

Figuur 5. Voorbeeld van een slechte lokale respons op radioembolisatie. Patiënt is bekend met enkele levermetastasen die onder chemotherapie blijven toenemen in omvang. Besloten wordt over te gaan tot radioembolisatie (^{90}Y-dosis 1,7 GBq, totale levervolume 3200 ml, geschat tumorvolume 980 ml), waarbij een goede accumulatie gezien wordt ter plaatse van de laesies op de ^{90}Y-PET/CT. Echter, drie maanden na therapie worden op de FDG PET/CT en diagnostische CT meerdere nieuwe hepatische en pulmonale laesie gezien. Ook zijn de forse afwijkingen in de rechter leverkwab verder toegenomen in omvang.

Daardoor wordt momenteel radioembolisatie uitgevoerd in een beperkt aantal specialistische centra.
Daarnaast is de toepassing van deze therapie nog niet volledig uitgekristalliseerd. Vooral op het gebied van dosis-respons relatie is nog veel winst te behalen. Door een bredere inzet van image-based dosimetrie na radioembolisatie binnen klinische studies kan een beter beeld verkregen worden van de geabsorbeerde dosis, waardoor op termijn mogelijk de optimale therapeutische dosis voor colorectale metastasen bepaald kan worden. Ook wordt het dan eenvoudiger om resultaten van patiënten uit verschillende centra met elkaar te vergelijken. Deze aanpak bij colorectale metastasen kan geëxtrapoleerd worden naar andere tumortypen zoals metastasen van neuroendocriene tumoren. Zodra accurate dosimetrie een belangrijke rol gaat spelen bij deze nucleaire therapie, zal er ook meer aandacht komen voor het nauwkeurig kwantificeren van de ^{90}Y-verdeling met PET. Door de ademhaling is kwantificatie van laesies tegen de diafragmakoepel nu nog een grote uitdaging. Nieuwe beeldvormende technieken zoals 4D-PET of ademhalings-getriggerde PET kunnen mogelijk een oplossing bieden.

l.vd.veen@nki.nl

Referenties

1. Lam MGEH, van den Bosch MAAJ, Vente MAD, et al. Yttrium-90-radioembolisatie ter behandeling van niet-reseceerbare levermaligniteiten: nieuw in Nederland! Tijdschr Nucl Geneesk. 2010; 32(1):438-44
2. Dezarn WA, Cessna JT, DeWerd LA, et al. Recommendations of the American Association of Physicists in Medicine on dosimetry, imaging, and quality assurance procedures for 90Y microsphere brachytherapy in the treatment of hepatic malignancies. Med Phys. American Association of Physicists in Medicine. 2011;38(8):4824–45
3. Giammarile F, Bodei L, Chiesa C, et al. EANM procedure guideline for the treatment of liver cancer and metastases with intra-arterial radioactive ligands. Eur J Nucl Med Mol Imaging. 2011;38(7):1393-406
4. Kennedy AS, Ball D, Cohen SJ, et al. Multicenter evaluation of the safety and efficacy of radioembolization in patients with unresectable colorectal liver metastases selected as candidates for (90)Y resin microspheres. J Gastrointest Oncol. 2015;6(2):134–42
5. Hickey R, Lewandowski RJ, Prudhomme T, et al. 90Y Radioembolization of Colorectal Hepatic Metastases Using Glass Microspheres: Safety and Survival Outcomes from a 531-Patient Multicenter Study. J Nucl Med. 2016;57(5):665–71
6. Giantonio BJ, Catalano PJ, Meropol NJ, et al. Bevacizumab in combination with oxaliplatin, fluorouracil, and leucovorin (FOLFOX4) for previously treated metastatic colorectal cancer: results from the Eastern Cooperative Oncology Group Study E3200. J Clin Oncol. 2007;25(12):1539–44
7. Van Cutsem E, Tabernero J, Lakomy R, Prenen H. Addition of aflibercept to FOLFIRI improves survival in a phase III randomized trial in patients with metastatic colorectal cancer previously treated with an oxaliplatin-based regimen. J Clin Oncol. 2012;30(28):3499-506
8. Kennedy AS, Ball D, Cohen SJ, et al. Multicenter evaluation of the safety and efficacy of radioembolization in patients with

unresectable colorectal liver metastases selected as candidates for (90)Y resin microspheres. J Gastrointest Oncol. 2015;6(2):134–42
9. Bester L, Meteling B, Pocock N, et al. Radioembolization versus standard care of hepatic metastases: comparative retrospective cohort study of survival outcomes and adverse events in salvage patients. J Vasc Interv Radiol. 2012;23(1):96–105
10. Hendlisz A, Van Den Eynde M, Peeters M, et al. Phase III trial comparing protracted intravenous fluorouracil infusion alone or with yttrium-90 resin microspheres radioembolization for liver-limited metastatic colorectal cancer refractory to standard chemotherapy. J Clin Oncol. 2010;28(23):3687–94
11. van Hazel GA, Heinemann V, Sharma NK, et al. SIRFLOX: Randomized Phase III Trial Comparing First-Line mFOLFOX6 (Plus or Minus Bevacizumab) Versus mFOLFOX6 (Plus or Minus Bevacizumab) Plus Selective Internal Radiation Therapy in Patients With Metastatic Colorectal Cancer. J Clin Oncol. 2016;34(15):1723–31
12. Chua TC, Bester L, Saxena A, Morris DL. Radioembolization and systemic chemotherapy improves response and survival for unresectable colorectal liver metastases. J Cancer Res Clin Oncol. 2011;137(5):865–73
13. Jakobs TF, Paprottka KJ, Raeßler F, et al. Robust evidence for long-term survival with (90)Y radioembolization in chemorefractory liver-predominant metastatic colorectal cancer. Eur Radiol. 2016. Apr 8:1–7
14. Wondergem M, Smits MLJ, Elschot M, et al. 99mTc-macroaggregated albumin poorly predicts the intrahepatic distribution of 90Y resin microspheres in hepatic radioembolization. J Nucl Med. 2013;54(8):1294–301
15. Elschot M, Vermolen BJ, Lam MGEH, et al. Quantitative comparison of PET and Bremsstrahlung SPECT for imaging the in vivo yttrium-90 microsphere distribution after liver radioembolization. Villa E, editor. PLoS ONE. 2013;8(2):e55742.
16. Zade AA, Rangarajan V, Purandare NC, et al. 90Y microsphere therapy: does 90Y PET/CT imaging obviate the need for 90Y Bremsstrahlung SPECT/CT imaging? Nuclear Medicine Communications. 2013;34(11):1090–6
17. Pasciak AS, Bourgeois AC, Bradley YC. A Comparison of Techniques for (90)Y PET/CT Image-Based Dosimetry Following Radioembolization with Resin Microspheres. Front Oncol. Frontiers. 2014;4(8):121
18. Willowson KP, Tapner M, QUEST Investigator Team, Bailey DL. A multicentre comparison of quantitative (90)Y PET/CT for dosimetric purposes after radioembolization with resin microspheres : The QUEST Phantom Study. Eur J Nucl Med Mol Imaging. 2015;42(8):1202–22
19. Kao YH, Steinberg JD, Tay YS, et al. Post-radioembolization yttrium-90 PET/CT - part 1: diagnostic reporting. EJNMMI Res. 2013;3(1):56
20. Pasciak AS, Bourgeois AC, Bradley YC. A Comparison of Techniques for 90Y PET/CT Image-Based Dosimetry Following Radioembolization with Resin Microspheres. Front Oncol. 2014;4(8):947
21. Kao YH, Steinberg JD, Tay YS, et al. Post-radioembolization yttrium-90 PET/CT - part 2: dose-response and tumor predictive dosimetry for resin microspheres. EJNMMI Res. 2013;3(1):57
22. Rosenbaum CENM, van den Bosch MAAJ, Veldhuis WB, et al. Added value of FDG-PET imaging in the diagnostic workup for yttrium-90 radioembolisation in patients with colorectal cancer liver metastases. Eur Radiol. 2013;23(4):931–7
23. Benson AB, Geschwind J-F, Mulcahy MF, et al. Radioembolisation for liver metastases: results from a prospective 151 patient multi-institutional phase II study. Eur J Cancer. 2013;49(15):3122–30
24. Cohen SJ, Konski AA, Putnam S, et al. Phase I study of capecitabine combined with radioembolization using yttrium-90 resin microspheres (SIR-Spheres) in patients with advanced cancer. British Journal of Cancer. 2014;111(2):265–71
25. Sabet A, Meyer C, Aouf A, et al. Early post-treatment FDG PET predicts survival after 90Y microsphere radioembolization in liver-dominant metastatic colorectal cancer. Eur J Nucl Med Mol Imaging. 2015;42(3):370–6
26. Cosimelli M, Golfieri R, Cagol PP, et al. Multi-centre phase II clinical trial of yttrium-90 resin microspheres alone in unresectable, chemotherapy refractory colorectal liver metastases. British Journal of Cancer. 2010;103(3):324–31
27. Turkmen C, Ucar A, Poyanli A, et al. Initial outcome after selective intraarterial radionuclide therapy with yttrium-90 microspheres as salvage therapy for unresectable metastatic liver disease. Cancer Biother Radiopharm. 2013;28(7):534–40
28. Sofocleous CT, Garcia AR, Pandit-Taskar N, et al. Phase I trial of selective internal radiation therapy for chemorefractory colorectal cancer liver metastases progressing after hepatic arterial pump and systemic chemotherapy. Clin Colorectal Cancer. 2014;13(1):27–36
29. Lewandowski RJ, Memon K, Mulcahy MF, et al. Twelve-year experience of radioembolization for colorectal hepatic metastases in 214 patients: survival by era and chemotherapy. Eur J Nucl Med Mol Imaging. 2014;41(10):1861–9
30. Saxena A, Meteling B, Kapoor J, et al. Is yttrium-90 radioembolization a viable treatment option for unresectable, chemorefractory colorectal cancer liver metastases? A large single-center experience of 302 patients. Ann Surg Oncol. 2015;22(3):794–802
31. Golfieri R, Mosconi C, Giampalma E, et al. Selective transarterial radioembolisation of unresectable liver-dominant colorectal cancer refractory to chemotherapy. Radiol Med. 2015;120(8):767–76
32. Abbott AM, Kim R, Hoffe SE, et al. Outcomes of Therasphere Radioembolization for Colorectal Metastases. Clin Colorectal Cancer. 2015;14(3):146–53
33. Hickey R, Mulcahy MF, Lewandowski RJ, et al. Chemoradiation of hepatic malignancies: prospective, phase 1 study of full-dose capecitabine with escalating doses of yttrium-90 radioembolization. Int J Radiat Oncol Biol Phys. 2014;88(5):1025–31
34. Evans KA, Richardson MG, Pavlakis, et al. Survival outcomes of a salvage patient population after radioembolization of hepatic metastases with yttrium-90 microspheres. J Vasc Interv Radiol. 2010;21(10):1521-6

Holmium-166 radioembolisation for liver tumours

J.F. Prince, MD, PhD; Prof. M.A.A.J. van den Bosch, MD; J.F.W. Nijsen, PhD; Prof. M.G.E.H. Lam, MD; M.L.J. Smits, MD, PhD

Department of Radiology and Nuclear Medicine, University Medical Centre Utrecht, the Netherlands

Abstract

Prince JF, Van den Bosch MAAJ, Nijsen JFW, Lam MGEH, Smits MLJ. Holmium-166 radioembolisation for liver metastases. Since 2016, radioembolisation is a reimbursed treatment option for patients with colorectal carcinoma liver metastases in the Netherlands. This image-guided treatment consists of injection of radioactive microspheres in the hepatic arterial system, selectively targeting the arterially vascularised metastases. Radioembolisation is usually performed with microspheres containing yttrium-90 (^{90}Y). As an alternative to these microspheres, holmium-166 (^{166}Ho) microspheres have been developed with improved imaging characteristics. One of the advantages is that a small number of ^{166}Ho-microspheres can be given as a scout dose to predict distribution before treatment. This paper describes the characteristics of ^{166}Ho-microspheres, the treatment procedure, clinical results and ongoing developments.
Tijdschr Nucl Geneesk 2016; 38(4):1622-1626

Origin of radioembolisation

In the early 1960s, Dr. Irving Ariel noticed that cancer in the liver was resistant to treatment with external beam radiation therapy and chemotherapy. He wanted to try a new treatment using a medical device that he and several colleagues had previously tried in animals: ceramic microspheres loaded with radioactivity. The microspheres contained the radioisotope ^{90}Y that emits beta radiation and induces cell death through DNA damage. To administer the microspheres, he placed a catheter at the level of the celiac artery in the aorta via a groin puncture and femoral artery access. He protected the patient's legs from the radioactive microspheres by strapping tourniquets on both of them. After injecting the microspheres, a photoscan was obtained to illustrate the distribution of the radioisotopes. Unfortunately, the complications were sometimes severe. One patient experienced a paresis of the right leg, while another became completely paraplegic. It was hypothesised that these complication arose from microspheres entering the spinal canal because the patients were positioned on their back and gravity would pull the microspheres towards the arteries in the spinal canal. Still, several of his patients reported a temporary relief of complaints; their sense of wellbeing improved, appetite returned and pain decreased (1).

Around 50 years later, the intra-arterial injection of radioactive microspheres evolved into radioembolisation and became mainstream clinical practice performed in hospitals worldwide. Microspheres with ^{90}Y gained European CE market approval in two forms, resin microspheres in 2002 (SIR-Spheres, SIRTeX Medical Ltd., Australia) and glass microspheres in 2006 (TheraSphere, BTG, Canada). Three randomised controlled trials have been published and several other trials are recruiting patients or awaiting follow up (2). Multiple oncology guidelines now include radioembolisation as a treatment option and reimbursement is recently established for colorectal cancer (and hepatocellular carcinoma) patients in the Netherlands (3, 4).

^{90}Y-radioembolisation technique

To be eligible for radioembolisation with ^{90}Y-radioembolisation, candidates should have primary or metastatic hepatic disease that is liver-dominant (figure 1), and have a life expectancy of more than three months (5). A contrast enhanced CT is acquired to assess the hepatic vasculature. In a pretreatment procedure, injection positions are determined and optionally, extrahepatic arteries are embolised (6). A scout dose consisting of technetium-99m macroaggregated albumin (^{99m}Tc-MAA) is injected as a surrogate particle. It functions as a surrogate for the microspheres. ^{99m}Tc-MAA emits only gamma rays that can be visualised on SPECT/CT, while keeping radiation exposure to patients low. Extrahepatic deposition in a gastrointestinal organ (e.g., stomach, duodenum or pancreas) is a contraindication for treatment and requires another pretreatment procedure with different injection positions, additional embolisation or the use of an anti-reflux catheter (7). If targeted liver segments are missed, different injection positions can be chosen or intrahepatic embolisation can redirect flow to ensure all desired segments (i.e., tumours) are reached (8). Some of the particles will inadvertently shunt to the lungs, but this is a contraindication only if an absorbed dose of more than 30 Gy is expected in the lungs (often approximated as a shunt percentage of >20%) (9). After an adequate pretreatment procedure, microspheres loaded with ^{90}Y are administered at the injection position(s) and their distribution is confirmed using PET/CT. The microspheres remain in the liver indefinitely; most radiation is deposited in a week.

^{166}Ho-microspheres

As an alternative to ^{90}Y-microspheres, ^{166}Ho-microspheres were developed to provide superior imaging capabilities (10). ^{166}Ho also

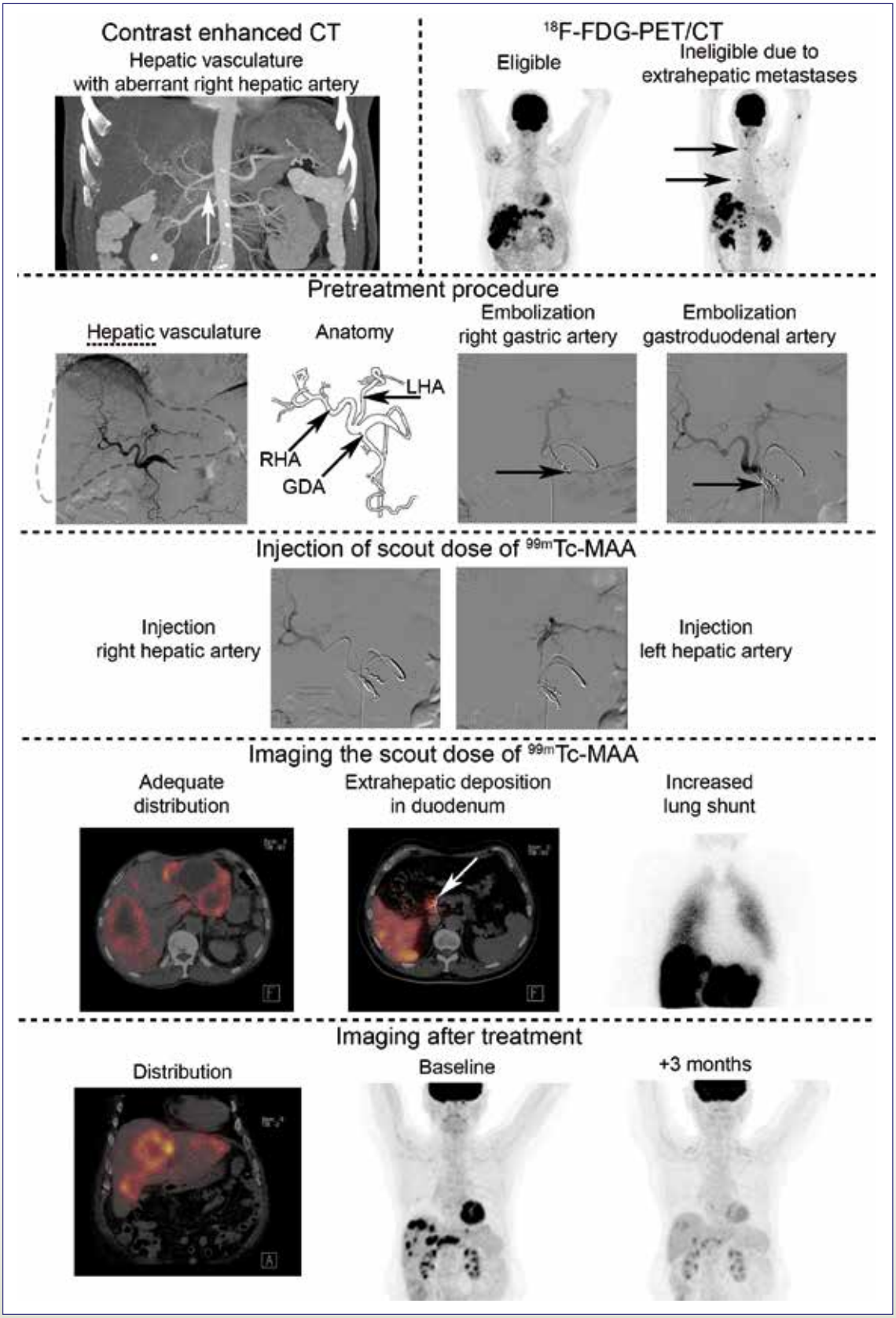

RHA = right hepatic artery, LHA = left hepatic artery, GDA = gastroduodenal artery

Figure 1. Imaging of radioembolisation during all procedures.

emits beta radiation for tumour destruction and additionally emits gamma rays (81 keV, 6.2%) that can be detected using SPECT/CT. Also, holmium is paramagnetic and can be visualised on MR imaging (figure 2) (11). The half-life of ^{166}Ho is shorter than the half-life of ^{90}Y (27 versus 64 hours), thus more activity is needed to obtain the same absorbed dose (table 1). ^{166}Ho-microspheres can improve radioembolisation, mainly because a scout dose of ^{166}Ho-microspheres can replace ^{99m}Tc-MAA and pre- and post-treatment dosimetry can be performed more accurately.

^{166}Ho-radioembolisation technique

^{166}Ho-radioembolisation is performed in a similar fashion to ^{90}Y-radioembolisation. The main difference is that the scout dose of ^{99m}Tc-MAA can be replaced by a scout dose of ^{166}Ho-microspheres. A scout dose prior to treatment is used to: 1) identify non-target gastrointestinal deposition of activity, 2) calculate the lung shunt fraction, and 3) predict the intrahepatic distribution of the microspheres (tumour and non-tumour absorbed doses).

Both ^{99m}Tc-MAA and a scout dose of ^{166}Ho-microspheres show extrahepatic deposition on the pre-treatment SPECT/CT (point 1), because both isotopes emit gamma radiation. A scout dose of ^{166}Ho-microspheres also emits beta radiation, but calculations and experiences in safety trials have shown that the absorbed dose of an extrahepatic deposition is not sufficient to cause complications (12, 13).

Studies have shown that ^{99m}Tc-MAA does not perform well enough to calculate the lung shunt fraction (14) (point 2).

In contrast, studies have also shown that using the ^{166}Ho-microspheres scout dose, the lung dose is estimated more accurately than with ^{99m}Tc-MAA. ^{99m}Tc-MAA provides a significant overestimation of the lung shunt fraction, especially when calculated on planar imaging. Overestimation of the lung shunt fraction results in patients falsely receiving a reduced amount of ^{90}Y-microspheres activity or no treatment at all (which is prescribed by the product manual).

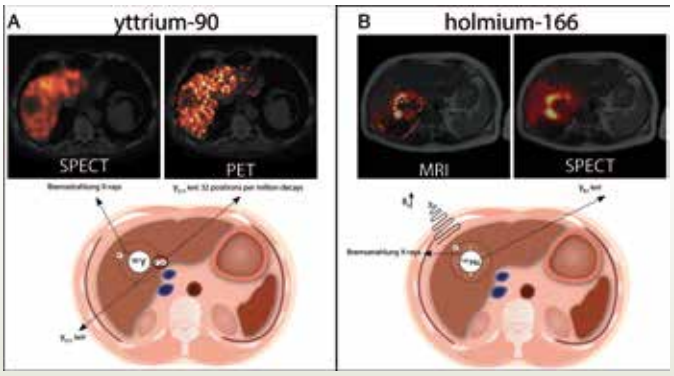

Figure 2. (A) Yttrium-90 microspheres can be visualised with Bremsstrahlung-SPECT and PET. (B)Holmium-166 microspheres can be visualised with SPECT and MRI. Reproduced from Smits et al. CVIR 2015, with permission from Springer (21).

^{99m}Tc-MAA also does not predict the intrahepatic distribution of microspheres (15, 16) (point 3). The differences between the distribution of ^{99m}Tc-MAA and the actual microspheres for therapy probably lie in the different shape, binding and size of the particles. In theory, distribution prediction is best performed with a scout dose of the same microspheres as used for treatment. For that reason, a small amount (10% of total amount of microspheres) is used for scout dose imaging in ^{166}Ho-radioembolisation. Data in terms of the intrahepatic distribution performance of the ^{166}Ho-microspheres scout dose are awaited. Better distribution prediction could lead to improved efficacy and reduced toxicity. The prescribed absorbed dose is currently averaged over the whole liver, but the dose per tumour varies per patient (and per tumour) because of heterogeneity in uptake (17). An accurate scout dose could determine the maximum amount of radioactivity that can safely be administered, maximising impact.

Another difference in the treatment with ^{90}Y- or ^{166}Ho-microspheres lies in the method of injection. The administration systems for the two types of ^{90}Y-microspheres and the ^{166}Ho-microspheres are only slightly different. All microspheres are contained in a vial positioned centrally in a Perspex box (to shield for beta radiation). The microspheres are flushed from the vial into the patient via a tubing system connected to the intra-arterial catheter. For resin ^{90}Y-microspheres and ^{166}Ho-microspheres the administration is performed intermittently to check for stasis and possible backflow. ^{90}Y glass microspheres only require a single injection after which flushing can start.

The final difference lies in post-treatment imaging. Quantitative ^{166}Ho-imaging can be performed with SPECT (using the gamma radiation) or MRI (using the paramagnetic properties of holmium). ^{90}Y can be quantified with PET (using the 34 positrons emitted per million decays) or indirectly and less accurately with Bremsstrahlung-SPECT.

Clinical results of ^{166}Ho-radioembolisation

After laboratory and animal testing, the first human trial in 2011 concluded that radioembolisation with ^{166}Ho-microspheres was feasible and safe with an aimed whole liver dose of 60 Gy (13, 18, 19). Efficacy of ^{166}Ho-radioembolisation was subsequently investigated in a phase 2 trial, the Holmium Embolization Particles for Arterial Radiotherapy (HEPAR) 2 trial. In this trial, patients were first given a scout dose of ^{99m}Tc-MAA to check for contraindications. A second scout dose, with ^{166}Ho-microspheres, preceded treatment to eventually compare both scout doses with treatment. SPECT/CT and MR-imaging were acquired after the scout and treatment dose of ^{166}Ho-microspheres to assess quantification accuracy. The primary outcome, efficacy, was evaluated using contrast enhanced CT and ^{18}F-FDG PET/CT every three months up to one year after treatment. The primary outcome was rated by three radiologists independently and blinded for time of imaging (baseline or follow up), alike central independent review (20). Adverse events were recorded in addition to frequent quality of life questionnaires. Because quality of life is important in

Table1. Microsphere characteristics.

characteristic	^{166}Ho microspheres	SIR-Spheres	TheraSphere
isotope	holmium-166	yttrium-90	
half-life (h)	26.8	64.1	
deposited energy (J/GBq)	15.9	49.4	
maximum β^- energy (MeV)	1.85 (50.0%) 1.77 (48.7%)	2.28 (100%)	
γ-energy (keV)	80.6 (6.6%) 1,379 (0.9%)	none[1]	
decay product	erbium-166	zirconium-90	
matrix material	poly(L-lactic acid)	resin	glass
diameter (μm)	30±15	32.5±2.5	25±10
density (g/mL)	1.4	1.6	3.3
number per dose	33,000,000	50,000,000	4,000,000
activity/ microsphere (Bq)	300-330	40-70	2,400-2,700

[1] Abundance of gamma photons is very low, 0.02% (1,761 keV)

a salvage setting, changes in quality of life were measured starting already one week after treatment. A sequential trial design with different stopping criteria after every interim analysis ensured timely completion; 30 to 48 patients were to be included with analyses following every six patients. Disease control rate (stable disease and partial response) in this heavily pretreated group of patients was 49% at 3-month follow-up. Figure 3 shows an example of partial tumour response. The most common serious toxicities (grade 3 or 4 toxicity according to CTCAE v4.03 criteria) were abdominal pain (18% of patients) and nausea (8%).
Data from the first two clinical studies were used to obtain CE-marking for ^{166}Ho-microspheres in 2015, making it the third commercially available microsphere (QuiremSpheres, Quirem Medical, The Netherlands).

Currently we are investigating the use of ^{166}Ho-radioembolisation in other tumour types like neuroendocrine tumours and hepatocellular carcinoma. In these trials, scout dose imaging will be used to individualise the amount of activity that patients receive by combining functional liver imaging and the ^{166}Ho-scout dose distribution.

Summary

In summary, Dr. Ariel and his colleagues pioneered a new treatment of liver cancers (radioembolisation) that has become a mainstream therapy for hepatic malignancies. The most recent innovation, ^{166}Ho-microspheres, has the potential to further improve both efficacy and safety of radioembolisation treatment by introducing personalised treatment planning.

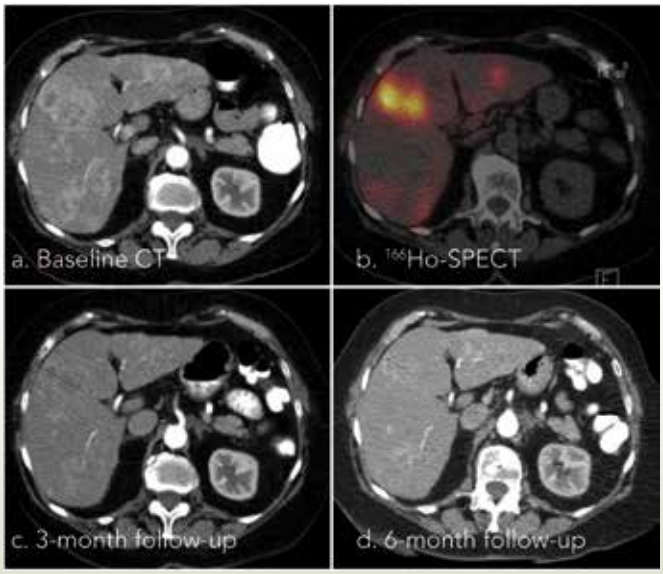

Figure 3. Example of partial response after 166Ho-radioembolisation in a NET patient.

Disclosure

J.F.W. Nijsen, PhD is inventor on several patents related to the ^{166}Ho-PLLA-microspheres, is co-founder and chief scientific officer of Quirem Medical, and has a minority share in the company Quirem Medical. Prof. M.G.E.H. Lam, MD is a consultant for Sirtex Medical, BTG and Mirada. The department of Radiology and Nuclear Medicine of the UMC Utrecht receives royalties from Quirem Medical.

m.l.j.smits-3@umcutrecht.nl

References

1. Ariel IM. Treatment of Inoperable Primary Pancreatic and Liver Cancer by the Intra-Arterial Administration of Radioactive Isotopes (Y90 Radiating Microspheres). Annals of surgery. 1965;162:267-78
2. Braat AJ, Huijbregts JE, Molenaar IQ, Borel Rinkes IH, van den Bosch MA, Lam MG. Hepatic radioembolization as a bridge to liver surgery. Frontiers in oncology. 2014;4:199
3. Van Cutsem E, Cervantes A, Adam R, et al. ESMO consensus guidelines for the management of patients with metastatic colorectal cancer. Annals of oncology : official journal of the European Society for Medical Oncology / ESMO. 2016;27(8):1386-422
4. Frilling A, Modlin IM, Kidd M, et al. Recommendations for management of patients with neuroendocrine liver metastases. The lancet oncology. 2014;15(1):e8-21
5. Kennedy A, Nag S, Salem R, et al. Recommendations for radioembolization of hepatic malignancies using yttrium-90 microsphere brachytherapy: a consensus panel report from the radioembolization brachytherapy oncology consortium. International journal of radiation oncology, biology, physics. 2007;68(1):13-23
6. Salem R, Thurston KG. Radioembolization with 90Yttrium microspheres: a state-of-the-art brachytherapy treatment for primary and secondary liver malignancies. Part 1: Technical and methodologic considerations. Journal of vascular and interventional radiology : JVIR. 2006;17(8):1251-78
7. Fischman AM, Ward TJ, Patel RS, et al. Prospective, randomized study of coil embolization versus Surefire infusion system during yttrium-90 radioembolization with resin microspheres. Journal of vascular and interventional radiology : JVIR. 2014;25(11):1709-16
8. Bilbao JI, Garrastachu P, Herraiz MJ, et al. Safety and efficacy assessment of flow redistribution by occlusion of intrahepatic vessels prior to radioembolization in the treatment of liver tumors. Cardiovascular and interventional radiology. 2010;33(3):523-31
9. Ho S, Lau WY, Leung TW, Chan M, Johnson PJ, Li AK. Clinical evaluation of the partition model for estimating radiation doses from yttrium-90 microspheres in the treatment of hepatic cancer. European journal of nuclear medicine. 1997;24(3):293-8
10. Nijsen JF, Zonnenberg BA, Woittiez JR, et al. Holmium-166 poly lactic acid microspheres applicable for intra-arterial radionuclide therapy of hepatic malignancies: effects of preparation and neutron activation techniques. European journal of nuclear medicine. 1999;26(7):699-704
11. Seevinck PR, Seppenwoolde JH, de Wit TC, et al. Factors affecting the sensitivity and detection limits of MRI, CT, and SPECT for multimodal diagnostic and therapeutic agents. Anti-cancer agents in medicinal chemistry. 2007;7(3):317-34
12. Prince JF, van Rooij R, Bol GH, de Jong HW, van den Bosch MA, Lam MG. Safety of a Scout Dose Preceding Hepatic Radioembolization with 166Ho Microspheres. Journal of nuclear medicine : official publication, Society of Nuclear Medicine. 2015;56(6):817-23
13. Smits ML, Nijsen JF, van den Bosch MA, et al. Holmium-166 radioembolisation in patients with unresectable, chemorefractory liver metastases (HEPAR trial): a phase 1, dose-escalation study. The lancet oncology. 2012;13(10):1025-34
14. Elschot M, Nijsen JF, Lam MG, et al. 99mTc-MAA overestimates the absorbed dose to the lungs in radioembolization: a quantitative evaluation in patients treated with 166-Ho-microspheres. European journal of nuclear medicine and molecular imaging. 2014;41(10):1965-75
15. Wondergem M, Smits ML, Elschot M, et al. 99mTc-macroaggregated albumin poorly predicts the intrahepatic distribution of 90Y resin microspheres in hepatic radioembolization. Journal of nuclear medicine : official publication, Society of Nuclear Medicine. 2013;54(8):1294-301
16. Ulrich G, Dudeck O, Furth C, et al. Predictive value of intratumoral 99mTc-macroaggregated albumin uptake in patients with colorectal liver metastases scheduled for radioembolization with 90Y-microspheres. Journal of nuclear medicine : official publication, Society of Nuclear Medicine. 2013;54(4):516-22
17. Smits ML, Elschot M, van den Bosch MA, et al. In Vivo Dosimetry Based on SPECT and MR Imaging of 166Ho-Microspheres for Treatment of Liver Malignancies. Journal of nuclear medicine : official publication, Society of Nuclear Medicine. 2013;54(12):2093-100
18. Vente MA, Nijsen JF, de Wit TC, et al. Clinical effects of transcatheter hepatic arterial embolization with holmium-166 poly(L-lactic acid) microspheres in healthy pigs. European journal of nuclear medicine and molecular imaging. 2008;35(7):1259-71
19. Nijsen JF, Seppenwoolde JH, Havenith T, Bos C, Bakker CJ, van het Schip AD. Liver tumors: MR imaging of radioactive holmium microspheres--phantom and rabbit study. Radiology. 2004;231(2):491-9
20. Ford R, Schwartz L, Dancey J, et al. Lessons learned from independent central review. European journal of cancer. 2009;45(2):268-74
21. Smits ML, Elschot M, Sze DY, et al. Radioembolization dosimetry: the road ahead. Cardiovascular and interventional radiology. 2015;38(2):261-69

Lutetium-177 labelled PSMA ligands for the treatment of metastatic castrate-resistant prostate cancer

A.J.A.T. Braat, MD[1]; H. Ahmadzadehfar, MD, MSc[2]

[1]Department of Radiology and Nuclear Medicine, University Medical Centre Utrecht, Utrecht, the Netherlands
[2]Department of Nuclear Medicine, University Hospital Bonn, Bonn, Germany

Abstract

Braat AJAT, Ahmadzadehfar H. Lutetium-177 labelled PSMA ligands for the treatment of metastatic castrate-resistant prostate cancer. The use of ^{68}Ga-PSMA-HBED-CC PET/CT has increased immensely in the last year. Based on ^{68}Ga-PSMA-HBED-CC success, ^{177}Lu-labelled PSMA ligands have peaked everyone's interest. This article discusses several articles on radionuclide treatments in prostate cancer and the initial results on ^{177}Lu-PSMA therapy with either ^{177}Lu-PSMA-617 or ^{177}Lu-PSMA-I&T as a salvage therapy. ^{177}Lu-PSMA is very promising, based on the recently published papers describing a total of 165 patients. ^{177}Lu-PSMA was administered intravenously with 4–8 GBq per treatment cycle (varying 1–6 cycles in total). Any PSA decrease, >30% PSA decline and >50% PSA decline was reached in approximately 75%, 60% and 50%, respectively. Additionally, assessment with ^{68}Ga-PSMA-HBED-CC PET/CT showed high imaging response rates as well. No toxicities occurred directly after therapy administration and early toxicities were mild. Apart from one case with a Common Terminology Criteria for Adverse Events (CTCAE) grade III anaemia and one case with a CTCAE grade III thrombocytopenia, no significant myelosuppression occurred in these initial studies. Toxicities to the salivary glands were limited and transient and no renal toxicities where described, even though these organs were most at risk from a dosimetry point of view. Long term toxicities are currently unknown, however future studies will tell. ^{177}Lu-PSMA therapy is a promising imaging based treatment. A need exists for well-designed prospective studies or randomised controlled trials comparing ^{177}Lu-PSMA therapy to chemotherapy or ^{223}Ra-chloride in patients with bone-limited disease. An opportunity for nuclear medicine physicians and urologists for the development of a patient personalised treatment.**Tijdschr Nucl Geneesk 2016; 38(4):1627-1634**

Introduction

Prostate cancer (PCa) is the second most common cancer in males. In patients with localised PCa, the five-year survival rate approximates 100%. In patients with distant metastases on the other hand, the five-year survival rate drops radically to 31% (1). First-line treatments include surgery, external beam radiotherapy (EBRT), brachytherapy and/or hormonal treatments. Once first-line treatment failure occurs, mostly stated as a biochemical recurrence under hormonal treatment (e.g. castration resistant prostate cancer), radiation oncologists could apply pelvic EBRT or medical oncologists add a chemotherapeutic regimen to the patient's treatment. In the case of chemotherapy, after an initial docetaxel treatment a switch to novel agents occurs, in which abiraterone and enzalutamide provide limited survival benefit of 3.9 and 4.8 months, respectively (2, 3). Looking at novel radionuclide treatments in patients with diffuse or painful bone metastases, patients are treated with ^{223}Ra-chloride. Overall survival after ^{223}Ra-chloride has been reported to improve with 3.6 months (4).

To assess the risk in first-, second- or third-line treatment failures, prostate-specific antigen (PSA) kinetics is used. Fiercely debated in literature, PSA has been mentioned to be unreliable for active surveillance (5). Even a stable PSA during the first two years after diagnosis does not preclude the formation of distant metastases and the possibility of lethal cancer (6-8). Thus, a need exists for a more accurate diagnostic modality for initial diagnosis and follow-up.

Choline tracers labelled with ^{11}C or ^{18}F have been widely used for the staging and detection of recurrent disease. In patients with low PSA levels however, numerous studies report a low sensitivity and specificity of these tracers (9, 10). In light of the rapid developments in recent years, an improved imaging modality has become available. Prostate specific membrane antigen (PSMA) is a 750-amino acid type II transmembrane glycoprotein (also called folate hydrolase I or glutamate carboxypeptidase II (GCPII)) (11-13). PSMA is upregulated in PCa and the glycoprotein's expression is low on normal prostate tissue. Its target specificity is maintained after radiolabelling with ^{68}Ga (11, 12). The most commonly used type is ^{68}Ga-PSMA-HBED-CC, which has been successfully used for the imaging of prostate cancer with high sensitivity and specificity, even in patients with very low PSA levels (<2 ng/ml) (14). Direct comparison studies support the superiority of ^{68}Ga-PSMA-HBED-CC in lymph node assessment over CT 3D volumetric based lymph node assessment (15) and in overall disease assessment

compared to ^{18}F-methylcholine, especially in patients with low PSA-levels (16).
These staggering results will lead or have already led to a paradigm shift in the use of imaging in primary staging of PCa. In a recent study by Hijazi et al. diagnostic accuracy of ^{68}Ga-PSMA-HBED-CC in the pre-operative assessment of nodal metastases is very high for macro- and even micro- metastases in lymph nodes. Correlating imaging and tissue specimens of 213 removed nodes provided a 94% sensitivity, 99% specificity, 89% positive predictive value and 99.5% negative predictive value (17).

Detection of unsuspected locoregional or distant metastases with ^{68}Ga-PSMA has a major impact on patient management, ranging from 51% to 63% in several studies (16, 18, 19).
Targeted radionuclide therapy is an attractive, minimal invasive and quickly developing therapy option for PCa, like it has been for many different cancers before, such as CD20-positive lymphomas and somatostatin receptor positive neuroendocrine tumours, i.e. respectively ^{90}Y-ibritumomab tiuxetan (Zevalin®) and ^{177}Lu-DOTATATE (commonly referred to as peptide receptor radionuclide therapy = PRRT). We will discuss several articles on radionuclide treatments in PCa, leading to ^{177}Lu-PSMA therapy, and discuss the published initial results of ^{177}Lu-PSMA therapy.

Different radiopharmaceuticals

Table 1 shows a summary of the different radiopharmaceuticals used for imaging and therapy of PCa. In the evolvement of radionuclide treatments in metastatic prostate cancer a switch has been made from monoclonal antibodies labelled with ^{90}Y, that bind to the intracellular domain of PSMA (20), to small molecules labelled with ^{131}I (21) and later on labelled to ^{177}Lu (22-27). We will discuss these different radionuclide treatments in short.
The initial phase I study with ^{90}Y-CYT-356 monoclonal antibodies by Deb et al. was unsuccessful with no objective response on radiologic imaging and high biochemical and clinical toxicities (20). Phase I and II trials using other monoclonal antibodies, called J591 labelled to either ^{90}Y or ^{177}Lu, showed more promising results. In the phase II study with ^{177}Lu-J591, Tagawa et al. showed a PSA decline in 59.6% following a single treatment and one out of twelve patients with measurable disease had a partial response on imaging studies (28). However, myelosuppression was common with 46.8% experiencing a Common Terminology Criteria for Adverse Events (CTCAE) grade IV thrombocytopenia and 25.5% experiencing a CTCAE grade IV neutropenia with one episode of febrile neutropenia (28). Thus radionuclide treatment ^{90}Y-J591 and ^{177}Lu-J591 was limited by myelosuppression and non-haematological toxicity, with a maximum tolerated activity per cycle of 650 MBq/m^2 and 2,450 MBq/m^2, respectively (29, 30).
Due to the fact that monoclonal antibodies are large molecules, a poor permeability in solid tumours and slow clearance from the circulation is inevitable, leading to suboptimal tumour targeting and an increased absorbed dose to red marrow. These factors contribute to the narrow therapeutic window of radionuclide treatments with monoclonal antibodies. The more recently used

Table 1. Different radiopharmaceuticals used for prostate cancer (11).

imaging tracer	**physiology**
^{18}Fluorodeoxyglucose	glucose metabolism
^{11}C-acetate	fatty acid de novo synthesis
^{11}C-/^{18}F-choline, ^{18}F-(m)ethylcholine	phospholipid biosynthesis
^{18}F-FACBC	synthetic leucine analogue*
^{111}In-J591, ^{64}Cu-J591, ^{89}Zr-J591	PSMA antibody
^{99m}Tc-MIP-1404	PSMA small molecule inhibitor
^{125}I-MIP-1072, ^{125}I-MIP-1095	PSMA small molecule inhibitor
^{18}F-DCFBC	PSMA small molecule inhibitor
^{68}Ga-PSMA-HBED-CC (PSMA-11)	PSMA small molecule inhibitor
^{68}Ga-PSMA-DOTAGA-(I-y)fk(Sub-KuE)**	PSMA small molecule inhibitor
therapeutic tracer	**physiology**
^{90}Y-CYT-356	PSMA antibody
^{90}Y-J591, ^{177}Lu-J591	PSMA antibody
^{131}I-MIP-1466	PSMA small molecule inhibitor
^{177}Lu-PSMA-617	PSMA small molecule inhibitor
^{177}Lu-PSMA-DOTAGA-(I-y)fk(Sub-KuE)**	PSMA small molecule inhibitor

*amino acid transport; **also called PSMA-'imaging and therapy' = PSMA-I&T

small molecules (or low molecular weight compounds) have higher permeability into solid tumours, offering a significant advantage. Small molecules have a very specific binding, thus achieving higher uptake in tumour tissue. Furthermore, small molecules display more rapid tissue distribution and faster blood clearance. These properties contribute to an enhanced target to non-target tissue ratio, which is important not just for imaging but also for successful application of therapeutic absorbed doses.

Zechmann et al. used a PSMA small molecule ligand labelled with ^{131}I instead of monoclonal antibodies, ^{131}I-MIP-1095 (21). In their study, 25 men were evaluated after treatment with one cycle of ^{131}I-MIP-1095 showing a PSA decline in 84%, >50% PSA decline in 61% and >75% PSA decline in 25%. Imaging follow up consisted of ^{68}Ga-PSMA-HBED-CC PET/CT's on which a decreased uptake was noticed in the metastatic lesions. Myelosuppression was lower than the studies using PSMA antibodies, with grade III leukopenia in 4.2% (one patient) and grade III thrombopenia in 8.3% (two patients) (21).

^{131}I has a long half-life of 8.02 days, with a mean beta-particle range in soft tissue of just 0.9 mm and maximum range of 2.5–3 mm ($E_{\beta,mean}$ 192 keV, $E_{\beta,max}$ 606 keV). Due to the gamma-emitting properties and long half-life, ^{131}I is less attractive from a radiation safety point of view. 90Y has a half-life of 64 hours, but only has a high-energy beta-emission ($E_{\beta,mean}$ 935 keV and $E_{\beta,max}$ 2284 keV) resulting in a long mean beta-particle range of 3.6 mm and maximum range of 10 mm in soft tissue. Due to its long beta-particle range, collateral damage to surrounding tissues is quite high.
^{177}Lu has a half-life of 6.7 days and a low energy beta-particles emission (β1: $E_{\beta,mean}$ 47 keV, $E_{\beta,max}$ 176 keV; β2: $E_{\beta,mean}$ 111 keV, $E_{\beta,max}$ 384 keV; β3: $E_{\beta,mean}$ 149 keV, $E_{\beta,max}$ 497 keV) with a mean range of 0.7 mm and maximum range of 2 mm in soft tissue. So the practical issues surrounding radiation safety with ^{131}I and the limited collateral damage to surrounding tissues compared to ^{90}Y, make a ^{177}Lu labelled radionuclide treatment the most attractive option from a physical point of view.

^{177}Lu-labelled PSMA

One year after the publication of Zechmann et al., ^{177}Lu-labelled small molecules were introduced (31). Currently six studies are published using either ^{177}Lu-PSMA-617 (22, 23, 26, 27) and ^{177}Lu-DOTAGA-(I-y)fk(Sub-KuE), also named PSMA-I&T for 'imaging and therapy' (24, 25). The latter compound can be labelled to either ^{68}Ga, ^{111}In or ^{177}Lu for diagnostic or therapeutic purposes (32, 33). These six articles show promising results for the future application of ^{177}Lu-labelled PSMA. Table 2 summarises the baseline characteristics of the studied populations, in which the baseline PSA levels are the most remarkable difference. An overlap of six patients exists between the first and second study by Ahmadzadehfar et al. (22, 23).

Based on preliminary experience in different centres, patients are treated with 4–8 GBq of ^{177}Lu-PSMA intravenously (13). Multiple cycles can be given based on individual responses and tolerance. In our personal experience, up to six cycles can be given in selected patients (unpublished data by dr. Ahmadzadehfar) (24).

Efficacy

Although the study populations differ at baseline, the reported efficacy on PSA levels is remarkable (table 3). An overall PSA decline after one or more cycles was reported in 68–82%, in which the degree of PSA decline is quite comparable between the five studies: >30% decline in approximately 60% (range 29–66%) and >50% decline in approximately 50% (range 24–73%). Logically, a greater PSA decline can be accomplished by repeated cycles in selected patients (23, 25, 26).

Objective response on imaging studies differ between modalities and the five studies. The study by Ahmadzadehfar et al. describes the objective response rates, in which they conclude that the follow up with ^{68}Ga-PSMA-HBED-CC PET/CT is deemed superior due to a strong correlation with PSA levels (p=0.004) (23). Although response on imaging has also been described, while PSA levels are increasing (26). Based on European Organization for Research and Treatment of Cancer (EORTC) criteria, applied to the ^{68}Ga-PSMA-HBED-CC PET/CT images, partial response was seen in 56% and 80%, stable disease in 8% and progressive disease in 20% and 36% (23, 24). An example is shown in the figure. The studies by Heck et al. and Kratochwil et al. are difficult to interpret on this subject, due to the use of different imaging modalities in their patient populations.

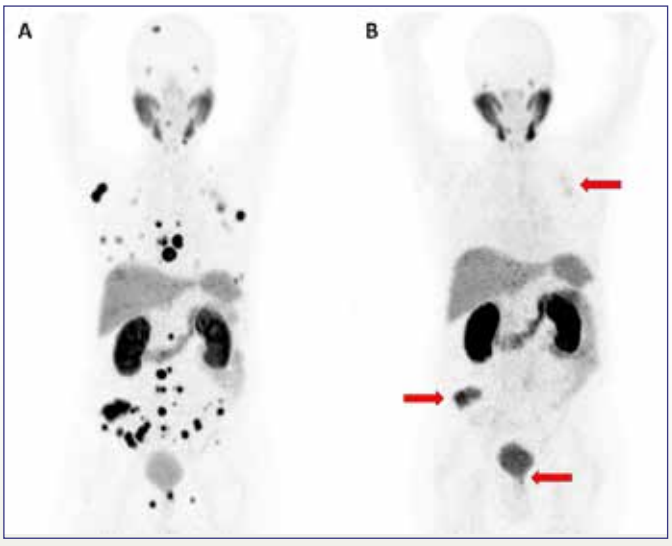

Example of a patient treated with ^{177}Lu-PSMA-671. A 74-year-old patient with diffuse bone and lymph node metastases (MIP image; A). History of chemotherapy and therapy with abiraterone. The patient underwent two cycles of Lu-PSMA therapy. Continuing PSA decline from 42 ng/ml to 18 ng/ml as well as partial response on Ga-PSMA PET images after two cycles (MIP image; B). Red arrows show residual disease two months after the second cycle.

Table 2. Baseline characteristics of current available literature.

	Ahmadzadehfar 2015 (22)	Baum 2016 (24)	Ahmadzadehfar 2016 (23)	Heck 2016 (25)	Kratochwil 2016 (26)	Rahbar 2016 (27)
age in years (range)	mean 73.5 (62–81)	median 72 (50–88)	mean 75.2 (64–82)	median 71 (46–77)	mean 71,9 (61–85)	median 73.4 (45–87)
number of patients	10	56	24	22	30	28
ECOG in n						
0	10%	-	63%	18%	NA	18%
1	70%	59%		82%	NA	60%
2	10%	41%	33%	-	NA	18%
3	10%	-	4%	-	NA	4%
median PSA in ng/ml	298.5	43.2	522	349	NA	381
tumour load						
local recurrence	30%	18%	46%	NA	NA	NA
regional lymph nodes	60%	79%	33%	82%	NA	-
distant lymph nodes	30%		50%		NA	75%
bone metastases	80%	77%	100%	95%	NA	93%
liver metastases	10%	9%	13%	18%	27%	29%
lung metastases	-	13%	-	14%	17%	14%
other	-	11%	-	-	13%	-
prior treatments						
prostatectomy	NA	71%	54%	NA	73%	29%
EBRT*	NA	84%	NA	NA	80%	NA
hormonal therapy and chemotherapy**	100%	100%	92%	100%	100%	96%
Ra-223-chloride	40%	2%	50%	14%	20%	NA

NA = not available; *external beam radiotherapy; **including novel agents abiraterone and enzalutamide

Myelosuppression

The most remarkable difference between the study populations, apart from baseline PSA levels, are the prior ^{223}Ra-chloride treatments. In the study population of Baum et al. just 2% had prior ^{223}Ra-chloride therapy, as opposed to the studies by Ahmadzadehfar et al., in which 40% and 50% of the study population had received multiple ^{223}Ra-chloride cycles (median of five cycles; range: 1-6 cycles) prior to ^{177}Lu-PSMA-617 therapy. Regardless of earlier EBRT, ^{223}Ra-chloride treatments, and the number of ^{177}Lu-PSMA cycles, the severity of the haematotoxicity is minimal, with a grade III anaemia or thrombocytopenia according to CTCAE criteria in ≤10% of the treated patients (table 4). No other relevant biochemical toxicities (CTCAE grade III or IV) were reported.

Salivary glands

Feared by many, is the induction of xerostomia and/or hypogeusia, due to the high binding of PSMA ligands to the salivary glands. In the studies by Ahmadzadehfar et al., Heck et al. and Rahbar et al., patients receive an ice-packing collar from thirty minutes prior to and up to four hours after administration of ^{177}Lu-PSMA-617, in the hope to induce vasoconstriction and reduced PSMA-binding to the salivary glands (34). But with or without an ice packing collar, current reports are less concerning, all describing a transient xerostomia or hypogeusia in 4-37%. Based on salivary gland scintigraphy, no significant decrease in salivary function is seen either (22). Besides fatigue, no other significant long term complaints were noticed (table 4).

Renal toxicity

Another fear surrounding ^{177}Lu-PSMA therapy is a decrease of kidney function. In the articles published by Ahmadzadehfar et al., Kratochwil et al. and Rahbar et al., the therapy solution was

Table 3. Administered activities, amount of therapeutic cycles and reported PSA response.

	Ahmadzadehfar 2015 (22)	**Baum 2016 (24)**	**Ahmadzadehfar 2016 (23)**		**Heck 2016 (25)**					**Kratochwil 2016 (26)**		**Rahbar 2016 (27)**	
compound used	PSMA-617	PSMA-I&T	PSMA-617		PSMA-617					PSMA-I&T		PSMA-617	
activity in GBq per cycle (range)	5.6 (4.1–6.1)	5.76 (3.6–8.7)	6.0 (4.1–7.1)		3.7 in 3 pts 7.3 in 19 pts (7.0–7.8)					4 in 11 pts 6 in 24 pts (NA)		5.9 (NA)	
number of cycles													
1	10	10	2		12					30		6	
2	-	15	22		4					NA		22	
3	-	17	-		2					9		-	
4	-	6	-		4					-		-	
5	-	2	-		-					-		-	
PSA follow up													
reported (per cycle)	1st	All	1st	2nd	1st	2nd	3rd	4th	All	1st	3rd	1st	2nd
overall decline	70%	80%	79%	68%	NA	NA	NA	NA	NA	70%	82%	59%	75%
>25-30% decline	60%	66%	54%	68%	29%	50%	67%	50%	56%	60%	82%	NA	NA
>50% decline	50%	59%	42%	60%	24%	40%	67%	50%	33%	43%	73%	32%	50%
>80-90% decline	10%	23%	8%	32%	6%	10%	33%	25%	11%	NA	NA	NA	NA
PSA increase	30%	20%	21%	32%	27%	NA	NA	NA	NA	27%	18%	41%	25%

pts = patients; NA = not available

administered by hand within one minute followed by 1000 ml of NaCl or Ringer. Whereas the group of Baum et al. and Heck et al. administered the therapy under amino acid infusion during 10-15 minutes (like in PRRT). Even though renal protection measurements differed, no significant renal toxicities were reported. In line with PRRT in neuroendocrine tumours, late renal toxicity of ^{177}Lu-PSMA is subject of longer follow-up and further research.

Other safety parameters and toxicities

Although renal protection measurements differ between the studies (additional intravenous fluids versus amino acid transfusion in line with PRRT), the difference in therapy administration seems irrelevant as no direct adverse events were encountered (by hand injection in 1 minute versus 10-15 minutes infusion) (22-27). No adverse events were reported directly after injection. Early transient side effects are mild and include nausea, vomiting, dry lips and headache.

Survival

One study reported a potential survival benefit of ^{177}Lu-PSMA. Rahbar et al. matched their patient population (n=28) to a historical cohort of 20 patients receiving best supportive care (BSC) to look at potential survival benefits. Apart from more heavily pre-treated patients and more visceral metastases in the ^{177}Lu-PSMA group, the groups were quite comparable.

Median survival in the ^{177}Lu-PSMA group was significantly longer than in BSC group; 29.4 weeks versus 19.7 weeks, respectively (p=0.032; 95% CI 0.20-0.95).

Dosimetry

The distribution of small molecule PSMA ligands in tissue is fast. Over time, uptake in PCa tissue increases, whereas uptake in normal tissue declines (24, 35). Of all normal tissues the salivary glands have the highest PSMA binding, followed by normal kidney tissue (35).
Delker et al. reported their dosimetry results with ^{177}Lu-PSMA-617 and calculated a mean absorbed dose to the bone marrow, kidneys, liver, spleen and salivary glands of 0.012 Gy/GBq, 0.6 Gy/GBq, 0.1 Gy/GBq, 0.1 Gy/GBq and 1.4 Gy/GBq, respectively (35). These results were reproduced in the clinical studies (26). Dosimetry with ^{177}Lu-PSMA-I&T results in a mean absorbed doses to whole-body, red marrow and kidneys of median 0.02 Gy/GBq, 0.014 Gy/GBq, and 0.8 Gy/GBq, respectively (24). So looking at current available literature on dosimetry, no significant differences are seen between ^{177}Lu-PSMA-617 or ^{177}Lu-PSMA-I&T. Both ligands do have a significantly lower dose on healthy tissue than in patients treated with PSMA antibody therapy ^{177}Lu-DOTA-J591 or PSMA small molecule therapy ^{131}I-MIP-1095 (21, 30).

As mentioned before, the biggest fear is damage to the salivary glands. Based on external radiotherapy data, irreversible damage to salivary glands occurs after administration of 30–40 Gy (35). With a mean absorbed dose of 1.4 Gy/GBq of ^{177}Lu-PSMA-617 and absence of permanent xerostomia or hypogeusia in the initial treatment studies, the salivary glands don't seem to be the dose limiting organ.

The second fear is the absorbed dose to kidney tissue. Based on external radiotherapy data a dose of 23 Gy is considered to result in permanent damage. The mean absorbed kidney dose of ^{177}Lu-PSMA is 0.53–0.8 Gy/GBq, quite similar to the absorbed kidney dose mentioned in published data on ^{177}Lu-DOTATATE (0.64 ± 0.16 Gy/GBq) (24, 26, 35-37). So based on PRRT literature, the kidneys could be a dose limiting organ for ^{177}Lu-PSMA therapy as well. Learned from PRRT and equally valuable for ^{177}Lu-PSMA, it's important to take impaired renal function into consideration. In the study by Svensson et al. on dosimetry with ^{177}Lu-DOTATATE therapy, treatment results in a higher kidney absorbed dose in patients with impaired renal function (GFR ≤ 60 ml/min = 0.83 ± 0.35 Gy/GBq versus GFR ≥ 90 ml/min = 0.49 ± 0.09 Gy/GBq; p <0.01) (36).

Discussion

These initial results on ^{177}Lu-labelled PSMA therapy are very promising. Remarkable PSA and imaging response can be

Table 4. Reported myelosuppression according to CTCAE v4.03 and complaints after treatment.

	Ahmadzadehfar 2015 (22)	Baum 2016* (24)	Ahmadzadehfar 2016 (23)	Heck 2016 (25)	Kratochwil 2016 (26)	Rahbar 2016 (27)
number of patients	10	56	24	22	30 (28 evaluated)	28 (22 evaluated)
anaemia						
grade 1	10%	25%	13%	32%	43%	5%
grade 2	-	5%	17%		13%	9%
grade 3	10%	-	8%	-	3%	-
leukopenia						
grade 1	10%	7%	8%	5%†	20%	14%
grade 2	10%	9%	13%		7%	-
thrombopenia						
grade 1	10%	-	17%	25%	13%	23%
grade 2	10%	-	-		3%	-
grade 3	-	-	-	-	3%	-
complaints						
nausea	20%	-	13%	-	-	5%
vomiting	10%	-		-	-	-
dry lips or xerostomia	10%	4%	4%	37%	7%‡	14%
hypogeusia	10%	-	8%	-	-	-
headache	10%	-	4%	-	-	NA
fatigue	10%	-	17%	-	7%‡	NA

*no changes in CTCAE score in myelosuppression before and after therapy; †neutropenia; ‡patients reported, needing substitution of saliva or affecting daily life, however the true number of transient xerostomia or fatigue after treatment is not reported

obtained with just two ^{177}Lu-PSMA cycles and even further improved with more cycles. Furthermore, its clinical and biochemical toxicity profile seems limited and a potential survival benefit is a promising result as well.
As often stated, the main advantage of radionuclide treatment and of ^{177}Lu-PSMA therapy is: 'you see what you treat'. Baum et al. already employed this paradigm in their study, by treating patients with multiple cycles based on their ^{68}Ga-PSMA-HBED-CC PET/CT results (24). Thus application of ^{177}Lu-PSMA should be evaluated on a patient-to-patient basis, resulting in imaging based personalised treatment.

At the same time, normal tissue dose-limiting substances are being developed. One example of a dose-limiting substance is PSMA-inhibitor 2-(phosphonomethyl-)pentanedioic acid (PMPA). Blocking of specific PSMA binding in the kidney tissue by PMPA has been validated in pre-clinical studies (38). As significant renal toxicity has not been reported yet, the use of PMPA seems unnecessary or just for selected patients with reduced renal function. The use of PMPA is even less attractive, as it blocks tumour uptake as well, resulting in a lower tumour absorbed dose and probably a decline in efficacy (38).

Future research on ^{177}Lu-PSMA treatment is needed and will improve our knowledge on efficacy, long term toxicities, survival, dosimetry and indications. Besides these parameters, we might learn even more interesting features of ^{177}Lu-PSMA therapy in PCa.
Recently, Schlenkhoff et al. reported two interesting cases (39, 40). The first case was a patient with extensive bone marrow disease with haematological depressions requiring blood transfusions. After ^{177}Lu-PSMA treatment an improved bone marrow function or recovery was reported and no blood transfusions were needed afterwards (39). The second case was a patient with hormone refractory PCa metastases, who was treated with two cycles of ^{177}Lu-PSMA under growth hormone releasing hormone (GHRH) analogues resulting in a partial response. Afterwards the patient continued GHRH analogues, had a continuing PSA decrease and imaging response on ^{68}Ga-PSMA-HBED-CC PET/CT. The authors stated that ^{177}Lu-PSMA could have a long term response, or the PCa metastases might have become hormone sensitive again (40). Upregulation of PSMA on the neovasculature of several other human solid malignancies has been described in multiple case reports. So the use of ^{177}Lu-PSMA might not be limited to PCa. This is especially interesting and valuable in tumours in which the current treatment options are limited.
As stated by Pfestroff et al., we as nuclear medicine physicians in Europe have the opportunity to collaborate with urologists in conducting early well-designed studies (13). But instead of being a salvage therapy, a more upfront role of ^{177}Lu-PSMA could be advantageous. Proper prospective randomised controlled trials comparing ^{177}Lu-PSMA to, or combining ^{177}Lu-PSMA with (first-/second-line) chemotherapy or ^{223}Ra-chloride (in patients with bone-limited disease) are needed.

Conclusion

Although additional research and prospective studies are needed, initial results on ^{177}Lu-PSMA therapy are very promising with high response rates and a limited toxicity profile.

a.j.a.t.braat@umcutrecht.nl

References

1. Jemal A, Siegel R, Xu J, Ward E. Cancer statistics, 2010. CA Cancer J Clin. 2010;60:277-300
2. Morris MJ, Molina A, Small EJ, et al. Radiographic progression-free survival as a response biomarker in metastatic castration-resistant prostate cancer: COU-AA-302 results. J Clin Oncol. 2015;33:1356-63
3. Ramadan WH, , Kabbara WK, Al Basiouni, Al Masri HS. Enzalutamide for patients with metastatic castration-resistant prostate cancer. Onco Targets Ther. 2015;17:871-6
4. Parker C, Nilsson S, Heinrich D, et al. Alpha emitter radium-223 and survival in metastatic prostate cancer. N Engl J Med. 2013;369:213-23
5. Ross AE, Loeb S, Landis P, et al. Prostate-specific antigen kinetics during follow-up are an unreliable trigger for intervention in a prostate cancer surveillance program. J Clin Oncol. 2010;28:2810-6
6. Lees K, Durve M, Parker C. Active surveillance in prostate cancer: patient selection and triggers for intervention. Curr Opin Urol. 2012;22:210-5
7. Loblaw A, Zhang L, Lam A, et al. Comparing prostate specific antigen triggers for intervention in men with stable prostate cancer on active surveillance. J Urol. 2010;184:1942-6
8. Fall K, Garmo H, Andrén O, et al. Prostate-specific antigen levels as a predictor of lethal prostate cancer. J Natl Cancer Inst. 2007;99:526-32
9. Umbehr MH, Müntener M, Hany T, et al. The role of 11C-choline and 18F-fluorocholine positron emission tomography (PET) and PET/CT in prostate cancer: a systematic review and meta-analysis. Eur Urol. 2013;64:106-17
10. Bauman G, Belhocine T, Kovacs M, et al. 18F-fluorocholine for prostate cancer imaging: a systematic review of the literature. Prostate Cancer Prostatic Dis. 2012;15:45-55
11. Haberkorn U, Eder M, Kopka K, Babich JW, Eisenhut M. New Strategies in Prostate Cancer: Prostate-Specific Membrane Antigen (PSMA) Ligands for Diagnosis and Therapy. Clin Cancer Res. 2016;22:9-15
12. Banerjee SR, Pullambhatla M, Byun Y, et al. 68Ga-labeled inhibitors of prostate-specific membrane antigen (PSMA) for imaging prostate cancer. J Med Chem. 2010;53:5333-41
13. Pfestroff A, Luster M, Jilg CA, et al. Current status and future perspectives of PSMA-targeted therapy in Europe: opportunity knocks. Eur J Nucl Med Mol Imaging. 2015;42:1971-5
14. Eiber M, Maurer T, Souvatzoglou M, et al. Evaluation of Hybrid 68Ga-PSMA Ligand PET/CT in 248 Patients with Biochemical Recurrence After Radical Prostatectomy. J Nucl Med. 2015;56:668-74

15. Giesel FL, Fiedler H, Stefanova M, et al. PSMA PET/CT with Glu-urea-Lys-(Ahx)-[68Ga(HBED-CC)] versus 3D CT volumetric lymph node assessment in recurrent prostate cancer. Eur J Nucl Med Mol Imaging. 2015;42:1794-1800
16. Morigi JJ, Stricker PD, van Leeuwen PJ, et al. Prospective Comparison of 18F-Fluoromethylcholine Versus 68Ga-PSMA PET/CT in Prostate Cancer Patients Who Have Rising PSA After Curative Treatment and Are Being Considered for Targeted Therapy. J Nucl Med. 2015;56:1185-90
17. Hijazi S, Meller B, Leitsmann C, et al. Pelvic lymph node dissection for nodal oligometastatic prostate cancer detected by 68Ga-PSMA-positron emission tomography/computerized tomography. Prostate. 2015;75:1934-40
18. Shakespeare TP. Effect of prostate-specific membrane antigen positron emission tomography on the decision-making of radiation oncologists. Radiat Oncol. 2015;10:233
19. Sterzing F, Kratochwil C, Fiedler H, et al. (68)Ga-PSMA-11 PET/CT: a new technique with high potential for the radiotherapeutic management of prostate cancer patients. Eur J Nucl Med Mol Imaging. 2016;43:34-41
20. Deb N, Goris M, Trisler K, et al. Treatment of hormone-refractory prostate cancer with 90Y-CYT-356 monoclonal antibody. Clin Cancer Res. 1996;2:1289-97
21. Zechmann CM, Afshar-Oromieh A, Armor T, et al. Radiation dosimetry and first therapy results with a (124)I/ (131)I-labeled small molecule (MIP-1095) targeting PSMA for prostate cancer therapy. Eur J Nucl Med Mol Imaging. 2014;41:1280-92
22. Ahmadzadehfar H, Rahbar K, Kürpig S, et al. Early side effects and first results of radioligand therapy with (177)Lu-DKFZ-617 PSMA of castrate-resistant metastatic prostate cancer: a two-centre study. EJNMMI Res. 2015;5:114
23. Ahmadzadehfar H, Eppard E, Kürpig S, et al. Therapeutic response and side effects of repeated radioligand therapy with 177Lu-PSMA-DKFZ-617 of castrate-resistant metastatic prostate cancer. Oncotarget. 2016;7:12477-88
24. Baum RP, Kulkarni HR, Schuchardt C, et al. Lutetium-177 PSMA Radioligand Therapy of Metastatic Castration-Resistant Prostate Cancer: Safety and Efficacy. J Nucl Med. 2016;57:1006-13
25. Heck MM, Retz M, D Alessandria C, et al. Systemic radioligand therapy with 177Lu-PSMA-I&T in patients with metastatic castration-resistant prostate cancer. J Urol. 2016;[Epub ahead of print]
26. Kratochwil C, Giesel FL, Stefanova M, et al. PSMA-targeted radionuclide therapy of metastatic castration-resistant prostate cancer with Lu-177 labeled PSMA-617. J Nucl Med. 2016;[Epub ahead of print]
27. Kambiz Rahbar, Axel Bode, Matthias Weckesser, et al. Radioligand Therapy with 177Lu-PSMA-617 as a novel Therapeutic Option in Patients with Metastatic Castration Resistant Prostate Cancer. Clin Nucl Med. 2016;[Epub ahead of print]
28. Tagawa ST, Milowsky MI, Morris M, et al. Phase II study of Lutetium-177-labeled anti-prostate-specific membrane antigen monoclonal antibody J591 for metastatic castration-resistant prostate cancer. Clin Cancer Res. 2013;19:5182-91
29. Vallabhajosula S, Goldsmith SJ, Kostakoglu L, et al. Radioimmunotherapy of prostate cancer using 90Y- and 177Lu-labeled J591 monoclonal antibodies: effect of multiple treatments on myelotoxicity. Clin Cancer Res. 2005;11:7195s-7200s
30. Vallabhajosula S, Goldsmith SJ, Hamacher KA, et al. Prediction of myelotoxicity based on bone marrow radiation-absorbed dose: radioimmunotherapy studies using 90Y- and 177Lu-labeled J591 antibodies specific for prostate-specific membrane antigen. J Nucl Med. 2005;46:850-8
31. Kratochwil C, Giesel FL, Eder M, et al. [177Lu]Lutetium-labelled PSMA ligand-induced remission in a patient with metastatic prostate cancer. Eur J Nucl Med Mol Imaging. 2015;42:987-8
32. Weineisen M, Schottelius M,, Simecek J, et al. 68Ga- and 177Lu-Labeled PSMA I&T: Optimization of a PSMA-Targeted Theranostic Concept and First Proof-of-Concept Human Studies. J Nucl Med. 2015;56:1169-76
33. Schottelius M, Wirtz M, Eiber M, et al. [(111)In]PSMA-I&T: expanding the spectrum of PSMA-I&T applications towards SPECT and radioguided surgery. EJNMMI Res. 2015;5:68
34. Gaertner FC, Ahmadzadehfar H, Bundschuh RA, Kürpig S, Eppard E, Essler M. Does cooling of the salivary glands reduce uptake of radiolabeled PSMA-ligands? In: EAMN 2015; 2015
35. Delker A, Fendler WP, Kratochwil C, et al. Dosimetry for (177)Lu-DKFZ-PSMA-617: a new radiopharmaceutical for the treatment of metastatic prostate cancer. Eur J Nucl Med Mol Imaging. 2016;43:42-51
36. Svensson J, Berg G, Wängberg B, Larsson M, Forssell-Aronsson E, Bernhardt P. Renal function affects absorbed dose to the kidneys and haematological toxicity during 177Lu-DOTATATE treatment. Eur J Nucl Med Mol Imaging. 2015;42:947-55
37. Hohberg M, Eschner W, Schmidt M, et al. Lacrimal Glands May Represent Organs at Risk for Radionuclide Therapy of Prostate Cancer with [177Lu]DKFZ-PSMA-617. Mol Imaging Biol. 2016;18:437-45
38. Kratochwil C, Giesel FL, Leotta K, et al. PMPA for nephroprotection in PSMA-targeted radionuclide therapy of prostate cancer. J Nucl Med. 2015;56:293-8
39. Schlenkhoff CD, Gaertner F, Essler M, Schmidt M, Ahmadzadehfar H. Positive Influence of 177Lu PSMA-617 Therapy on Bone Marrow Depression Caused by Metastatic Prostate Cancer. Clin Nucl Med. 2016;41:478-80
40. Schlenkhoff CD, Knüpfer E, Essler M, Ahmadzadehfar H. Metastatic Prostate Cancer With Restored Hormone-Response After Radioligand Therapy With 177Lu-PSMA-617. Clin Nucl Med. 2016;41:572-3

Peptide receptor radionuclide therapy for neuroendocrine tumours

D.A. Smit Duijzentkunst, MD; J.J.M. Teunissen, MD, PhD; B.L.R. Kam, MD; Prof. D.J. Kwekkeboom, MD

Department of Nuclear Medicine, Erasmus Medical Centre, Rotterdam, the Netherlands

Abstract

Smit Duijzentkunst DA, Teunissen JJM, Kam BLR, Kwekkeboom DJ. Peptide receptor radionuclide therapy for neuroendocrine tumours. Neuroendocrine tumours have a low incidence and generally a slow growing pattern. With distant metastases frequently being present at presentation or developed in follow up, there is need for a systemic, and preferably targeted, approach. Most neuroendocrine tumours express high levels of somatostatin receptors. Radiolabelled somatostatin analogues have been developed for targeted imaging and therapy. The two most applied radiopharmaceuticals for therapy are ^{90}Y-DOTATOC and ^{177}Lu-DOTATATE. With fractionated administration, disease control rates up to 95% have been reported. Along with objective response, both increased survival and improved quality of life are the most important outcomes that have been reported. Subacute toxicity to the kidneys and bone marrow is usually mild and self-limiting. Long-term adverse events, myelodysplastic syndrome and acute leukaemia, are reported in up to 2-3% of patients; an annual decrease in renal function is observed but renal failure is rare. Peptide receptor radionuclide therapy offers an effective and safe therapeutic option for patients with inoperable and/or metastatic neuroendocrine tumours and can be used in the treatment algorithm, on its own, combined with additional therapies, and in the neo-adjuvant and salvage setting.
Tijdschr Nucl Geneesk 2016; 38(4):1635-1644

Introduction

Neuroendocrine tumours (NETs) can arise throughout the body and originate most often in the digestive tract and lungs. Although all called NETs, the primary site of origin is important in diagnosis, therapy and prognosis. Often thought of as rare tumours, the relatively slow-growing nature of NETs and relatively good prognosis make it the second most prevalent gastrointestinal tumour (1). A large observational study estimated the incidence to be 5.25/100.000/y and the prevalence to be 35/100.000 in 2004 in the USA, and these figures are presumed rising since (1-3). In the Netherlands, the incidence increased from 2.1/100.000/y in 1990 to 4.9 in 2010 (excluding high grade small cell NETs)(4). According to the WHO classification of 2010, NETs are currently graded upon mitotic rate (mitoses per 10 high power fields (HPF)) and Ki67 index (percentage of cells that show immunohistochemical signs of proliferation) (5). Grade 1 (G1) (< 2 mitoses / 10 HPF, Ki67 < 2%) and G2 (3-20 mitoses / 10 HPF, Ki67 3-20%) NETs are considered a separate entity from G3 (> 20 mitoses /10 HPF, Ki67 > 20%) tumours, deemed neuroendocrine carcinomas (NECs). However, more recent insights show significant heterogeneity in G3 tumours, in which there can be a discordance in mitotic rate and Ki67 index. Relatively well-differentiated tumours with relatively lower mitotic rate than Ki67 index are thought to have a better prognosis than poorly differentiated NECs that show a high mitotic rate (6).
NETs can be hormonally active and the excessive hormonal secretion can cause a variety of symptoms, based on the type of hormone produced (e.g. serotonin, gastrin, insulin). The typical symptoms of the carcinoid syndrome (referring to the initial name for NETs coined by Oberndorfer in 1907: 'karzinoid') are among others flushing, diarrhoea and bronchospasm, which are often attributed to menopause, irritable bowel disease and asthma, and thereby delaying the initial diagnosis. If not hormonally active, NETs can present with symptoms due to local growth and development of metastases. At diagnosis, 21-30% of NETs present with distant metastases, as do 50% of the NECs, however this may be an underestimation due to inadequate diagnostic testing (1). In a population-based cohort study, 21% of NET patients had metastatic disease at diagnosis, and this increased to 38% during follow up (2). Metastases are most often found in regional lymph nodes and the liver (7). Metastatic spread limits therapeutic options, with surgery being the only potentially curative treatment (8). For pancreatic NETs and NECs, chemotherapy is being prescribed using mostly platinum-based or alkalizing agents. More targeted therapies (e.g. everolimus, sunitinib) are being approved for NETs from various origins (9). For most NETs, treatment with somatostatin analogues (SSA) (e.g. octreotide) is prescribed as first line treatment (7). In addition to a minor cytostatic effect, SSAs can significantly decrease hormonally induced symptoms (10,11).

One of the major breakthroughs in the therapeutic management of metastatic or inoperable NETs in the past decades has been the development of peptide receptor radionuclide therapy (PRRT). This technique uses the overexpression of somatostatin receptors (SSTRs), a characteristic that is very specific to NETs, to target tumour

cells. Linking a radionuclide to an SSA, this radiopharmaceutical is internalised by the transmembrane protein, facilitating internal irradiation in highly specific target locations. This review intends to give an oversight of the clinical use and the current evidence for the efficacy and safety of PRRT.

Principle of tumour targeting

Development and first use

The technique of tumour targeting with radionuclide-labelled SSAs was first applied in the late 1980's using ^{123}I-Tyr^{3}-octreotide for scintigraphic localisation of NETs (12). Soon thereafter a switch was made to ^{111}In-diethylenetriamine pentaacetic acid^{0}-octreotide (^{111}In-octreotide) for use in imaging and since 1992 in therapy at Erasmus MC Rotterdam, using the Auger and conversion electron emission of the radionuclide (12,13). At that time, it was understood that an alpha or beta emitting radionuclide would have more favourable physical characteristics for use in therapy, but these were not available until later that decade. With the development of the chelator 1,4,7,10-tetraazacyclotetradecane-1,4,7,10-tetraacetic acid (DOTA), SSAs could be linked to beta emitters. In human NETs, there are five SSTR subtypes found, with SSTR2 being the predominant subtype (14,15). With modification of the SSA octreotide into octreotate (threonine substitutes C-terminal threoninol), a nine-fold higher affinity for SSTR2 was achieved (16,17). The most frequently used radiolabelled SSAs ^{90}Y-DOTA^{0},Tyr^{3}-octreotide and ^{177}Lu-DOTA^{0},Tyr^{3}-octreotate are also known as ^{90}Y-DOTATOC and ^{177}Lu-DOTATATE, respectively.

Yttrium-90 is a pure beta emitter with a half-life of 2.7 days, decay energy of 2.28 MeV and a maximum tissue penetration of 12 mm. Contrary, Lutetium-177 emits both beta- particles (half-life 6.7 days, decay energy 0.5 MeV, maximum tissue penetration 2 mm) and gamma rays. The advantage is that post-therapy scintigraphy for target evaluation and dosimetry can be performed using the therapeutic dose (see figure), as opposed to the use of yttrium-90, that relies on a small dose of indium-111 added in the labelling process for intra-therapeutic imaging. In large, heterogeneous tumours, yttrium-90 is more likely to irradiate both SSTR-positive and more surrounding SSTR-negative tumour cells. Lutetium-177 on the other hand would theoretically be more advantageous to treat small tumours (18).

Uptake assessment and imaging

The radiation dose to the tumour is partially dependent on the radiopharmaceutical being used, but more importantly on the level of expression of SSTRs on the tumour cell membrane, a characteristic that is assessed using ^{111}In-octreotide planar and single photon emission computed tomography (SPECT) imaging or ^{68}Ga-SSA positron emitting tomography (PET). For diagnostic purposes, both modalities are combined with low- or full-dose computed tomography (CT) to enhance diagnostic accuracy. Originally, tracer uptake was scored as follows: tumour uptake less than (grade 1), equal to (grade 2) or higher than (grade 3) uptake in physiological liver tissue, or higher than uptake in kidneys/spleen (grade 4), assessed visually on planar scintigraphic images (Krenning score). The Krenning score has shown to be an independent predictor for objective response in multivariable analysis (19). With ^{68}Ga-SSA PET, lacking planar imaging, the standardised uptake value (SUV) can be used. PRRT is thought to be feasible when tumour uptake is at least equal to uptake in liver tissue (grade 2). Although treatment outcome using a ^{68}Ga-SSA based selection method prior to PRRT has not been studied, the correlation of the amount of uptake according the SUV and achieved absorbed dose with PRRT suggests that this approach of selecting the appropriate candidates for PRRT is reliable (20).

Recent developments have led to a shift in imaging, replacing ^{111}In-octreotide-based SPECT/CT and establishing ^{68}Ga-SSA-based PET/CT as the dominant modality for diagnostics and staging. Studies show superior diagnostic accuracy for ^{68}Ga-SSA PET/CT scans, and sensitivity and specificity are estimated

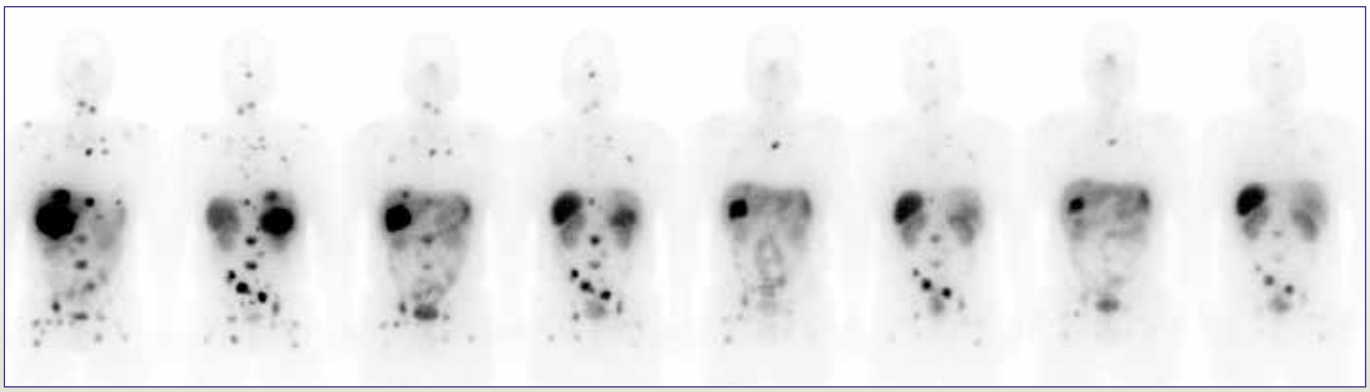

Uptake and response. From left to right anterior and posterior planar post-therapy scintigraphy images using the therapeutic dose, results 24-hours after each administration of 7.4 GBq ^{177}Lu-DOTATATE with 8 week intervals in a patient with metastatic pancreatic NEC (Ki67: 25%). Note the decrease in number of metastatic laesions and decrease uptake indicating a favourable response.

to be around 90%, according to a recent systematic review (21-24). With ^{68}Ga-SSA PET/CT, interobserver variability is very low, but assessment of the viability of PRRT showed to be more difficult; a higher rate of false positive recommendations for PRRT was observed in less experienced assessors (25). Furthermore, PET imaging offers greater patient convenience, because the scans can be performed between 45 and 90 minutes after tracer administration, as opposed to 4, 24 and 48 hours for planar and SPECT imaging. However, it is important to note that both modalities are frequently inadequate to assess high grade tumours (G3), since the majority of these tumours do not express (sufficient) SSTRs (26,27). Hence, PRRT is predominantly used in G1 and G2 NETs. To illustrate the exceptions, the figure shows planar post-therapy scintigraphy images in a patient with G3 (Ki67: 25%) pancreatic NEC with high tumour uptake.

Efficacy

Tumour response

Starting this technique with ^{111}In-octreotide, results from Rotterdam in the 1990's were encouraging. Their largest case series report on 40 patients with at least grade 2 tumour uptake and evaluable results after fractionated administration of 20-160 GBq (28). One (2.5%) patient showed partial remission (PR) and 20 (50%) patients with previously progressive disease showed stable disease (SD).

The first, very early phase II trials using ^{90}Y-DOTATOC provided supportive results. In 2001, Waldherr et al. reported on 41 patients with predominantly (83%) progressive NETs (of which 71% gastroenteropancreatic (GEP) or bronchial) that were treated with a total of 6 GBq ^{90}Y-DOTATOC in a dose escalation schedule, resulting in disease control rate (complete remission (CR) + PR + SD) of 85% (respectively 2% + 22% + 61%)(29). One year later, this group published results of a second phase II trial, in which 39 patients with progressive NETs (of which 72% GEP/bronchial NET) received four cycles with a total of 7.2GBq/m^2 ^{90}Y-DOTATOC; the disease control rate was 92% (5% CR + 18% PR + 69% SD)(30). The first results of PRRT using ^{177}Lu-DOTATATE in a large cohort were published in 2005 and again with additional patients in 2008 (31). Table 1a shows an overview of clinical trials, limited to populations greater than fifty patients.

The largest series of tumours stratified by origin are found in the study of Imhof et al. (32). In 295 non-functioning (i.e. without hormonal hypersecretion) pancreatic (P) NETs, morphological response (any reduction in the sum of all pre-therapeutic lesions' longest diameters) was 49.2%, in 265 small bowel NETs, morphological response was 26.8%. It should be noted that patients in this cohort were treated with a relatively low dose ^{90}Y-DOTATOC and the overall disease control rate was 40%, far lower than in other studies.

Quality of life

In addition to tumour size, PRRT can have an effect on quality of life. By reducing disease activity and hormone hypersecretion, it can alleviate symptoms like fatigue, pain and diarrhoea. In a group of 265 patients with metastatic or inoperable NETs, receiving 22.2-29.6 GBq ^{177}Lu-DOTATATE (completed by 241/265), European Organisation for Research and Treatment of Cancer quality of life questionnaire scores were prospectively registered, measuring global health status/quality of life (GHS/QoL), several symptoms and several domains of functioning (33). Independent of tumour response, there was an increase in GHS/QoL, emotional and social functioning and a decrease of insomnia, appetite loss and diarrhoea. In patients who reported decreased GHS/QoL at baseline, clinically relevant improvements were seen in 36%, in patients who reported fatigue, in 49%; for nausea/vomiting, in 70%; for pain, in 53%; for dyspnoea, in 44%; for insomnia, in 59%; for appetite loss, in 63%; for constipation in 60%; and for diarrhoea in 67% (34).

Prognostic factors for survival

Results on progression free survival (PFS) and overall survival (OS) are shown in table 1. Several studies have crudely tried to identify factors that predict response and survival. The largest series of patients used for prediction modelling consists of 1109 patients with NETs of mixed origin treated with ^{90}Y-DOTATOC (32). With a total of 491 deaths and median follow-up of 23 months, multivariable analysis showed overall survival benefit for: younger patients; with no previous surgery; no previous chemotherapy; no liver or bone metastases; tumour uptake score grade 3 (versus grade 1) and with tumour response.

Kwekkeboom et al. analysed overall and disease-specific survival in 310 patients (81 deaths, median follow-up 18 months) treated with ^{177}Lu-DOTATATE (31). In multivariable analysis, there were six independent factors influencing survival: treatment outcome, liver involvement, Karnofsky performance index (< 70%), baseline weight loss, bone metastases and tumour type (with shorter survival for gastrinoma, insulinoma and VIPoma). Tumour uptake score was not statistically confirmed as an independent predictor in this study, most likely because 75% of the patients had grade 3 tumour uptake (versus 23% grade 4, only 2% grade 2 and no grade 1).

Toxicity

(Sub)acute toxicity

Acute and subacute side effects of PRRT are generally mild. Nausea and vomiting are mostly related to the co-infusion of amino acids, administered for renal protection. Other side effects are fatigue, mild hair loss and mild abdominal pain. Toxicity to the bone marrow is usually self-limiting. Platelets and white blood cells are most often affected, with the nadir to be expected 4-6 weeks after each therapy. Large series report grade 3/4 haematotoxicity in 3.1-11.3% for ^{177}Lu-DOTATATE and in 12.8-14.2% for ^{90}Y-DOTATOC (table 2). In general, blood counts restore within 3-6 months after treatment

Table 1a. Clinical trials using ^{90}Y and/or ^{177}Lu-labelled somatostatin analogues.

first author	year	radio-pharmaceutical	schedule	n	tumour type	baseline PD (%)	CR (%)	PR (%)	SD (%)	DCR (%)	PD (%)	n.a. (%)	response	FU (months)	survival (median) (months)
Valkema (74)	2006	^{90}Y-DOTATOC	8.2-14.9 GBq in 4 cy	58	GEP	81	0	9	62	71	24	5	SWOG	n.a.	PFS 14.3, OS 36.7
Forrer (75)	2006	^{90}Y-DOTATOC	6.1-7.4 GBq/m^2 in 2-4 cy	116	NET	94	4	23	62	89	11	-	WHO	n.a.	n.a.
Bushnell (76)	2010	^{90}Y- DOTATOC	4.4 GBq x 3 cy	90	GEP+B	100	0	4	70	74	12	14	SWOG	n.a.	PFS 16.3, OS 26.9
Cwikla (77)	2010	^{90}Y-DOTATATE	mean 11.2 GBq, 3.7 GBq/cy	60	GEP	100	0	22	73	95	5	-	RECIST	n.a.	PFS 17, OS 22 ▲
Pfeifer(78)	2011	^{90}Y-DOTATOC	9.6-15.5 GBq in 2cy	53	NET	61	4	19	64	87	11	2	RECIST	17 •	PFS 29, OS n.r.
Imhof (32)	2011	^{90}Y- DOTATOC	3.7 GBq/m^2 x 2 (1-10) cy	1109	SSTR+	100	1	34	5	40	60*	0	other	23 ◦	n.a.
Kwekkeboom (31)	2008	^{177}Lu-DOTATATE	27.8-29.6 GBq in 4 cy	310	GEP	43	2	28	51	81	20 △	-	SWOG	19 ◦	PFS 33, OS 46
Bodei(79)	2011	^{177}Lu-DOTATATE	25.2-26.4 GBq in 4-6 cy	51	SSTR+	76	2	27	53	82	18	-	RECIST	29 ◦	TTP 36, OS n.r.
Sansovini (80)	2013	^{177}Lu-DOTATATE	17.8-25.5 GBq in 5 cy	51	p	100	8	21	52	81	19	-	SWOG	n.a.	PFS 29, OS n.r.
Ezziddin (81)	2014	^{177}Lu-DOTATATE	8 GBq x 4 cy	68	P	67	0	60	25	85	15	-	SWOG	58 ◦	PFS 34, OS 53
Sabet (82)	2015	^{177}Lu-DOTATATE	mean 27.2 GBq in 4 cy	61	SI	75	0	13	79	92	8	-	SWOG	62 ◦	PFS 33, OS 61
Baum (83)	2016	^{177}Lu-DOTATOC	7.0 GBq x 1-4 cy	56	NET	100	16	18	32	66	34	-	RECIST	16 •	PFS 17.4, OS 34.2

Table 1b. Clinical trials combining PRRT with other treatment modalities.

Claringbold (53)	2011	7.8 GBq ^{177}Lu-DOTATATE+ capecitabine (1650mg/m^2 x 14 days) x 4 cy	33	NET	100	0	24	70	94	6	-	RECIST	16	PFS n.r., OS n.r.
Claringbold (54)	2012	7.8 GBq ^{177}Lu-DOTATATEt + capecitabine (1500mg/m^2 x 14 days) + temozolomide (100-200mg/m^2 x 5 days) x 4 cy	34	GEP+B	100	15	38	38	91	9	-	RECIST	18	PFS 31, OS n.r.
Kong (84) ▲	2014	31 GBq ^{177}Lu-DOTATATE in 4 cy + 5-FU (200mg/m^2 x 25 days) x 3 cy	68	NET	85	0	30	37,5	67,5	32,5*	-	RECIST	60	PFS n.a., OS n.r.
Claringbold (85)	2015	7.8 GBq ^{177}Lu-DOTATATE x 4 cy + everolimus 5-10mg daily for 24 weeks	16	GEP	100	0	44	50	94	0	6	RECIST	34	PFS n.a., OS n.r.

year – year of publication; n - number of patients; PD - progressive disease; CR - complete response; PR - partial response; SD - stable disease; DCR - disease control rate (CR + PR + SD); n.a. - not available/assessable; FU - follow-up; cy - cycles; GEP - gastroenteropancreatic; NET - (all) neuroendocrine tumours; B - bronchial; SSRT+ - (all) somatostatin receptor positive tumours; SI - small intestine; SWOG - Southwest Oncology Group Criteria; WHO - World Health Organisation Criteria; RECIST - Response Evaluation Criteria In Solid Tumours; PFS - progression free survival; OS - overall survival; TTP - time to progression; n.r. - not reached

*including n=1 mixed response; ▲in 57/60 (3 deaths during trail due to progression); △cumulative 101% due to rounding of; • mean; ◦ median

(31,32,35). The most commonly found predictors for subacute haematotoxicity are poor renal function, low blood cell counts at baseline and previous chemotherapy (32,35-38). Long-term adverse events relate mainly to the kidneys and the bone marrow.

Long-term nephrotoxicity

It is known that PRRT can lead to a yearly decline of renal function due to radiation damage. In radiotherapy, the maximal dose to the kidneys is considered to be 23 Gy. In developing PRRT regimens, this, along with a maximal dose of 2 Gy to the bone marrow, were the dose limiting factors. An important part of the dose to the kidneys is due to reabsorption of the radiolabelled peptide in the proximal tubule cells. This can partially be prevented by co-infusion of positively charged amino acids (39-42). A combination of lysine and arginine has shown to be safe and effective, resulting in a dose reduction of up to 40%, allowing for escalation of administered activity. In a cohort of 42 patients treated with ^{90}Y-DOTATOC without this co-infusion, performed before 1999, Bodei et al. reported

60% nephrotoxicity (any grade), of which 45% was persistent (35). This compares poorly to the post-1999 cohort treated with the amino-acid co-infusion, which showed 33.2% nephrotoxicity (any grade), of which 23.1% was persistent ($p<0.002$). Currently, the use of amino acids is standard of care and implemented in all guidelines (43). The most commonly found risk factors for nephrotoxicity are old age, hypertension, diabetes mellitus, high renal dose, impaired renal function at baseline and previous chemotherapy (32,35,44-47).

In 209 patients treated with ^{177}Lu-DOTATATE, long-term (> 1 year) renal function was assessed using baseline 24-hour urine creatinine clearance (CrCl) and subsequent glomerular filtration rate estimation (eGFR) using the Cockcroft-Gault formula (48). The average annual decrease in CrCl was estimated to be 3.4±0.4%. Out of 208 patients, 5 (2.4%) showed an annual decrease in CrCl > 10%. Remarkably, no independent risk factor could be identified in this study. Overall, severe and persisting renal toxicity is considered to be rare (see also table 2).

Long-term myelotoxicity

A known risk of PRRT is the induction of secondary myelodysplastic syndrome (MDS) and acute leukaemia (AL), occurring in 1-2% and <1% of patients, respectively (see also table 2). These events are considered stochastic and are observed at least two years after PRRT (38). A recent comprehensive review identified several risk factors associated with MDS/AL, most importantly previous use of chemotherapy, especially with alkalizing agents. An unusual high incidence was reported by Brieau et al. (49). In 20 patients, heavily pre-treated with alkalizing chemotherapeutic agents and receiving ^{177}Lu-DOTATATE (intended dose 22.2-29.6 GBq), 3 (15%) patients developed MDS and one (5%) patient developed AL. These patients were pre-treated with 6-20 cycles chemotherapy with alkalizing agents; the high incidence of this alarming effect most likely reflects the natural course after treatment with myelotoxic chemotherapies. Therefore, PRRT should preferably be given prior to these therapies or at the point no alternative therapeutic option is left.

Alternative PRRT strategies

Choice of radionuclide and individualised treatment

Protocols comparing and/or combining ^{90}Y-DOTATOC and ^{177}Lu-DOTATATE have been proposed and described in retrospective case series. Mariniello et al. compared patients with bronchial NETs treated with ^{177}Lu-DOTATATE (n=48), ^{90}Y-DOTATOC (n=45) or a combination (n=21) (44). The authors conclude that in terms of both survival and toxicity ^{177}Lu-DOTATATE monotherapy seems the best option. Bodei et al. reported lower rates of both haemato- and nephrotoxicity for patients treated with ^{177}Lu-DOTATATE (n=278) compared to patients treated with a combination (n=157), which had lower toxicity rates compared to patients treated with ^{90}Y-DOTATOC (n=358) as well. (see table 2)(35). Choosing an individualised approach, Gabriel et al. reported on an algorithm that takes into account the uptake on ^{68}Ga-DOTATOC PET/CT: if positive, treatment is performed with ^{90}Y-DOTATOC or ^{177}Lu-DOTATATE depending on tumour size; if negative ^{68}Ga-DOTALAN PET/CT is used and, if positive, treatment with ^{90}Y-DOTALAN is performed; both with treatment schedules that take into account presumed risk factors (50). However, in each of the studies comparing radiolabelled SSAs the difficulty lies in that 1) selection criteria were either not specified or 2) choice of treatment was based on clinical factors (e.g. tumour diameter, disease extent, renal function) and 3) independent effects were not assessed in proper multivariable models, making the comparison between ^{90}Y-DOTATOC and ^{177}Lu-DOTATATE hard to interpret (35,44,51,52). The benefits of either radiopharmaceutical are still to be determined in a randomised trial.

Concomitant chemotherapy

Based on experiences in oncology and external beam radiotherapy, several groups have studied the efficacy and safety of PRRT combined with chemotherapy. Efficacy results are shown in table 1b. The combination of PRRT with the radiosensitizing drugs 5-fluorouracil or its pro-drug capecitabine have not shown evident survival benefit in small patient series (53,54). In 65 patients treated with ^{177}Lu-DOTATATE combined with capecitabine (n=28) or capecitabine/temozolomide(n=37), haematological toxicity was mild and mostly reversible, MDS occurred in 2 (3%) of patients (median follow-up 60 months), suggesting this strategy can be adopted for larger, randomised trials.

Salvage therapy

For patients who initially had benefit from PRRT (i.e. significant and lasting clinical, biochemical and/or radiological response), salvage treatment can be considered in case of disease progression. The effects of ^{177}Lu-based PRRT after prior treatment with either ^{90}Y-DOTATOC or ^{177}Lu-DOTATATE were presented in four articles (55-58). In all studies, patients had benefit from primary PRRT, had progressive disease at the time of salvage treatment and had tumour uptake score > 2 on SSTR scintigraphy. Pooled data from 119 patients showed PR in 11%, SD in 49% and PD in 40% of patients. Interestingly, Forrer et al.(55), administering an additional 7.4 GBq, and Sabet et al., administering an additional median 17.7 GBq, both reach a disease control rate of around 70% (57). Toxicity rates are in line with primary treatment and no cases of MDS/AL have been reported, however, only one article reported a median follow-up of more than 24 months (58). Predictors commonly associated with benefit from salvage treatment are prolonged time to progression after the initial PRRT cycles and better radiographic response after initial PRRT.

Intra-arterial administration to the liver

The most frequent location for distant metastases of NETs is the liver (7). Furthermore, liver failure is one of the most common causes of death in end-stage NET disease, making

Table 2. Toxicity.

first author	year	radiopharmaceutical	n	FU	renal toxicity	haematoxicity	MDS	AL
Imhof (32)	2011	^{90}Y-DOTATOC	1109	23	9.2% G4/5 v3	12.8% G3/4 v3	0.1%	0.1%
Bodei (35)	2015	^{90}Y-DOTATOC	358	30	2.8% G3/4 v4	3.1% G3/4 v4	2.1%*	0.7%*
Kwekkeboom (31)	2008	^{177}Lu-DOTATATE	504	19	0.4% G3/4 WHO	9.5% G3/4 WHO	0.8%	0%
Sabet (86)	2013	^{177}Lu-DOTATATE	203	31	n.a.	11.3% G3/4 v4	1.4%	0%
Bodei (35)	2015	^{177}Lu-DOTATATE	278	30	0% G3/4 v4	14.2% G3/4 v4	2.0%*	1.4%*

year - year of publication; n - number of patients; FU - median follow up (months); haematoxicity - in % of patients; MDS - myelodysplastic syndrome; AL - acute leukaemia; G - Grade; v3/v4 - version of Common Terminology Criteria for Adverse Events; WHO - World Health Organisation; n.a. – not available
*stratified figures derived from Bodei et al. 2016 (87)

the liver a logical target of cytoreductive therapy. Several groups have experimented with intra-arterial administration of radiolabelled SSAs, which shows a high first-pass effect. Limouris et al. reported higher success rates with intra-arterial ^{111}In-octreotide treatments compared to intravenous ^{111}In-octreotide treatments, the latter of which had shown rather limited results (59). Kratochwil et al. reported a (mean) 3.75-fold higher uptake of ^{68}Ga-DOTATOC with selective intra-arterial administration compared to intravenous administration (60). At a later stage, after their switch to beta emitting radionuclides in PRRT, this group performed a pilot study in fifteen patients with progressive, abdominally confined GEP-NETs which resulted in CR in 7% (n=1), PR in 53%, and SD in 40% (61). No patients had PD during treatment, three (20%) patients showed disease progression during follow-up (median: 20 months). In this study, ^{90}Y was used for metastases > 2 cm in diameter, ^{177}Lu for metastases < 2 cm in diameter and a mix for patients with heterogeneous lesions. These optimistic results have not yet been confirmed in a randomised trial, but seem promising for patients with disease confined to the liver. A somewhat different approach is currently studied in the Netherlands, in which patients with disease predominantly restricted to the liver receive 166-holmium radioembolisation additional to previous treatment with four cycles of 7.4 GBq ^{177}Lu-DOTATATE (62).

Neo-adjuvant treatment

With surgery being the only treatment with curative intent, PRRT is also applied in a neo-adjuvant setting. Although objective, radiographical response is rather limited in many trials, successful pre-surgical tumour size reduction has been described in several case reports and series (63,64). In a group of 29 patients with borderline or unresectable non-functioning P-NETS, localised or with < 3 liver metastases, successful surgery was performed in 9 (31%) (65). In these patients receiving successful surgery, median PFS was 69 months, versus 49 months in the other 20 patients. The neo-adjuvant use of PRRT can be very beneficial and careful selection of patients may increase the fraction of patients qualifying for surgery after neo-adjuvant PRRT.

PRRT for other SSTR positive diseases

Several malignancies other than NETs can overexpress SSTRs, including meningiomas, paragangliomas, small cell lung carcinomas, melanomas and thyroid cancer. However, even high expression of SSTRs (and thus a high effective dose) may not be enough to be effective, since the tumour cell type has to be radiosensitive as well. Moreover, tumours with a high growth rate, such as small cell lung carcinomas, may not be sufficiently treated in an 8 week interval schedule (66). In 34 patients with inoperable, progressive meningioma treated with ^{90}Y- and/or ^{177}LU-DOTATOC, the best response was SD in 68%, with severe toxicity in 12% (66). Recently, a review on PRRT used in thyroid cancer identified 88 patients in fifteen articles treated with four different radiopharmaceuticals (67). Best outcome was PR in 4.5% and SD in 43%. Though in the latter study the fraction of disease progression at baseline is unknown and unsuccessful cases may be unreported, it shows that treatment with radiolabelled SSAs can be a viable option for patients with non-NET SSTR positive tumours, especially when alternative therapeutic options are lacking.

Implementation into the treatment algorithm

Limitations

Over the past decades, PRRT has been growing as a treatment modality for metastatic or inoperable NETs. Efficacy and toxicity considered, PRRT seems to provide a valuable option in disease management. However, PRRT is not yet wholeheartedly embraced by all professionals involved with NET patient care; the level of evidence for PRRT is still limited. Up until now evidence relies on uncontrolled non-randomised phase I/II trials and retrospectively analysed case series. There is great diversity in patient selection, treatment schedule (radiopharmaceutical, administered activity, number of cycles) and methods of outcome assessment. This significantly limits both comparison of studies within the realm of PRRT

and comparison of PRRT with other treatment modalities, such as SSAs, targeted therapies and chemotherapy. Furthermore, small trial size and differences in protocols hamper the development and validation of prognostic models. A major breakthrough in this field is the NETTER-1 trial, a trial randomising between ^{177}Lu-DOTATATE and high dose octreotide long acting release (LAR) (see below)(68).

Current guidelines

Several major randomised controlled trials have led to the registration of systemic, targeted approaches for the treatment of advanced and inoperable G1/G2 NETs. For intestinal and pancreatic NETs, treatment with non-radionuclide labelled ('cold') SSAs is accepted as standard first line treatment (7). In a randomised trial (PROMID) comparing octreotide LAR 30 mg per month versus placebo in midgut NETs, the median PFS was 14.3 versus 6 months, respectively (10). The effect of lanreotide (120 mg per 4 weeks) versus placebo was shown in pancreatic, midgut and hindgut NETs (11). In this trial (CLARINET), median PFS was not reached after 24 months in the lanreotide group (estimated PFS 65% at that time), versus a median PFS of 18 months in the placebo group. Next in line are other targeted drugs such as everolimus (an inhibitor of mammalian target of rapamycin) and sunitinib (a tyrosine kinase inhibitor). The RADIANT trials support the use of everolimus in advanced NETs associated with carcinoid syndrome (RADIANT-2)(69), advanced P-NETs (RADIANT-3) (70) and advanced non-functioning NETs from the lung and gastrointestinal tract (RADIANT-4)(71); results from these placebo controlled trials are shown in table 3. The effect of sunitinib was shown in a randomised trial in 2011, with a median PFS of 11.4 months in the sunitinib group versus 5.5 months in the placebo group (72).

A role for PRRT

As stated above, in terms of evidence-based medicine the most important step forward for PRRT is the NETTER-1 trial (73). This phase III trial randomised between ^{177}Lu-DOTATATE (3-4x 7.4 GBq) and octreotide LAR (60mg every 4 weeks, double the standard dose). Preliminary results showed that the median PFS was not reached in the ^{177}Lu-DOTATATE group versus 8.4 months in the control group (68). A hazard ratio of 0.21 (95% confidence interval 0.13 – 0.34) was reported, reflecting an almost fivefold lower hazard of disease progression for patients in the ^{177}Lu-DOTATATE group. Along with the comparison of PRRT cohorts (table 1) with other treatments (table 3), PRRT yields very favourable results. Treatment with cold SSAs will remain first-line due to its very limited side effects. With the first randomised controlled trial using ^{177}Lu-DOTATATE, PRRT may acquire a permanent place in the treatment algorithm. Considering the efficacy and safety, PRRT is the prime candidate to become the second-line treatment after SSAs for both midgut and pancreatic NETs. Future research should include randomised trials on the sequencing of treatments.

Conclusion

PRRT using radiolabelled SSAs has grown into a well-known, safe, and effective treatment for patients with metastasised or inoperable NETs. In terms of radiographical response, patients' quality of life and progression free survival, the results of PRRT are outstanding. Side effects from PRRT are usually mild and self-limiting. Severe adverse events in the form of secondary (pre-)malignancies are rare but occur in up to 2-3% of patients. In standardised ^{177}Lu-DOTATATE treatment schedules with renal protection, an annual decrease in renal function is reported, but severe renal toxicity is a sporadic event. For

Table 3. Randomised controlled trial for advanced NETs.

trial name	first author	year	domain	intervention	control	median PFS (months)	HR (95% CI) ▲
PROMID	Rinke (9)	2009	midgut NET	octreotide LAR 30 mg/month	placebo	14.3 vs. 6	0.34 (0.20 - 0.59) △
CLARINET	Caplin (11)	2014	P-, midgut, hindgut NET	lanreotide 120 mg/4 weeks	placebo	Not reached at 24 vs. 18	0.47 (0.30 - 0.73) △
RADIANT-2	Pavel (69)	2011	NET + carcinoid syndrome	everolimus 10 mg/day*	placebo*	16.4 vs. 11.3	0.77 (0.59 – 1.00) △
RADIANT-3	Yao (70)	2011	P-NET	everolimus 10 mg/day*	placebo*	11.0 vs. 4.6	0.35 (0.27 – 0.45) △
RADIANT-4	Yao (71)	2015	n-f lung, GI tract NET	everolimus 10 mg/day*	placebo*	11.0 vs. 3.9	0.48 (0.35 – 0.67) △
	Raymond (72)	2011	f + n-f P-NET	sunitinib 37.5 mg/day*	placebo*	11.4 vs. 5.5	0.42 (0.26 – 0.66) △
NETTER-1	Strosberg (68)	2016	midgut NET	^{177}Lu-DOTATATE (4x 7.4 GBq)	octreotide LAR 60 mg/month	not reached vs. 8.4	0.21 (0.13 – 0.34) ▲

year - year of publication; PFS – progression free survival; HR – Hazard ratio for ▲disease progression or △ disease progression and death; CI – confidence interval; LAR – long acting release; P – pancreatic; (n-)f – (non-)functioning
*with continuation of SSA therapy

PRRT to become part of the standard of care, it is imperative that efficacy and safety are proven in randomised controlled trials, providing valuable insight into factors predicting both disease response and toxicity. This leap forward is presented in the NETTER-1 trial, leading way towards an even more radiant future for PRRT.

d.smitduijzentkunst@erasmusmc.nl

References

1. Yao JC, Hassan M, Phan A, et al. One hundred years after "carcinoid": epidemiology of and prognostic factors for neuroendocrine tumors in 35,825 cases in the United States. J Clin Oncol. 2008;26:3063-72
2. Hallet J, Law CH, Cukier M, et al. Exploring the rising incidence of neuroendocrine tumors: a population-based analysis of epidemiology, metastatic presentation, and outcomes. Cancer. 2015;121:589-97
3. Mocellin S, Nitti D. Gastrointestinal carcinoid: epidemiological and survival evidence from a large population-based study (n = 25 531). Ann Oncol. 2013;24:3040-4
4. Korse CM, Taal BG, van Velthuysen ML, Visser O. Incidence and survival of neuroendocrine tumours in the Netherlands according to histological grade: experience of two decades of cancer registry. Eur J Cancer. 2013;49:1975-83
5. Bosman FT, Carneiro F, Hruban RH, Theise ND. WHO Classification of Tumours of the Digestive System. Lyon: IARC; 2010.
6. Basturk O, Yang Z, Tang LH, et al. The high-grade (WHO G3) pancreatic neuroendocrine tumor category is morphologically and biologically heterogenous and includes both well differentiated and poorly differentiated neoplasms. Am J Surg Pathol. 2015;39:683-90
7. Pavel M, O'Toole D, Costa F, et al. ENETS Consensus Guidelines Update for the Management of Distant Metastatic Disease of Intestinal, Pancreatic, Bronchial Neuroendocrine Neoplasms (NEN) and NEN of Unknown Primary Site. Neuroendocrinology. 2016;103:172-85
8. Knigge U, Hansen CP. Surgery for GEP-NETs. Best Pract Res Clin Gastroenterol. 2012;26:819-31
9. Lee A, Chan DL, Wong MH, et al. Systematic Review on the Role of Targeted Therapy in Metastatic Neuroendocrine Tumor (NET). Neuroendocrinology. 2016.
10. Rinke A, Muller HH, Schade-Brittinger C, et al. Placebo-controlled, double-blind, prospective, randomized study on the effect of octreotide LAR in the control of tumor growth in patients with metastatic neuroendocrine midgut tumors: a report from the PROMID Study Group. J Clin Oncol. 2009;27:4656-63
11. Caplin ME, Pavel M, Cwikla JB, et al. Lanreotide in metastatic enteropancreatic neuroendocrine tumors. N Engl J Med. 2014;371:224-33
12. Krenning EP, Bakker WH, Breeman WA, et al. Localisation of endocrine-related tumours with radioiodinated analogue of somatostatin. Lancet. 1989;1:242-4
13. Krenning EP, Kooij PP, Bakker WH, et al. Radiotherapy with a radiolabeled somatostatin analogue, [111In-DTPA-D-Phe1]-octreotide. A case history. Ann N Y Acad Sci. 1994;733:496-506
14. Schaer JC, Waser B, Mengod G, Reubi JC. Somatostatin receptor subtypes sst1, sst2, sst3 and sst5 expression in human pituitary, gastroentero-pancreatic and mammary tumors: comparison of mRNA analysis with receptor autoradiography. Int J Cancer. 1997;70:530-7
15. Reubi JC, Schaer JC, Waser B, Mengod G. Expression and localization of somatostatin receptor SSTR1, SSTR2, and SSTR3 messenger RNAs in primary human tumors using in situ hybridization. Cancer Res. 1994;54:3455-9
16. Kwekkeboom DJ, Bakker WH, Kooij PP, et al. [177Lu-DOTAOTyr3] octreotate: comparison with [111In-DTPAo]octreotide in patients. Eur J Nucl Med. 2001;28:1319-25
17. Reubi JC, Schar JC, Waser B, et al. Affinity profiles for human somatostatin receptor subtypes SST1-SST5 of somatostatin radiotracers selected for scintigraphic and radiotherapeutic use. Eur J Nucl Med. 2000;27:273-82
18. De Jong M, Breeman WA, Valkema R, Bernard BF, Krenning EP. Combination radionuclide therapy using 177Lu- and 90Y-labeled somatostatin analogs. J Nucl Med. 2005;46 Suppl 1:13S-17S.
19. Kwekkeboom DJ, Teunissen JJ, Bakker WH, et al. Radiolabeled somatostatin analog [177Lu-DOTA0,Tyr3]octreotate in patients with endocrine gastroenteropancreatic tumors. J Clin Oncol. 2005;23:2754-62
20. Ezziddin S, Lohmar J, Yong-Hing CJ, et al. Does the pretherapeutic tumor SUV in 68Ga DOTATOC PET predict the absorbed dose of 177Lu octreotate? Clin Nucl Med. 2012;37:e141-7
21. Gabriel M, Decristoforo C, Kendler D, et al. 68Ga-DOTA-Tyr3-octreotide PET in neuroendocrine tumors: comparison with somatostatin receptor scintigraphy and CT. J Nucl Med. 2007;48:508-18
22. Srirajaskanthan R, Kayani I, Quigley AM, et al. The role of 68Ga-DOTATATE PET in patients with neuroendocrine tumors and negative or equivocal findings on 111In-DTPA-octreotide scintigraphy. J Nucl Med. 2010;51:875-82
23. Deppen SA, Liu E, Blume JD, et al. Safety and Efficacy of 68Ga-DOTATATE PET/CT for Diagnosis, Staging, and Treatment Management of Neuroendocrine Tumors. J Nucl Med. 2016;57:708-14
24. Deppen SA, Blume J, Bobbey AJ, et al. 68Ga-DOTATATE Compared with 111In-DTPA-Octreotide and Conventional Imaging for Pulmonary and Gastroenteropancreatic Neuroendocrine Tumors: A Systematic Review and Meta-Analysis. J Nucl Med. 2016;57:872-8
25. Fendler WP, Barrio M, Spick C, et al. 68Ga-DOTATATE PET/CT interobserver agreement for neuroendocrine tumor assessments: results from a prospective study on 50 patients. J Nucl Med. 2016.
26. Mizutani G, Nakanishi Y, Watanabe N, et al. Expression of Somatostatin Receptor (SSTR) Subtypes (SSTR-1, 2A, 3, 4 and 5) in Neuroendocrine Tumors Using Real-time RT-PCR Method and Immunohistochemistry. Acta Histochem Cytochem. 2012;45:167-76
27. Ezziddin S, Opitz M, Attassi M, et al. Impact of the Ki-67 proliferation index on response to peptide receptor radionuclide therapy. Eur J Nucl Med Mol Imaging. 2011;38:459-66
28. Valkema R, De Jong M, Bakker WH, et al. Phase I study of peptide receptor radionuclide therapy with [In-DTPA]octreotide: the Rotterdam experience. Semin Nucl Med. 2002;32:110-22
29. Waldherr C, Pless M, Maecke HR, Haldemann A, Mueller-Brand J. The clinical value of [90Y-DOTA]-D-Phe1-Tyr3-octreotide

(90Y-DOTATOC) in the treatment of neuroendocrine tumours: a clinical phase II study. Ann Oncol. 2001;12:941-5
30. Waldherr C, Pless M, Maecke HR, et al. Tumor response and clinical benefit in neuroendocrine tumors after 7.4 GBq (90)Y-DOTATOC. J Nucl Med. 2002;43:610-6
31. Kwekkeboom DJ, de Herder WW, Kam BL, et al. Treatment with the radiolabeled somatostatin analog [177 Lu-DOTA 0,Tyr3]octreotate: toxicity, efficacy, and survival. J Clin Oncol. 2008;26:2124-30
32. Imhof A, Brunner P, Marincek N, et al. Response, survival, and long-term toxicity after therapy with the radiolabeled somatostatin analogue [90Y-DOTA]-TOC in metastasized neuroendocrine cancers. J Clin Oncol. 2011;29:2416-23
33. Aaronson NK, Ahmedzai S, Bergman B, et al. The European Organization for Research and Treatment of Cancer QLQ-C30: a quality-of-life instrument for use in international clinical trials in oncology. J Natl Cancer Inst. 1993;85:365-76
34. Khan S, Krenning EP, van Essen M, et al. Quality of life in 265 patients with gastroenteropancreatic or bronchial neuroendocrine tumors treated with [177Lu-DOTA0,Tyr3]octreotate. J Nucl Med. 2011;52:1361-8
35. Bodei L, Kidd M, Paganelli G, et al. Long-term tolerability of PRRT in 807 patients with neuroendocrine tumours: the value and limitations of clinical factors. Eur J Nucl Med Mol Imaging. 2015;42:5-19
36. Bergsma H, Konijnenberg MW, Kam BL, et al. Subacute haematotoxicity after PRRT with (177)Lu-DOTA-octreotate: prognostic factors, incidence and course. Eur J Nucl Med Mol Imaging. 2016;43:453-63
37. Svensson J, Berg G, Wangberg B, Larsson M, Forssell-Aronsson E, Bernhardt P. Renal function affects absorbed dose to the kidneys and haematological toxicity during (1)(7)(7)Lu-DOTATATE treatment. Eur J Nucl Med Mol Imaging. 2015;42:947-55
38. Kesavan M, Turner JH. Myelotoxicity of Peptide Receptor Radionuclide Therapy of Neuroendocrine Tumors: A Decade of Experience. Cancer Biother Radiopharm. 2016;31:189-98
39. Rolleman EJ, Valkema R, de Jong M, Kooij PP, Krenning EP. Safe and effective inhibition of renal uptake of radiolabelled octreotide by a combination of lysine and arginine. Eur J Nucl Med Mol Imaging. 2003;30:9-15
40. Bodei L, Cremonesi M, Zoboli S, et al. Receptor-mediated radionuclide therapy with 90Y-DOTATOC in association with amino acid infusion: a phase I study. Eur J Nucl Med Mol Imaging. 2003;30:207-16
41. Jamar F, Barone R, Mathieu I, et al. 86Y-DOTA0)-D-Phe1-Tyr3-octreotide (SMT487)–a phase 1 clinical study: pharmacokinetics, biodistribution and renal protective effect of different regimens of amino acid co-infusion. Eur J Nucl Med Mol Imaging. 2003;30:510-8
42. Rolleman EJ, Melis M, Valkema R, Boerman OC, Krenning EP, de Jong M. Kidney protection during peptide receptor radionuclide therapy with somatostatin analogues. Eur J Nucl Med Mol Imaging. 2010;37:1018-31
43. Bodei L, Mueller-Brand J, Baum RP, et al. The joint IAEA, EANM, and SNMMI practical guidance on peptide receptor radionuclide therapy (PRRNT) in neuroendocrine tumours. Eur J Nucl Med Mol Imaging. 2013;40:800-16
44. Mariniello A, Bodei L, Tinelli C, et al. Long-term results of PRRT in advanced bronchopulmonary carcinoid. Eur J Nucl Med Mol Imaging. 2016;43:441-52
45. Bodei L, Cremonesi M, Ferrari M, et al. Long-term evaluation of renal toxicity after peptide receptor radionuclide therapy with 90Y-DOTATOC and 177Lu-DOTATATE: the role of associated risk factors. Eur J Nucl Med Mol Imaging. 2008;35:1847-56
46. Valkema R, Pauwels SA, Kvols LK, et al. Long-term follow-up of renal function after peptide receptor radiation therapy with (90) Y-DOTA(0),Tyr(3)-octreotide and (177)Lu-DOTA(0), Tyr(3)-octreotate. J Nucl Med. 2005;46 Suppl 1:83S-91S
47. Erbas B, Tuncel M. Renal Function Assessment During Peptide Receptor Radionuclide Therapy. Semin Nucl Med. 2016;46:462-78
48. Bergsma H, Konijnenberg MW, van der Zwan WA, et al. Nephrotoxicity after PRRT with 177Lu-DOTA-octreotate. Eur J Nucl Med Mol Imaging. 2016.
49. Brieau B, Hentic O, Lebtahi R, et al. High risk of myelodysplastic syndrome and acute myeloid leukemia after 177Lu-octreotate PRRT in NET patients heavily pretreated with alkylating chemotherapy. Endocr Relat Cancer. Vol 23. England; 2016:L17-23
50. Gabriel M, Andergassen U, Putzer D, et al. Individualized peptide-related-radionuclide-therapy concept using different radiolabelled somatostatin analogs in advanced cancer patients. Q J Nucl Med Mol Imaging. 2010;54:92-9
51. Romer A, Seiler D, Marincek N, et al. Somatostatin-based radiopeptide therapy with [177Lu-DOTA]-TOC versus [90Y-DOTA]-TOC in neuroendocrine tumours. Eur J Nucl Med Mol Imaging. 2014;41:214-2
52. Villard L, Romer A, Marincek N, et al. Cohort study of somatostatin-based radiopeptide therapy with [(90)Y-DOTA]-TOC versus [(90) Y-DOTA]-TOC plus [(177)Lu-DOTA]-TOC in neuroendocrine cancers. J Clin Oncol. 2012;30:1100-6
53. Claringbold PG, Brayshaw PA, Price RA, Turner JH. Phase II study of radiopeptide 177Lu-octreotate and capecitabine therapy of progressive disseminated neuroendocrine tumours. Eur J Nucl Med Mol Imaging. 2011;38:302-11
54. Claringbold PG, Price RA, Turner JH. Phase I-II study of radiopeptide 177Lu-octreotate in combination with capecitabine and temozolomide in advanced low-grade neuroendocrine tumors. Cancer Biother Radiopharm. 2012;27:561-9
55. Forrer F, Uusijarvi H, Storch D, Maecke HR, Mueller-Brand J. Treatment with 177Lu-DOTATOC of patients with relapse of neuroendocrine tumors after treatment with 90Y-DOTATOC. J Nucl Med. 2005;46:1310-6
56. Van Essen M, Krenning EP, Kam BL, et al. Salvage therapy with (177) Lu-octreotate in patients with bronchial and gastroenteropancreatic neuroendocrine tumors. J Nucl Med. 2010;51:383-90
57. Sabet A, Haslerud T, Pape UF, et al. Outcome and toxicity of salvage therapy with 177Lu-octreotate in patients with metastatic gastroenteropancreatic neuroendocrine tumours. Eur J Nucl Med Mol Imaging. 2014;41:205-10
58. Severi S, Sansovini M, Ianniello A, et al. Feasibility and utility of re-treatment with (177)Lu-DOTATATE in GEP-NENs relapsed after treatment with (90)Y-DOTATOC. Eur J Nucl Med Mol Imaging. 2015;42:1955-63
59. Limouris GS, Chatziioannou A, Kontogeorgakos D, et al. Selective

hepatic arterial infusion of In-111-DTPA-Phe1-octreotide in neuroendocrine liver metastases. Eur J Nucl Med Mol Imaging. 2008;35:1827-37
60. Kratochwil C, Giesel FL, Lopez-Benitez R, et al. Intraindividual comparison of selective arterial versus venous 68Ga-DOTATOC PET/CT in patients with gastroenteropancreatic neuroendocrine tumors. Clin Cancer Res. 2010;16:2899-905
61. Kratochwil C, Lopez-Benitez R, Mier W, et al. Hepatic arterial infusion enhances DOTATOC radiopeptide therapy in patients with neuroendocrine liver metastases. Endocr Relat Cancer. 2011;18:595-602
62. https://clinicaltrials.gov/ct2/show/NCT02067988.
63. Kaemmerer D, Prasad V, Daffner W, et al. Neoadjuvant peptide receptor radionuclide therapy for an inoperable neuroendocrine pancreatic tumor. World J Gastroenterol. 2009;15:5867-70
64. Sowa-Staszczak A, Pach D, Chrzan R, et al. Peptide receptor radionuclide therapy as a potential tool for neoadjuvant therapy in patients with inoperable neuroendocrine tumours (NETs). Eur J Nucl Med Mol Imaging. 2011;38:1669-74
65. van Vliet EI, van Eijck CH, de Krijger RR, et al. Neoadjuvant Treatment of Nonfunctioning Pancreatic Neuroendocrine Tumors with [177Lu-DOTA0,Tyr3]Octreotate. J Nucl Med. 2015;56:1647-53
66. van Essen M, Krenning EP, Kooij PP, et al. Effects of therapy with [177Lu-DOTA0, Tyr3]octreotate in patients with paraganglioma, meningioma, small cell lung carcinoma, and melanoma. J Nucl Med. 2006;47:1599-606
67. Salavati A, Puranik A, Kulkarni HR, Budiawan H, Baum RP. Peptide Receptor Radionuclide Therapy (PRRT) of Medullary and Nonmedullary Thyroid Cancer Using Radiolabeled Somatostatin Analogues. Semin Nucl Med. 2016;46:215-24
68. Strosberg JR, Wolin EM, Chasen B, et al. NETTER-1 phase III: Efficacy and safety results in patients with midgut neuroendocrine tumors treated with 1 7 7Lu- DOTATATE. Journal of Clinical Oncology. 2016;34.
69. Pavel ME, Hainsworth JD, Baudin E, et al. Everolimus plus octreotide long-acting repeatable for the treatment of advanced neuroendocrine tumours associated with carcinoid syndrome (RADIANT-2): a randomised, placebo-controlled, phase 3 study. Lancet. 2011;378:2005-12
70. Yao JC, Shah MH, Ito T, et al. Everolimus for advanced pancreatic neuroendocrine tumors. N Engl J Med. 2011;364:514-23
71. Yao JC, Fazio N, Singh S, et al. Everolimus for the treatment of advanced, non-functional neuroendocrine tumours of the lung or gastrointestinal tract (RADIANT-4): a randomised, placebo-controlled, phase 3 study. Lancet. 2016;387:968-77
72. Raymond E, Dahan L, Raoul JL, et al. Sunitinib malate for the treatment of pancreatic neuroendocrine tumors. N Engl J Med. 2011;364:501-13
73. https://clinicaltrials.gov/ct2/show/NCT01578239.

MIBG-therapy in neuroblastoma patients

G. Bleeker, MD, PhD[1]; F. van der Zant, MD, PhD[1]; G.A.M. Tytgat, MD, PhD[2]

[1]Department of Medical Imaging, Noord-West Ziekenhuis Groep, Alkmaar, the Netherlands
[2]Department of Paediatric oncology, Emma Children's Hospital, Academic Medical Centre, Amsterdam and Princess Máxima centre for Paediatric Oncology, Utrecht, the Netherlands

Partly adapted from:
Bleeker G. The use of both diagnostic and therapeutic MIBG in neuroblastoma patients. Buijten & Schipperheijn. Amsterdam. ISBN: 978-90-9028217-6

Abstract

Bleeker G, van der Zant F, Tytgat GAM. MIBG-therapy in neuroblastoma patients. Neuroblastoma is the most common extracranial malignant solid tumour of childhood. It is an embryonic tumour derived from the sympathetic adrenal lineage of the neural crest. Consequently, neuroblastomas may arise anywhere in the sympathetic nervous system.Neuroblastoma is a tumour with very heterogeneous clinical and biological behaviour. The clinical course ranges from spontaneous regression to rapid and fatal tumour progression despite extensive treatment. Despite the use of a wide range of therapies, chemotherapy-resistant neuroblastoma is still a major problem, especially in the high-risk group MIBG is a compound that is structurally analogous to the neurotransmitter norepinephrine and therefore cellular accumulation of MIBG occurs by two distinct mechanisms: active uptake via the uptake-1 system (NET) and passive diffusion. Once labelled with radioactive iodine (^{123}I or ^{131}I), MIBG scintigraphy can be used for imaging tumours of neural crest and neuroendocrine origin, like neuroblastomas. Currently, ^{131}I-MIBG therapy is part of clinical trials. The number of centres participating in these trials is increasing. Three types of studies with ^{131}I-MIBG therapy can be identified in high-risk patients: induction studies with ^{131}I-MIBG therapy as first line treatment upfront in newly diagnosed neuroblastoma patients; consolidation studies with ^{131}I-MIBG therapy given in conjunction with myeloablative chemotherapy after initial chemotherapy; and relapsed/refractory studies with ^{131}I-MIBG therapy in patients with progressive disease after an initial response to treatment, or with failure to respond well to induction chemotherapy.
Till recently, in the Dutch Childhood Oncology Group (DCOG) – neuroblastoma protocol, ^{131}I-MIBG therapy was incorporated in the treatment of newly diagnosed stage 4 neuroblastoma patients before the start of induction chemotherapy (upfront). Although a lot of studies have been published on the use of ^{131}I-MIBG therapy and ^{131}I-MIBG therapy seems to be a promising treatment modality in neuroblastoma treatment protocol, more data is needed to implement this treatment modality in international neuroblastoma protocols. Especially data on upfront ^{131}I-MIBG therapy is limited.
Tijdschr Nucl Geneesk 2016; 38(4):1645-1654

Introduction

Neuroblastoma is the most common extracranial malignant solid tumour of childhood (1-3). It accounts for 7 to 10% of all childhood cancers and for approximately 15% of cancer deaths in children (2-8). About 25 patients per year are diagnosed in the Netherlands. Ninety percent of patients are younger than five years of age at diagnosis with a median age of 22 months (6-9).
Neuroblastoma is an embryonic tumour derived from the sympathetic adrenal lineage of the neural crest. Consequently, neuroblastomas may emerge anywhere in the sympathetic nervous system, but most frequently they arise in the abdomen (65%) with half of them in the adrenal glands (3, 4, 10).

Presentation

Clinical presentation depends on extent and site of disease. Patients can present with localised neuroblastoma at diagnosis, varying from incidentally diagnosed adrenal tumours to large locally invasive neuroblastomas with a large abdominal mass, abdominal distension and pain (3, 4). Distant metastases are present at diagnosis in 50% of the patients (4, 10, 11). Dissemination occurs through lymphatic and haematogenous routes and tumour cells affect predominantly bone, bone marrow and lymph nodes and less frequently liver and lungs (4, 10, 11). Children with metastatic disease are frequently quite ill at presentation. As the tumour disseminates to the skeleton, patients often present with bone pain, limping or both. Patients may show anaemia at diagnosis because of marrow failure or tumour bleedings.

Staging

Staging of neuroblastomas was previously performed according to the International Neuroblastoma Staging System (INSS) (12, 13). Because the INSS system is a postsurgical staging system, in 2008 the International Neuroblastoma

Research Group (INRG) published a new clinical staging system that uses image defined risk factors on computed tomography (CT) or magnetic resonance imaging (MRI) instead of surgical evaluation (table 1) (14, 15). Image defined risk factors include the involvement of vital structures with the risk of injury to these structures during surgery (15). In the INRG staging system, stage L tumours are localised; L1 tumours do not involve vital structures as defined by the image defined risk factors, and the tumour must be confined to one body compartment; L2 tumours are locoregional tumours with one or more image defined risk factors, and possible extension in adjacent body compartments ipsilaterally. Stage M tumours show distant metastatic disease and in stage MS tumours, as in stage 4S, metastases are confined to the skin, liver and bone marrow (less than 10%) in patients younger than 18 months (14).

Neuroblastoma is a tumour with very heterogeneous clinical and biological behaviour. The clinical course ranges from spontaneous regression to rapid and fatal tumour progression despite extensive treatment.
The current risk classification system of the INRG uses stage, age at diagnosis, histology, MYCN amplification, 11q aberration and DNA content to identify four risk groups: very low, low, intermediate and high, with event-free survivals (EFS) of >85%, 75 to 85%, 50 to 75% and <50%, respectively (15).

Diagnosis

Initial assessment of all patients suspected of neuroblastoma should include histopathological confirmation of the diagnosis and determination of tumour characteristics and extent of the disease, which is necessary for risk classification. This should be performed prior to any therapy and consists mostly of (histo-)pathology and imaging (16, 17).
To evaluate the primary tumour, international consensus was achieved in the INRG. MRI and/or CT with three-dimensional measurements are recommended (14) and necessary to address image-defined risk factors (IDRF). In addition, metastatic sites should also be measured by CT and/or MRI, because the results are useful for evaluation of treatment response (14). Furthermore, all patients should have iodine-123 (^{123}I)- metaiodobenzylguanidine (MIBG) scintigraphy according to the guidelines of the European Association of Nuclear Medicine (EANM) (18, 19). One unequivocal MIBG-positive lesion at a distant site is sufficient to define metastatic disease. A single dubious lesion on MIBG scintigraphy requires confirmation by another imaging modality (14).
A recently published Cochrane review reported a high MIBG scintigraphy sensitivity (67-100%) (20). Specificity could not be calculated, but other studies reported specificities of 83-92% (21). SPECT increases the accuracy of localisation of the primary tumour and metastases, and enables differentiation of lesions from physiological uptake areas (22).

Table 1. Description of International Neuroblastoma Risk Group Staging System (14)

stage	explanation
L1	localised tumour not involving vital structures as defined by the list of image-defined risk factors and confined to one body compartment
L2	locoregional tumour with presence of one or more image-defined risk factors
M	distant metastatic disease (except stage MS)
MS	metastatic disease in children younger than 18 months with metastases confined to skin, liver and/or bone marrow

Patients with multifocal primary tumours should be staged according to the greatest extent of disease as defined in the table.

Treatment

Patient with neuroblastoma are treated according to risk groups (figure 1). In patients with low-risk neuroblastoma a wait-and-see policy might fulfil, while high-risk patients are treated with dose-intensive regimens.

Low-risk and medium-risk neuroblastoma

Most localised neuroblastomas (INRG stage L1) have favourable clinical biological features. Some do not need any treatment, because they regress spontaneously. Most other localised tumours can be treated with surgery alone (4, 24).
Treatment of more invasive locoregional tumours (INRG stage L2) is controversial. Chemotherapy is administered to enable surgical resection (23-27). Since the prognosis of these locoregional neuroblastomas is good, toxicity and late effects should be prevented as much as possible, for example by avoiding radical surgery and radiotherapy (4, 23).
The majority of patients with stage MS neuroblastomas without MYCN amplification show spontaneous regression and therefore need no or little intervention. However, chemotherapy or low-dose radiotherapy may be indicated for patients with large tumours or massive hepatomegaly with consequently mechanical obstruction, respiratory insufficiency or liver dysfunction (3, 28).

High-risk neuroblastoma

Treatment of high-risk neuroblastomas currently consists of induction, local control, consolidation and maintenance.
To improve outcome, it has been shown that dose intense chemotherapy (the same dose administered in shorter time frame) is better than conventional treatment (29). Local control consists of a combination of surgical resection and external-beam radiotherapy of the primary tumour site.
Consolidation aims to eliminate any remaining tumour cell with myeloablative cytotoxic agents and stem cell rescue.
Maintenance treatment has been added at the end of treatment protocols with the aim to treat persistent minimal

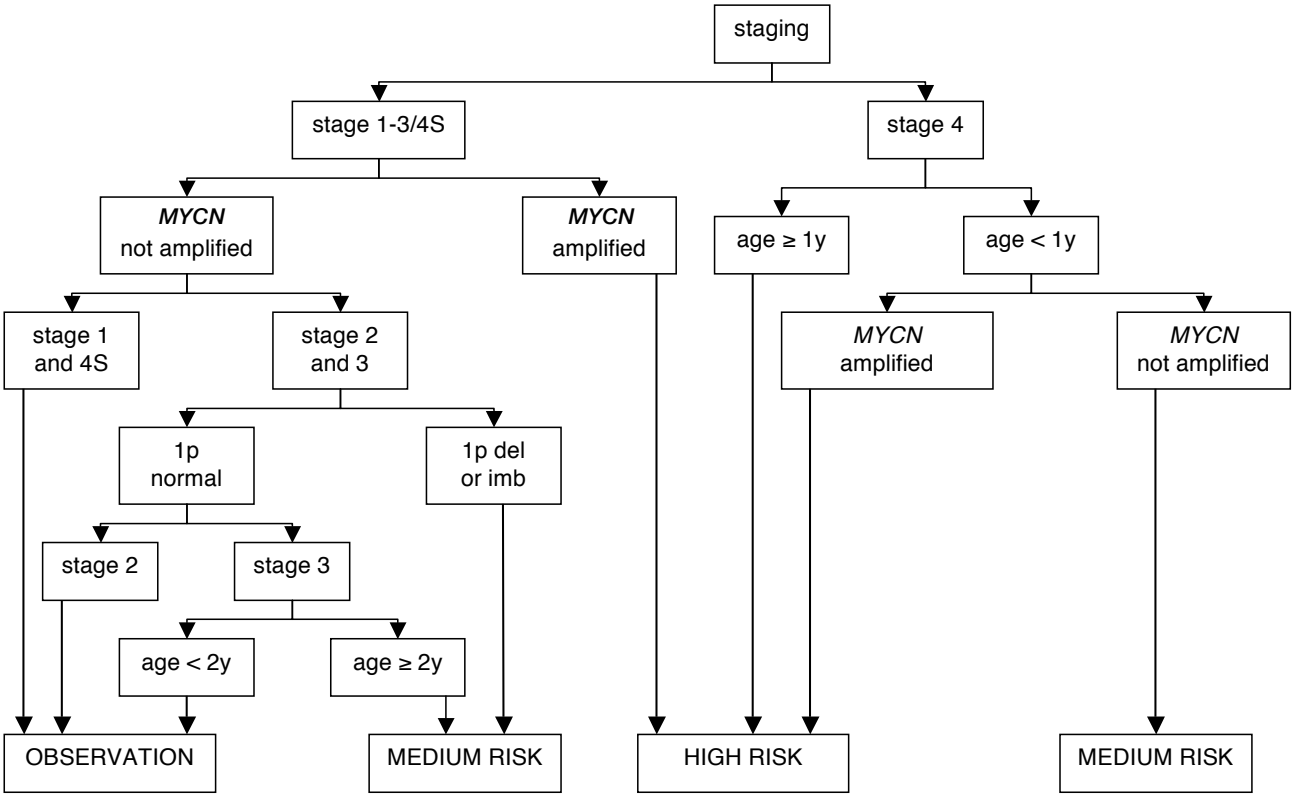

Staging according to INSS-staging system. del=deletion; imb=imbalance; y=year.

Figure 1. Risk groups according to the DCOG NBL 2009 protocol.

residual disease. Retinoic acid induces terminal differentiation of neuroblastoma cells in vitro.

The Children's Oncology Group (COG) reported that immunotherapy with ch14.18 (anti-GD2), GM-CSF and interleukin-2 was associated with a significantly improved outcome as compared with 13-cis-retinoic acid alone (EFS 66% vs 46% and overall survival (OS) 86% vs 75% at two years). Future studies are needed to find ways to administer this therapy without severe toxic effects (pain, capillary leak syndrome, hypersensitivity reaction) (30).

^{131}I-MIBG therapy

Despite the use of this range of therapies, chemotherapy-resistant neuroblastoma is still a major problem, especially in the high-risk group (31). Chemotherapy dose escalation studies improved initial tumour response rates. However, refractory or progressive disease still occurs in 10 to 20% of patients (31-33). Further dose intensification of induction therapy is limited because of haematopoietic and mucosal toxicity (31). Therefore, it is important to investigate different types of therapies to improve response and survival in high-risk neuroblastoma.
The number of clinical trials investigating ^{131}I-MIBG therapy in neuroblastoma patients is increasing.

Biology of metaiodobenzylguanidine
Radiolabelled MIBG was initially developed in the late 1970s by Dr. Donald Wieland and colleagues at the University of Michigan Medical School, Ann Arbor, as a diagnostic agent for imaging of the adrenal medulla (34, 35).
MIBG is a compound that is structurally analogous to the neurotransmitter norepinephrine (figure 2). Norepinephrine is a stress hormone and neurotransmitter. In the sympathetic nervous system it is released from noradrenergic neurons. It is synthesized from dopamine by dopamine-hydroxylase in the presynaptic neuron. It is then transported into vesicles and released into the synapse. It binds on the presynaptic and postsynaptic membrane of adrenergic receptors.
Norepinephrine and dopamine are transported back to the cytosol by the norepinephrine transporter (NET), a monoamine transporter. In the cytosol other vesicular monoamine transporters collect dopamine and norepinephrine into vesicles for later storage and release.
Because MIBG is a physiological analogue of norepinephrine, cellular accumulation of MIBG occurs by two distinct mechanisms (36-42) (figure 3):

Norepinephrine

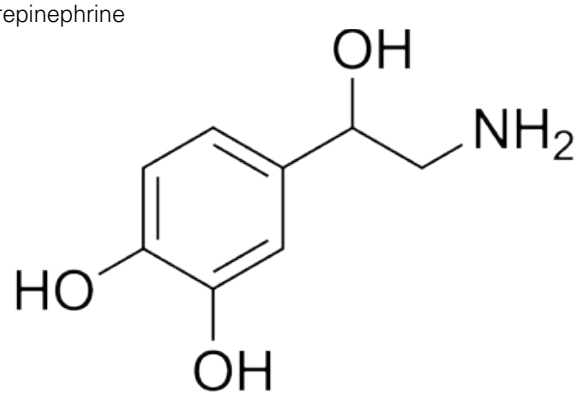

metaiodobenzylguandine

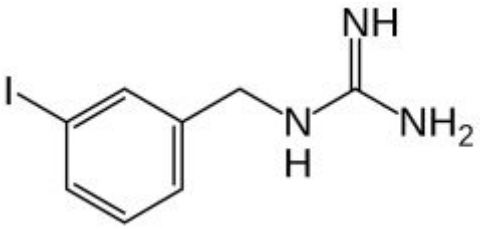

Figure 2. Norepinephrine versus MIBG.

1. Active uptake (uptake-1 system) via the NET previously called uptake-1 in cells that synthesize NET, which is sodium dependent, specific and saturable. MIBG is than stored in the noradrenergic neurosecretory granules, resulting in a high specific concentration in contrast to cells of other tissue.
2. Passive diffusion, which is sodium independent, nonspecific, and unsaturable, taking place in all cells.

Under ideal conditions in vitro, the specific uptake process is about fifty times more efficient than passive uptake (36). Discriminating tumour from non-tumoural tissues is possible because tumour cells express high affinity NET and most normal tissues accumulate MIBG inefficiently by passive diffusion. The active mechanism predominates when the extracellular concentration of ^{131}I-MIBG is low, passive diffusion occurs at higher concentrations (36-42).
NET expression is predictive for MIBG uptake capacity and quantification of NET mRNA has potential for the selection of patients for ^{131}I-MIBG therapy (36, 43, 44).

Metaiodobenzylguanidine in neuroblastoma

Neuroblastoma is a catecholamine secreting embryonic tumour of the peripheral sympathetic nervous system. Neuroblastomas express the NET and more than 90% of all tumours are MIBG-positive (21, 36).
Once labelled with radioactive iodine (^{123}I or ^{131}I), MIBG

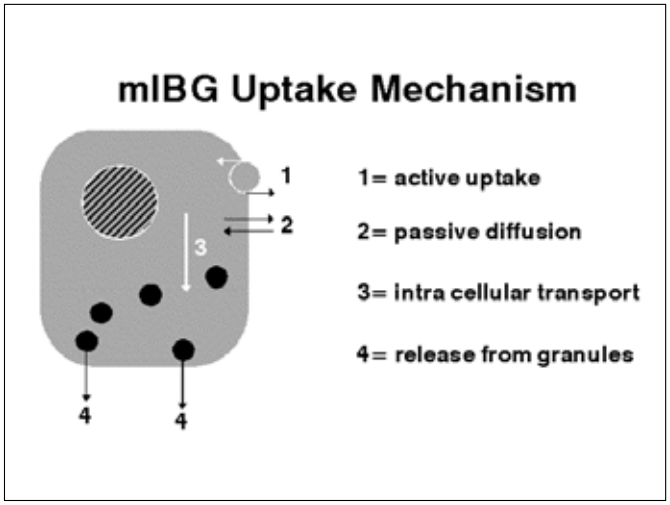

Figure 3. MIBG uptake mechanism.

scintigraphy can be used for imaging tumours of neural crest and neuroendocrine origin that express neurohormonal receptors, like neuroblastomas (36, 38, 39).
Initially MIBG was labelled with ^{131}I, followed by ^{123}I. ^{123}I-MIBG scintigraphy results in superior image quality compared to ^{131}I-MIBG at a lower patient radiation burden. The first explanation for this is that ^{123}I-MIBG has a shorter half-life than ^{131}I-MIBG (13 hours vs 8 days). Secondly, ^{123}I-MIBG has a lower gamma-emission energy (159 keV) than ^{131}I-MIBG (364 keV) making it more ideal for gamma camera imaging. Finally, ^{123}I-MIBG lacks beta particle emission (14, 38). Image quality is better for ^{123}I-MIBG than for ^{131}I-MIBG. However, both radiopharmaceuticals perform equally in the prediction of outcome by the use of a semi-quantitative scoring system (45). However, the physical characteristics that make ^{131}I-MIBG less suitable for imaging, make it a good candidate for radionuclide therapy of neuroblastoma.
MIBG has also been successfully used for diagnosis and treatment of other neuroendocrine tumours like pheochromocytoma/paraganglioma, gastroenteropancreatic neuroendocrine tumours and carcinoid tumours of the enterochromaffin cell type (36).
The physiological distribution of MIBG consists of accumulation in structures that excrete catecholamines, like urinary tract and gastrointestinal system. MIBG is also physiologically taken up by the liver and in a lesser extent by the spleen, lungs, salivary glands, thyroid, hypophysis, skeletal muscles, myocardium and brown adipose tissue (18, 46, 47).
About 10% of the neuroblastomas are MIBG non-avid causing false negative results. Pharmacological interference is probably the most frequent cause for false-negative MIBG uptake. Many drugs can interfere with the uptake and/or vesicular storage of ^{123}I-MIBG (18, 46,47).

Currently, ^{131}I-MIBG therapy is part of clinical trials. The number of centres participating in these trials is increasing.

^{131}I-MIBG therapy in the Dutch protocol

Till recently, in the Dutch Childhood Oncology Group (DCOG) neuroblastoma protocol, ^{131}I-MIBG therapy was incorporated in the treatment of newly diagnosed stage 4 neuroblastoma patients before start of induction chemotherapy (upfront) (48). ^{131}I-MIBG therapy was indicated in patients with a higher MIBG uptake level in the primary tumour than physiological liver activity combined with MIBG uptake in known metastases.
Patients were excluded from ^{131}I-MIBG therapy when they were in poor clinical condition (uncontrollable hypertension, orbital masses, pleural effusion) or in case of insufficient MIBG uptake (in primary tumour and/or metastases).

The protocol consisted of two courses of upfront ^{131}I-MIBG therapy, followed by six courses of induction chemotherapy (interval aimed at 21 days), followed by surgery. Patients that reached complete response (CR), very good partial response (VGPR) and partial response (PR) proceeded to myeloablative chemotherapy and autologous stem cell transplantation (ASCT), followed by radiotherapy to the primary tumour site and retinoic acid.
The first course of ^{131}I-MIBG was preferably started within two weeks from diagnosis. The scheduled interval between the two ^{131}I-MIBG courses was four weeks. If platelet counts were below 50 x 10^9/L, the second course could be postponed, or, if platelet counts allowed, a 3 week interval was permitted.
To reduce bone marrow toxicity the dose regimen was aimed at a whole body exposure of 4 Gy for the combined 2 cycles of ^{131}I-MIBG.
However, recently upfront ^{131}I-MIBG therapy was removed from the DCOG neuroblastoma treatment protocol, because upfront ^{131}I-MIBG therapy was frequently not feasible because of a weak clinical condition of patients, lack of MIBG-uptake or logistic reasons.
At this moment, patients that still have MIBG avid lesions before ASCT, or patients with refractory disease, are being treated with ^{131}I-MIBG in combination with ASCT (49-51). However, an independent advantage of ^{131}I-MIBG therapy could not be proven in a retrospective analysis of the German Neuroblastoma trial NB 2004 (49) and of the COG (50). The ongoing German Neuroblastoma Trial NB2004 will address the influence of ^{131}I-MIBG therapy with emphasis on tumour dosimetry (49).

When treated with ^{131}I-MIGB therapy, patients are admitted to a special nuclear medicine ward and thyroid prophylaxis is prescribed (52). Patients remain in radiation protective isolation until the exposure rate is less than 20 µSv/h, at 1 m distance. If possible, parents are involved in nursing during the admission of their child at the nuclear medicine ward.
Although prescription of interfering drugs is rare in paediatric patients, the use of these drugs has to be excluded before any MIBG administration. The most common interfering drugs prescribed in paediatric patients are bronchodilators, decongestants and cardiovascular medication.
To prevent hypertensive reaction on the infusion of MIBG, it is advised to infuse no more than 3700 MBq/h.

Toxicity of ^{131}I-MIBG therapy

^{131}I-MIBG toxicity has predominantly been reported in patients with refractory or relapsed neuroblastoma who received extensive chemotherapy treatment before ^{131}I-MIBG therapy. Toxicity of ^{131}I-MIBG alone has therefore been difficult to determine (53).
Over twenty years preceding the DCOG neuroblastoma 2009 study, in the Academic Medical Centre (AMC) in Amsterdam, neuroblastoma patients have been treated with upfront ^{131}I-MIBG. Therefore, this AMC cohort is unique in investigating toxicity of ^{131}I-MIBG only (53).
Upfront ^{131}I-MIBG therapy caused only little acute toxicity in patients with newly diagnosed neuroblastoma. The most frequently encountered acute toxicity was haematological, followed by nausea and vomiting (53).
Haematological toxicity was the main toxicity observed in pre-treated patients and consisted of severe and persistent thrombocytopenia (54, 55). With upfront ^{131}I-MIBG therapy, grade IV thrombocytopenia occurred in only 1% of patients after the first ^{131}I-MIBG therapy and in 3% of patients after the second (53). These percentages are lower than would be expected with induction chemotherapy (55). Mastrangelo et al. also reported only haematological and acceptable toxicity after upfront ^{131}I-MIBG in combination with chemotherapy (cisplatin, cyclophosphamide, etoposide, vincristine and doxorubicin) in newly diagnosed neuroblastoma patients (56).
Infections have been reported during and after ^{131}I-MIBG therapy in heavily pre-treated patients and in patients treated with myeloablative ^{131}I-MIBG therapy (57). In contrast, only a few patients in the upfront ^{131}I-MIBG therapy cohort of the AMC were diagnosed with infections not exceeding grade II in severity. As these patients were chemotherapy-naive, they might have had better bone marrow reserve (53).
Although upfront ^{131}I-MIBG therapy in newly diagnosed neuroblastoma patients seemed to be effective without serious toxicity, one should keep in mind that four serious adverse events occurred and in one toxicity of ^{131}I-MIBG therapy could not be excluded. This last patient had a posterior reversible encephalopathy syndrome (PRES), a rare complication in paediatric oncology patients, causing seizures. The PRES was presumably caused by pre-existing hypertension (53). In the literature only two other cases of PRES have been described in neuroblastoma patients, and none of these patients were treated with ^{131}I-MIBG (58).
Because acute toxicity of ^{131}I-MIBG therapy could not be excluded in the case of the serious adverse event with PRES and because hypertensive episodes can occur many hours after ^{131}I-MIBG infusion, blood pressure should be monitored for at least 48 hours after administration of ^{131}I-MIBG.
Besides acute toxicity it is important to further investigate

whether ^{131}I-MIBG therapy causes long-term toxicity, like thyroid toxicity, primary ovarian insufficiency and/or secondary malignancies.
Thyroid protection during ^{131}I-MIBG therapy mostly prevents ^{131}I thyroid uptake, but late effects of ^{131}I-MIBG therapy on thyroid function cannot be ruled out. Recently, two patients from the AMC were reported to have differentiated thyroid carcinoma following ^{131}I-MIBG therapy (52, 59). These patients received adequate thyroid protection during ^{131}I-MIBG therapy, and no ^{131}I-MIBG uptake was seen in their thyroid glands on post ^{131}I-MIBG imaging. Recently two cases of primary ovarian insufficiency, after ^{131}I-MIBG therapy only, have been described indicating that ^{131}I-MIBG therapy may have a causative role (60). Lastly, second malignancies have been described in patients that were treated with ^{131}I-MIBG therapy (61).

^{131}I-MIBG therapy in high-risk patients

In 2014 Wilson et al. distinguished three types of studies with ^{131}I-MIBG therapy in high-risk patients in a systematic review of ^{131}I-MIBG therapy in neuroblastoma patients (62):

1. Induction studies: ^{131}I-MIBG therapy used as first line treatment upfront in newly diagnosed neuroblastoma patients.
2. Consolidation studies: ^{131}I-MIBG therapy given in conjunction with myeloablative chemotherapy, after an initial response to initial chemotherapy.
3. Relapsed/refractory studies: ^{131}I-MIBG therapy in patients with progressive disease after initial response to treatment, or with failure to respond well to induction chemotherapy.

1. Induction studies

In 2008 De Kraker et al. already reported a response rate (according to the INRG) of 61% to a median of three fixed dose cycles of 3.7 GBq upfront ^{131}I-MIBG therapy to 41 newly diagnosed patients with high-risk neuroblastoma in the AMC. Median OS was fifteen months and 5-year OS was 15% (62, 63). Another European study of Mastrangelo et al. reported a response rate of 92% to one fixed dose of 7.4 MBq in thirteen newly diagnosed patients (54%). Median OS was not reported, median event-free survival (EFS) was ten months and 5-year EFS was 12% (56, 62).
As acute toxicity of upfront ^{131}I-MIBG therapy was low if the seriously ill condition of this patient population is taken into consideration, it was included in the protocol of the DCOG to investigate whether upfront ^{131}I-MIBG therapy was feasible in a high-risk treatment protocol compared to the induction chemotherapy regimen of the GPOH protocol.
In a pilot of this study, it was feasible to start upfront ^{131}I-MIBG therapy within two weeks after diagnosis of neuroblastoma (preliminary data Kraal/Bleeker et al). However, as stated before it has recently been removed from the treatment protocol.

2. Consolidation studies

Klingebiel et al. described eleven patients with INSS stage 4 neuroblastoma after initial chemotherapy from the GPOH-NB90 study. These patients were given the option to enrol for ^{131}I-MIBG therapy.
A single cycle of ^{131}I-MIBG, 0.58 GBq/kg, was immediately followed by chemotherapy and peripheral blood stem cell (PBSC) support and then anti-GD2 antibody.
Objective tumour responses were analysed after recovery from stem cell transplantation. Four out of eleven patients had a continued response from induction. Two had progressive disease and one suffered from a relapse.
Overall survival was 70% at 19 months, EFS was not reported (62, 64). As stated before the benefit of ^{131}I-MIBG therapy in patients with residual lesion before ASCT is still in investigation (49, 50). In addition, recently Simon et al. described in an abstract at the ANR in July 2016 that MIBG therapy can improve survival in patients with incomplete metastatic response to induction chemotherapy. They reported that EFS was very similar between patients who underwent MIBG therapy compared to no MIBG therapy. In contrast, a trend for better OS was found after MIBG therapy compared to no MIBG therapy (65).

3. Relapsed/refractory studies

Relapsed patients progressed after an initial partial or complete response, and often after consolidation with myeloablative therapy. Mostly, studies do not clearly distinguish these two types of patients.
In their systematic review, Wilson et al. describe twenty studies regarding ^{131}I-MIBG therapy given alone and seven studies about ^{131}I-MIBG therapy given with concurrent chemotherapy (62). When ^{131}I-MIBG therapy was given alone, the number of cycles ranged from 1 to 6, whereas ^{131}I-MIBG given with concurrent chemotherapy tended to have fewer cycles, ranging from 1 to 3. A wide range (2.5 - 9.5 GBq, not presented in some studies) of administered activity was given (62).
Overall mean tumour response of 25 studies was 32% (253/782) with a wide range of 4% (68) to 75% (67). In patients with ^{131}I-MIBG alone, response rate was 32% (199/629) (68-74) compared to 39% in the group with concomitant chemotherapy (48/124) (5, 66, 73-89). For refractory patients, the overall tumour response was 37% (61/164) and for relapsed patients this was 38% (43/113). In the studies with mixed populations response was 30% (149/505) (62). In 2015, Zhou et al. reported a response rate of 27% without difference in response rate between relapsed (n=146) and refractory patients (n=72) (90).
In the multivariable analysis of the systematic review of Wilson et al. there was a positive correlation between response rate and cumulative administered activity (62).
Median OS was reported in seven studies ranging from 6 to 48 months. Overall survival at 1 year was reported in eight studies and ranged from 38 to 100%. Median EFS was

reported in three studies ranging from 5 to 6.5 months and 1 year EFS from 18 to 33% (62).
Wilson et al. did not report detailed findings on toxicity, because the only significant acute toxicity was, as expected, myelosuppression. Haemopoietic support, typically with peripheral blood stem cells (PBSC), may be used to circumvent myelosuppression (62).
In 2016, George et al. reported that a personalised approach combining patient-specific dosimetry and clinical judgement, enabled delivery of high activities tolerated by patients, particularly with stem cell support. The overall response rate was 58% (complete or partial response) (91).

^{131}I-MIBG therapy in localised unresectable neuroblastoma

^{131}I-MIBG therapy also proved to be an effective treatment modality for unresectable localised neuroblastoma causing or in danger of causing organ or respiratory dysfunction and to offer a good alternative to chemotherapy if urgent treatment is needed (92).
Since the prognosis of localised neuroblastoma is good, toxicity and late effects should be avoided if possible. Schoot/Bleeker et al. reported a 10-year OS of 90.5%. Garaventa et al., reported a 5-year OS of 91% for patients with low-risk localised neuroblastoma with standard chemotherapy (vincristine, cyclophosphamide and doxorubicin) (93). In another study Rubie et al. reported a 5-year OS of 99 % for a heterogeneous patient group of 120 infants (94).
No treatment-related deaths were observed. However, progressive and recurrent events occurred in 12 of 120 patients. In the cohort of Schoot/Bleeker et al. two patients died. These deaths were not related to ^{131}I-MIBG therapy but to progression to high-risk disease and to complications of surgery (92).
Low-risk localised neuroblastomas were shown to have an excellent prognosis with standard-dose chemotherapy, although other studies reported that these patients with poor prognostic factors responded better to a high-dose protocol then when treated with a standard-dose protocol (93-95). Most treatment failures are caused by poor prognostic factors, like MYCN amplification (93, 94, 96).

Future perspectives

Although a lot of studies have been published on the use of ^{131}I-MIBG therapy, and ^{131}I-MIBG therapy seems to be a promising treatment modality, more data is needed to implement this treatment modality in international neuroblastoma protocols. Particularly data on upfront ^{131}I-MIBG therapy are limited to two European studies.
It is important to know how effective ^{131}I-MIBG therapy is compared to chemotherapy regimens. Furthermore it is important to know whether there is a benefit of concomitant chemotherapy compared to ^{131}I-MIBG therapy alone.

The relationship between administered activity and response should be investigated, as well as the optimum dose.

Furthermore it is important that future trials take account of distinction between relapsed and refractory patients.

Next to acute toxicity it is important to further investigate whether ^{131}I-MIBG therapy causes long-term toxicity, like thyroid toxicity, primary ovarian insufficiency and/or secondary malignancies.

To improve the known activity of ^{131}I-MIBG therapy, several studies are using different theoretical approaches. The first strategy combines ^{131}I-MIBG with cytotoxic chemotherapy agents known to also have activity in neuroblastoma. The second strategy involves combining ^{131}I-MIBG with radiation sensitizers that enhance the anti-tumour effect of ^{131}I-MIBG and may protect normal tissues from damaging effects of radiation. The third strategy involves increasing ^{131}I-MIBG uptake by neuroblastoma cells, either by combining ^{131}I-MIBG with drugs that increase NET expression, or through the use of high-specific active ^{131}I-MIBG (97).

To further adopt ^{131}I-MIBG therapy for safe and effective properties, it is important to replace fixed administered activity by scaling to size (weight) in future studies and use whole-body and tumour doses as measures to evaluate correlation with response rates and other outcome measures (62).

gbleeker78@gmail.com

References

1. Brodeur GM. Neuroblastoma: biological insights into a clinical enigma. Nat Rev Cancer. 2003;3:203-16
2. Castleberry RP. Neuroblastoma. Eur J Cancer. 1997;33:1430-7
3. Park JR, Eggert A, Caron H. Neuroblastoma: biology, prognosis, and treatment. Pediatr Clin North Am. 2008;55:97-120
4. Maris JM, Hogarty MD, Bagatell R, et al. Neuroblastoma. Lancet. 2007;369:2106-20
5. Spix C, Pastore G, Sankila R, et al. Neuroblastoma incidence and survival in European children (1978-1997): report from the Automated Childhood Cancer Information System project. Eur J Cancer. 2006;42:2081-91
6. Esiashvili N, Anderson C, Katzenstein HM. Neuroblastoma. Curr Probl Cancer. 2009;33:333-60
7. Gurney JG, Davis S, Severson RK, et al. Trends in cancer incidence among children in the U.S. Cancer. 1996;78:532-41
8. Gurney JG, Ross JA, Wall DA, et al. Infant cancer in the U.S.: histology-specific incidence and trends, 1973 to 1992. J Pediatr Hematol Oncol. 1997;19:428-32
9. Kaatsch P. Epidemiology of childhood cancer. Cancer Treat Rev. 2010;36:277-85
10. Maris JM. Recent advances in neuroblastoma. N Engl J Med. 2010;362:2202-11
11. Schwab M, Westermann F, Hero B, et al. Neuroblastoma: biology and molecular and chromosomal pathology. Lancet Oncol. 2003;4:472-80

12. Brodeur GM, Seeger RC, Barrett A, et al. International criteria for diagnosis, staging, and response to treatment in patients with neuroblastoma. J Clin Oncol. 1988;6:1874-81
13. Brodeur GM, Pritchard J, Berthold F, et al. Revisions of the international criteria for neuroblastoma diagnosis, staging, and response to treatment. J Clin Oncol. 1993;11:1466-77
14. Monclair T, Brodeur GM, Ambros PF, et al. The International Neuroblastoma Risk Group (INRG) Staging System: An INRG Task Force Report. J Clin Oncol. 2009; 27(2): 298–303
15. Cohn SL, Pearson AD, London WB, et al. The International Neuroblastoma Risk Group (INRG) classification system: an INRG Task Force report. J Clin Oncol. 2009;27:289-97
16. Shimada H, Chatten J, Newton WA, Jr., et al. Histopathologic prognostic factors in neuroblastic tumors: definition of subtypes of ganglioneuroblastoma and an age-linked classification of neuroblastomas. J Natl Cancer Inst. 1984;73:405-16
17. Shimada H, Ambros IM, Dehner LP, et al. The International Neuroblastoma Pathology Classification (the Shimada system). Cancer. 1999;86:364-72
18. Bombardieri E, Aktolun C, Baum RP, et al. 131I/123I-metaiodobenzylguanidine (MIBG) scintigraphy: procedure guidelines for tumour imaging. Eur J Nucl Med Mol Imaging. 2003;30:BP132-9
19. Olivier P, Colarinha P, Fettich J, et al. Guidelines for radioiodinated MIBG scintigraphy in children. Eur J Nucl Med Mol Imaging. 2003;30:B45-50
20. Bleeker G, Tytgat GA, Adam JA, et al. 123I-MIBG scintigraphy and 18F-FDG-PET imaging for diagnosing neuroblastoma. Cochrane Database of Systematic Reviews. 2015, issue 9.
21. Sharp SE, Parisi MT, Gelfand MJ, et al. Functional-metabolic imaging of neuroblastoma. Q J Nucl Med Mol Imaging. 2013;57:6-20
22. Matthay KK, Shulkin B, Ladenstein R, et al. Criteria for evaluation of disease extent by (123)I-metaiodobenzylguanidine scans in neuroblastoma: a report for the International Neuroblastoma Risk Group (INRG) Task Force. Br J Cancer. 2010;102:1319-26
23. Evans AE, Silber JH, Shpilsky A, et al. Successful management of low-stage neuroblastoma without adjuvant therapies: a comparison of two decades, 1972 through 1981 and 1982 through 1992, in a single institution. J Clin Oncol. 1996;14:2504-10
24. Plantaz D, Hartmann O, Kalifa C, et al. Dumbbell neuroblastoma. Experience at the Gustave Roussy Institute in 38 cases treated from 1982 to 1987. Arch Fr Pediatr. 1991;48:529-33
25. Plantaz D, Hartmann O, Kalifa C, et al. Localized dumbbell neuroblastoma: a study of 25 cases treated between 1982 and 1987 using the same protocol. Med Pediatr Oncol. 1993;21:249-53
26. Plantaz D, Rubie H, Michon J, et al. The treatment of neuroblastoma with intraspinall extension with chemotherapy followed by surgical removal of residual disease. A prospective study of 42 patients–results of the NBL 90 Study of the French Society of Pediatric Oncology. Cancer. 1996;78:311-9
27. Rubie H, De BB, Gerrard M, et al. Excellent outcome with reduced treatment in infants with nonmetastatic and unresectable neuroblastoma without MYCN amplification: results of the prospective INES 99.1. J Clin Oncol. 2011;29:449-55
28. Nickerson HJ, Matthay KK, Seeger RC, et al. Favorable biology and outcome of stage IV-S neuroblastoma with supportive care or minimal therapy: a Children's Cancer Group study. J Clin Oncol. 2000;18:477-86
29. Pearson AD, Pinkerton CR, Lewis IJ, et al. High-dose rapid and standard induction chemotherapy for patients aged over 1 year with stage 4 neuroblastoma: a randomised trial. Lancet Oncol. 2008;9:247-56
30. Yu AL, Gilman AL, Ozkaynak MF, et al. Anti-GD2 antibody with GM-CSF, interleukin-2, and isotretinoin for neuroblastoma. N Engl J Med. 2010;363:1324-34
31. Sharp SE, Trout AT, Weiss BD, Gelfand MJ. MIBG in Neuroblastoma Diagnostic Imaging and Therapy. Radiographics. 2016;36(1):258-78
32. Matthay KK. Intensification of therapy using hematopoietic stem-cell support for high-risk neuroblastoma. Pediatr Transplant. 1999;3(suppl 1):72–7
33. Pearson AD, Pinkerton CR, Lewis IJ, et al. High-dose rapid and standard induction chemotherapy for patients aged over 1 year with stage 4 neuroblastoma: a rondomised trial; European Neuroblastoma Study Group; Children's Cancer and Leukaemia Group (CCLG formerly United Kingdom Children's Cancer Study Group).Lancet Oncol. 2008;9(3):247-56
34. Wieland DM, Wu J, Brown LE, et al. Radiolabeled adrenergic neuron-blocking agents: adrenomedullary imaging with 131I iodobenzylguanidine. J Nucl Med. 1980;21(4):349–53
35. Wieland DM, Brown LE, Tobes MC, et al. Imaging the primate adrenal medulla with 123I and 131I meta-iodobenzylguanidine: concise communication. J Nucl Med. 1981;22(4):358–64
36. Vallabhajosula S, Nikolopoulou A. Radioiodinated metaiodobenzylguanidine (MIBG): radiochemistry, biology, and pharmacology. Semin Nucl Med. 2011;41(5):324-33
37. Smets LA, Loesberg C, Janssen M, et al. Active uptake and extravesicular storage of m-iodobenzylguanidine in human neuroblastoma SKNSH cells. Cancer Res. 1989;49:2941-4
38. Taggart D, Dubois S, Matthay KK. Radiolabeled metaiodobenzylguanidine for imaging and therapy of neuroblastoma. Q J Nucl Med Mol Imaging. 2008;52:403-18
39. Vaidyanathan G. Meta-iodobenzylguanidine and analogues: chemistry and biology. Q J Nucl Med Mol Imaging. 2008;52:351-68 .
40. Bomanji J, Levison DA, Flatman WD, et al. Uptake of iodine-123 MIBG by pheochromocytomas, paragangliomas, and neuroblastomas: A histopathological comparison. J Nucl Med. 1987;28:973-8
41. Jaques S, Tobes MC, Sisson JC, et al. Comparison of the sodium dependency of uptake of meta-iodobenzylguanidine and norepinephrine into cultured bovine adrenomedullary cells. Mol Pharmacol. 1984;26:539-46
42. Tobes MC, Jaques S, Wieland DM, et al. Effect of uptake-one inhibitors on the uptake of norepinephrine and metaiodobenzylguanidine. J Nucl Med. 1985;26:897-907
43. Mairs RJ, Livingstone AL, Gaze MN, et al. Prediction of accumulation of 131I-meta-iodo-benzyl guanidine in

neuroblastoma cell lines by means of reverse transcription and polymerase chain reaction. Br J Cancer. 1994;70:97-101
44. Carlin S, Mairs RJ, McCluskey AG, et al. Development of a real-time polymerase chain reaction assay for prediction of the uptake of [131I]meta-iodobenzylguanidine by neuroblastoma tumors. Clin Cancer Res. 2003;9:3338-44
45. Naranjo A, Parisi MT, Shulkin BL, et al. Comparison of (1)(2)(3) I-metaiodobenzylguanidine (MIBG) and (1)(3)(1)I-MIBG semi-quantitative scores in predicting survival in patients with stage 4 neuroblastoma: a report from the Children's Oncology Group. Pediatr Blood Cancer. 2011;56:1041-5
46. Boubaker A, Bischof DA. MIBG scintigraphy for the diagnosis and follow-up of children with neuroblastoma. Q J Nucl Med Mol Imaging. 2008;52:388-402
47. Bombardieri E, Giammarile F, Aktolun C, et al. 131I/123I-metaiodobenzylguanidine (mIBG) scintigraphy: procedure guidelines for tumour imaging. Eur J Nucl Med Mol Imaging. 2010;37:2436-46
48. Stichting Kinderoncologie Nederland (SKION, Dutch Childhood Oncology Group (DCOG). DCOG NBL 2009 TREATMENT PROTOCOL - for Risk Adapted Treatment of Children with Neuroblastoma. 2009.
49. Schmidt M, Simon T, Hero B, et al. Is there a benefit of 131 I-MIBG therapy in the treatment of children with stage 4 neuroblastoma? A retrospective evaluation of The German Neuroblastoma Trial NB97 and implications for The German Neuroblastoma Trial NB2004. Nuklearmedizin. 2006;45(4):145-51
50. French S, DuBois SG, Horn B, et al. 131I-MIBG followed by consolidation with busulfan, melphalan and autologous stem cell transplantation for refractory neuroblastoma. Pediatr Blood Cancer. 2013;60(5):879-84
51. Yanik GA, Villablanca JG, Maris JM, et al. 131I-metaiodobenzylguanidine with intensive chemotherapy and autologous stem cell transplantation for high-risk neuroblastoma. A new approaches to neuroblastoma therapy (NANT) phase II study. Biol Blood Marrow Transplant. 2015;21(4):673-81
52. van Santen HM, de Kraker J, van Eck BL, de Vijlder JJ, Vulsma T. High incidence of thyroid dysfunction despite prophylaxis with potassium iodide during (131)I-meta-iodobenzylguanidine treatment in children with neuroblastoma. Cancer. 2002;94(7):2081-9
53. Bleeker G, Schoot RA, Caron HN, et al. Toxicity of upfront ^{131}I-metaiodobenzylguanidine (^{131}I-MIBG) therapy in newly diagnosed neuroblastoma patients: a retrospective analysis. Eur J Nucl Med Mol Imaging. 2013;40(11):1711-7
54. DuBois SG, Messina J, Maris JM, et al. Hematologic toxicity of high-dose iodine-131-metaiodobenzylguanidine therapy for advanced neuroblastoma. J Clin Oncol. 2004;22:2452-60
55. Matthay KK, DeSantes K, Hasegawa B, et al. Phase I dose escalation of 131I-metaiodobenzylguanidine with autologous bone marrow support in refractory neuroblastoma. J Clin Oncol. 1998;16:229-36
56. Mastrangelo S, Rufini V, Ruggiero A, et al. Treatment of advanced neuroblastoma in children over 1 year of age: the critical role of (1)(3)(1)I-metaiodobenzylguanidine combined with chemotherapy in a rapid induction regimen. Pediatr Blood Cancer. 2011;56:1032-40
57. Matthay KK, Quach A, Huberty J, et al. Iodine-131–metaiodobenzylguanidine double infusion with autologous stem-cell rescue for neuroblastoma: a new approaches to neuroblastoma therapy phase I study. J Clin Oncol. 2009;27:1020-5
58. Won SC, Kwon SY, Han JW, et al. Posterior reversible encephalopathy syndrome in childhood with hematologic/oncologic diseases. J Pediatr Hematol Oncol. 2009;31:505-8
59. van Santen HM, Tytgat GA, van de Wetering MD, et al. Differentiated thyroid carcinoma after 131I-MIBG treatment for neuroblastoma during childhood: description of the first two cases. Thyroid. 2012;22:643-6
60. Clement SC, Kraal KC, van Eck-Smit BL, et al. Primary ovarian insufficiency in children after treatment with (131) i-metaiodobenzylguanidine for neuroblastoma: report of the first two cases. J Clin Endocrinol Metab. 2014;99:E112-6
61. Garaventa A, Gambini C, Villavecchia G, et al. Second malignancies in children with neuroblastoma after combined treatment with 131I-metaiodobenzylguanidine. Cancer. 2003;97:1332-8
62. Wilson JS, Gains JE, Moroz V, Wheatley K, Gaze MN. A systematic review of 131I-meta iodobenzylguanidine molecular radiotherapy for neuroblastoma. Eur J Cancer. 2014;50(4):801-15
63. de Kraker J, Hoefnagel KA, Verschuur AC, et al. Iodine-131-metaiodobenzylguanidine as initial induction therapy in stage 4 neuroblastoma patients over 1 year of age. Eur J Cancer. 2008;44(4):551–6
64. Klingebiel T, Bader P, Bares R, et al. Treatment of neuroblastoma stage 4 with 131I-meta-iodo-benzylguanidine, high-dose chemotherapy and immunotherapy. A pilot study. Eur J Cancer 1998;34(9):1398–402
65. Simon T, Schmidt M, Decarolis B, et al. I-131-meta-iodobenzylguanidine therapy improves survival in high-risk neuroblastoma patients with mIBG positive residual metastatic disease (#85). Abstract. ANR 2016.
66. Lumbroso J, Hartmann O, Schlumberger M. Therapeutic use of [131I]metaiodobenzylguanidine in neuroblastoma: a phase II study in 26 patients. "Societe Francaise d'Oncologie Pediatrique" and Nuclear Medicine Co-investigators. J Nucl Biol Med 1991;35(4):220–3
67. Castel V, Canete A, Melero C, et al. Results of the cooperative protocol (N-III-95) for metastatic relapses and refractory neuroblastoma. Med Pediatr Oncol. 2000;35(6):724–6
68. Dubois SG, Chesler L, Groshen S, et al. Phase I study of vincristine, irinotecan, and 131Imetaiodobenzylguanidine for patients with relapsed or refractory neuroblastoma: a new approaches to neuroblastoma therapy trial. Clin Cancer Res. 2012;18(9):2679–86
69. Klingebiel T, Feine U, Treuner J, et al. Treatment of neuroblastoma with [131I]metaiodobenzylguanidine: long-term results in 25 patients. J Nucl Biol Med. 1991;35(4):216–9
70. Matthay KK, Tan JC, Villablanca JG, et al. Phase I dose escalation of iodine-131-metaiodobenzylguanidine with myeloablative

chemotherapy and autologous stem-cell transplantation in refractory neuroblastoma: a new approaches to Neuroblastoma Therapy Consortium Study. J Clin Oncol. 2006;24(3):500–6
71. Miano M, Garaventa A, Pizzitola MR, et al. Megatherapy combining 131I metaiodobenzylguanidine and high-dose chemotherapy with haematopoietic progenitor cell rescue for neuroblastoma. Bone Marrow Transplant. 2001;27(6):571–4
72. Yanik GA, Levine JE, Matthay KK, et al. Pilot study of iodine-131-metaiodobenzylguanidine in combination with myeloablative chemotherapy and autologous stem-cell support for the treatment of neuroblastoma. J Clin Oncol. 2002;20(8):2142–9
73. Castellani MR, Rottoli L, Maffioli L, et al. Experience with palliative [131I]metaiodobenzylguanidine therapy in advanced neuroblastoma. J Nucl Biol Med. 1991;35(4):241–3
74. Claudiani F, Garaventa A, Bertolazzi L, et al. [131I] metaiodobenzylguanidine therapy in advanced neuroblastoma. J Nucl Biol Med. 1991;35(4):224–7
75. Garaventa A, Bellagamba O, Lo Piccolo MS, et al. 131I-metaiodobenzylguanidine (131IMIBG) therapy for residual neuroblastoma: a mono-institutional experience with 43 patients. Br J Cancer. 1999;81(8):1378–84
76. Hoefnagel CA, Voute PA, De KJ, et al. Radionuclide diagnosis and therapy of neural crest tumors using iodine-13 metaiodobenzylguanidine. J Nucl Med. 1987;28(3):308–14
77. Voûte PA, Hoefnagel CA, De KJ, et al. Results of treatment with 131I-metaiodobenzylguanidine (131I-MIBG) in patients with neuroblastoma. Future prospects of zetotherapy. Prog Clin Biol Res. 1991;366:439–45
78. Hutchinson RJ, Sisson JC, Shapiro B, et al. 131-I-metaiodobenzylguanidine treatment in patients with refractory advanced neuroblastoma. Am J Clin Oncol. 1992;15(3):226–32
79. Johnson K, McGlynn B, Saggio J, et al. Safety and efficacy of tandem 131I-metaiodobenzylguanidine infusions in relapsed/refractory neuroblastoma. Pediatr Blood Cancer. 2011;57(7):1124–9
80. Kang TI, Brophy P, Hickeson M, et al. Targeted radiotherapy with submyeloablative doses of 131I-MIBG is effective for disease palliation in highly refractor neuroblastoma. J Pediatr Hematol Oncol. 2003;25(10):769–73
81. Klingebiel T, Berthold F, Treuner J, et al. Metaiodobenzylguanidine (mIBG) in treatment of 47 patients with neuroblastoma: results of the German Neuroblastoma Trial. Med Pediatr Oncol. 1991;19(2):84–8
82. Lashford LS, Lewis IJ, Fielding SL, et al. Phase I/II study of iodine 131 metaiodobenzylguanidine in chemoresistant neuroblastoma: a United Kingdom Children's Cancer Study Group investigation. J Clin Oncol. 1992;10(12):1889–96
83. Matthay KK, Panina C, Huberty J, et al. Correlation of tumor and whole-body dosimetry with tumor response and toxicity in refractory neuroblastoma treated with 131I-MIBG. J Nucl Med. 2001;42(11):1713–21
84. Matthay KK, Yanik G, Messina J, et al. Phase II study on the effect of disease sites, age, and prior therapy on response to iodine-131-metaiodobenzylguanidine therapy in refractory neuroblastoma. J Clin Oncol. 2007;25(9):1054–60
85. Matthay KK, Weiss B, Villablanca JG, et al. Dose escalation study of no-carrier-added 131Imetaiodobenzylguanidine for relapsed or refractory neuroblastoma: new approaches to Neuroblastoma Therapy Consortium trial. J Nucl Med. 2012;2012:1155–63
86. Schwabe D, Sahm S, Gerein V, et al. 131-Metaiodobenzylguanedine therapy of neuroblastoma in childhood. One year of therapeutic experience. Eur J Pediatr. 1987;146(3):246–50
87. Treuner J, Klingebiel T, Bruchelt G, et al. Treatment of neuroblastoma with metaiodobenzylguanidine: results and side effects. Med Pediatr Oncol. 1987;15(4):199–202
88. Treuner J, Gerein V, Klingebiel T, et al. MIBG-treatment in neuroblastoma; experiences of the Tubingen/Frankfurt group. Prog Clin Biol Res. 1988;271:669–78
89. Troncone L, Rufini V, Riccardi R, et al. The use of [131I] metaiodobenzylguanidine in the treatment of neuroblastoma after conventional therapy. J Nucl Biol Med. 1991;35(4):232–6
90. Zhou MJ, Doral MY, DuBois SG, et al. Different outcomes for relapsed versus refractory neuroblastoma after therapy with (131)I-metaiodobenzylguanidine ((131)I-MIBG). Eur J Cancer. 2015;51(16):2465-72
91. George SL, Falzone N, Chittenden S, et al. Individualized 131I-mIBG therapy in the management of refractory and relapsed neuroblastoma. Nucl Med Commun. 2016;37(5):466-72
92. Schoot RA, Bleeker G, Caron HN, et al. The role of 131I-metaiodobenzylguanidine (MIBG) therapy in unresectable and compromising localised neuroblastoma. Eur J Nucl Med Mol Imaging. 2013;40(10):1516-22
93. Garaventa A, Boni L, Lo Piccolo MS, et al. Localized unresectable neuroblastoma: results of treatment based on clinical prognostic factors. Ann Oncol. 2002;13:956-64
94. Rubie H, De Bernardi B, Gerrard M, et al. Excellent outcome with reduced treatment in infants with nonmetastatic and unresectable neuroblastoma without MYCN amplification: results of the prospective INES 99.1. J Clin Oncol. 2011;29:449-55
95. Garaventa A, De Bernardi B, Pianca C, et al. Localized but unresectable neuroblastoma: treatment and outcome of 145 cases. Italian Cooperative Group for Neuroblastoma. J Clin Oncol. 1993;11:1770-9
96. Matthay KK, Perez C, Seeger RC, et al. Successful treatment of stage III neuroblastoma based on prospective biologic staging: a Children's Cancer Group study. J Clin Oncol. 1998;16:1256-64
97. DuBois SG, Matthay KK. 131I-Metaiodobenzylguanidine therapy in children with advanced neuroblastoma. Q J Nucl Med Mol Imaging. 2013;57:53-65

Radium-223 dichloride in the treatment of metastatic prostate cancer

D.N.J. Wyndaele, MD[1]; R. van der Voort, PhD[2]; E.L. Koldewijn, MD, PhD[3]; L.J.C. van Warmerdam, MD, PhD[4]

Departments of [1]Nuclear Medicine, [3]Urology & [4]Internal Medicine and Oncology, Catharina Hospital, Eindhoven, the Netherlands
[2]Vision Medical Communications, Nijmegen, the Netherlands

Abstract

Wyndaele DNJ, Van der Voort R, Koldewijn EL, Van Warmerdam LJC. Radium-223 dichloride in the treatment of metastatic prostate cancer. The recent introduction of a number of effective therapies has greatly improved the treatment of metastatic castration-resistant prostate cancer. In addition to chemotherapy and hormonal therapy, also treatment with the radiopharmaceutical radium-223 dichloride contributed to this improvement, especially in patients with symptomatic bone metastases. Consequently, nuclear medicine physicians are increasingly involved in the multidisciplinary management of metastatic castration-resistant prostate cancer. This review article summarises the results of key clinical studies and provides an overview of the current treatment options in metastatic prostate cancer, with a special focus on radium-223.
Tijdschr Nucl Geneesk 2016; 38(4):1655-1659

Introduction

With an estimated incidence of 1.1 million in 2012, prostate cancer is the second most common cancer in men worldwide (1). The incidence is highest in developed countries, including those of Western and Northern Europe, mostly due to routine testing for prostate-specific antigen (PSA) in these regions. Up to one third of prostate cancer patients present with metastatic disease at the time of diagnosis, while others develop metastases in the course of their disease, despite treatment with surgery or radiotherapy (2). Treatment of metastatic prostate cancer is palliative in nature and consists primarily of androgen deprivation therapy (ADT). Since prostate cancer cells are highly dependent on androgens, predominantly testosterone, ADT is an effective therapy. In the first line, ADT may include bilateral orchiectomy or chemical castration with luteinising hormone-releasing hormone (LHRH) agonists or antagonists, and/or anti-androgen therapy. Although the far majority of tumours initially responds to these hormonal therapies, they become hormone-refractory after a median of two years (3). Since the recent authorisation of a number of therapies, multiple options exist for the treatment of hormone- or castration-resistant prostate cancer (CRPC). These options include chemotherapy and second generation hormonal therapy with agents that block the androgen pathway, but also continuation of classical ADT. Moreover, since many CRPC patients suffer from symptomatic bone metastases, treatment with bone targeted agents such as bisphosphonates, denosumab and radiopharmaceuticals is common (4). In this setting the radiopharmaceutical radium-223 dichloride (^{223}Ra) gained particular attention last few years. This alpha emitter mimics calcium and consequently specifically targets osseous metastases. Recent studies demonstrated that ^{223}Ra not only improves the patients' quality of life, but also their time to first symptomatic skeletal event and overall survival (OS) (2). Furthermore, due to its favourable toxicity profile, ^{223}Ra seems an attractive agent to be combined with chemotherapy, hormonal therapy and even immunotherapy, although their clinical application remains limited because of ongoing clinical trials and financial issues (5). Indeed, there has been much research and debate on the optimal sequence and combination of the available therapies for metastatic CRPC (mCRPC), including the role and place of ^{223}Ra.
The aim of this review is to summarise the current knowledge and clinical practice regarding the management of mCRPC, including treatment with ^{223}Ra.

Chemotherapy for metastatic prostate cancer

Chemotherapy is a major option in the treatment of mCRPC, especially since the registration of docetaxel combined with prednisone by the FDA and EMA in 2004. This registration was preceded by TAX 327, a randomised phase 3 study demonstrating that docetaxel plus prednisone compared with mitoxantrone plus prednisone significantly improved the serum PSA level, quality of life and OS of mCRPC patients (6). Although docetaxel also reduced the pain experienced by the participating patients, it generally increased the occurrence of adverse events (AEs), including fatigue, diarrhoea and sensory neuropathy. Additional analyses indicated that the OS benefit of docetaxel versus mitoxantrone was greater in patients with poorly differentiated tumours (Gleason score ≥7) at diagnosis than in patients with more differentiated tumours (Gleason score ≤6) (7). At the time of the TAX 327 study, also

the randomised phase 3 SWOG 99-16 trial showed a survival benefit of docetaxel in the first line setting. In this study Petrylak et al. demonstrated that docetaxel and estramustine compared with mitoxantrone and prednisone significantly improved the OS, time to progression and objective tumour responses (8). However, the effectiveness of docetaxel and estramustine was accompanied with an increase in AEs, particularly grade 3 or 4 neutropenic fever, nausea and vomiting, and cardiovascular events such as impaired arterial circulation including ischaemic heart disease, venous thromboembolism, cardiac decompensation and cerebral depression.

Patients who fail on docetaxel can be treated with cabazitaxel, another member of the family of taxane-based chemotherapy. Registration of cabazitaxel in this setting followed the results of the TROPIC trial which showed that cabazitaxel plus prednisone versus mitoxantrone plus prednisone significantly improved the OS, PFS and several other endpoints (9). The most common grade ≥3 AEs were neutropenia (82% in the cabazitaxel arm vs. 58% in the control arm) and diarrhoea (6% vs. <1%, respectively). Furthermore, 8% of the patients in the cabazitaxel arm had febrile neutropenia compared with 1% in the mitoxantrone arm. The randomised phase 3 FIRSTANA trial currently compares cabazitaxel with docetaxel as a first-line therapy for mCRPC.

Following the positive results with docetaxel in mCRPC, several studies evaluated the value of docetaxel in the castration-sensitive setting. Although a study by Franke et al. demonstrated that castration was associated with a significantly increased docetaxel clearance, a number of randomised phase 3 studies showed great benefit of docetaxel in hormone-naïve patients (11). The CHAARTED and STAMPEDE trials convincingly demonstrated that the addition of docetaxel to ADT or standard of care, respectively, resulted in an improved OS of patients with metastatic hormone sensitive prostate cancer (12,13). In addition, although the GETUG-AFU 15 study did not show a statistically improved OS of mHSPC patients following the addition of docetaxel to ADT, it did also demonstrate an improvement in progression-free survival (PFS) (14). Two recent meta-analyses confirmed the benefit of upfront docetaxel (15,16). Based on these results it is now common practice to combine ADT with docetaxel in fit patients with newly diagnosed, hormone-naïve metastatic prostate cancer (17).

Agents targeting the androgen pathway

Another major treatment option in mCRPC is hormonal therapy with novel agents that target the androgen pathway. The most effective agents include abiraterone, a specific inhibitor of the enzyme CYP17A1 which catalyses two essential reactions in the biosynthesis of androgens, and enzalutamide, an inhibitor of the androgen receptor. For instance, the randomised phase 3 COU-AA-301 trial showed that abiraterone plus prednisone compared with placebo and prednisone significantly prolonged the OS of mCRPC patients previously treated with docetaxel (18,19). In addition, abiraterone improved the secondary endpoints time to progression, PFS and PSA response rate. Furthermore, abiraterone was shown to have a favourable toxicity profile. The most common grade 3-4 AEs were fatigue (9% in the abiraterone arm vs. 10% in the control arm), anaemia (8% in both arms) and back pain (7% vs. 10%).

Also enzalutamide was reported to be beneficial in the treatment of mCRPC. Thus, the randomised phase 3 AFFIRM trial demonstrated that enzalutamide compared with placebo significantly prolonged the survival of mCRPC patients who progressed on docetaxel (20). The superiority of enzalutamide over placebo was also shown with respect to all secondary endpoints, including the PSA response rate, PFS and quality of life. The rates of the most common AEs, fatigue, diarrhoea and hot flushes, were higher in the enzalutamide arm.

Although initially indicated as second line treatments, following chemotherapy with docetaxel, enzalutamide and abiraterone were also associated with positive results in the upfront treatment of mCRPC. Thus, the phase 3 COU-AA-302 trial demonstrated that abiraterone plus prednisone versus placebo plus prednisone improved the PFS and OS of chemotherapy-naïve mCRPC patients (21,22). Furthermore, abiraterone was superior over placebo with respect to time to initiation of chemotherapy, opiate use for cancer-related pain, PSA progression, and decline in performance status. The most common grade 3–4 AEs of special interest were cardiac disorders (8% in the abiraterone arm vs. 4% in the control arm), increased alanine aminotransferase (6% vs. <1%), and hypertension (5% vs. 3%).

In addition to abiraterone, also enzalutamide was shown to result in improved outcomes when given before chemotherapy. The landmark phase 3 PREVAIL trial showed that enzalutamide compared with placebo significantly improved the PFS and OS in mCRPC patients who had not received chemotherapy (23). Moreover, enzalutamide also improved all secondary endpoints, including the time until the initiation of chemotherapy, the first skeletal-related event (SRE) and PSA progression. The most common AEs of any grade were fatigue (36% in the enzalutamide arm vs. 26% in the placebo arm), back pain (27% vs. 22%) and constipation (22% vs. 17%). Head-to-head comparison trials of abiraterone and enzalutamide are necessary to determine the optimal sequencing of these agents.

Despite the significant efficacy of abiraterone and enzalutamide, a substantial number of patients develops resistance to these agents. Although our knowledge of the underlying mechanisms is still limited, some relevant factors have been revealed. For instance, Antonarakis and colleagues demonstrated that the expression of the constitutively active V7 isoform of the androgen receptor correlates with resistance to both enzalutamide and abiraterone (24). However, in view of contradicting results from recent studies, it remains uncertain if this isoform can be used as a biomarker in prostate cancer (25,26).

Treatment of bone metastases with ^{223}Ra

The majority of mCRPC patients develops bone metastases, typically in the axial skeleton and/or proximal appendicular skeleton (27). Since these metastases stimulate osteoblasts, they are associated with a number of SREs, including bone pain, elevated levels of serum alkaline phosphatase, and an increased risk of bone fractures and spinal cord compression. ^{223}Ra is an alpha particle emitting radiopharmaceutical that physically mimics calcium and hence targets osseous metastases. Since alpha particles cause more double-strand DNA breaks than beta particles but travel less far, ^{223}Ra might cause more DNA-damage within a shorter range than indicated beta emitters like samarium-153 and rhenium-188. These promising characteristics were evaluated in the phase 3 ALSYMPCA trial in which 921 mCRPC patients with symptomatic bone metastases were randomly assigned as 2:1 to treatment with ^{223}Ra or placebo in addition to the best standard of care. Every four weeks the patients in the ^{223}Ra arm received an intravenous injection at a dose of 50 kBq per kg body weight, for a total of six injections. The results demonstrated that ^{223}Ra as compared to placebo significantly improved the primary endpoint of OS, as well as the main secondary efficacy endpoints, including the time to first symptomatic skeletal event (SSE) and the time to increase in total alkaline phosphatase levels (28). Furthermore, treatment with ^{223}Ra was generally associated with less toxicity, including 56% grade 3 or 4 AEs versus 62% in the placebo arm. An extensive subgroup analysis showed that ^{223}Ra was effective and well tolerated in patients who were previously treated with docetaxel as well as those who were not (29). Another analysis demonstrated that the efficacy of ^{223}Ra was also independent of baseline opioid use (30). Prospective measurements of health-related quality of life (QOL) indicated that the improved survival associated with ^{223}Ra treatment was accompanied by significant QOL benefits (31). These benefits included a higher percentage of patients with improved QOL and a slower decrease in QOL over time in mCRPC patients treated with ^{223}Ra compared to those treated with placebo. Following the positive results of the ALSYMPCA study, the FDA and EMA authorised ^{223}Ra for the treatment of adults with CRPC, symptomatic bone metastases and no known visceral metastases (32,33).

Although the ALSYMPCA trial demonstrated that ^{223}Ra is beneficial with or without previous docetaxel treatment, it remained unclear if ^{223}Ra could be safely combined with or followed by chemo- or hormonal therapies. Hence, several studies evaluated the efficacy and safety of ^{223}Ra in a number of novel combinations and sequences. For instance, an exploratory analysis of prospectively collected data from patients participating in the ALSYMPCA trial showed that chemotherapy, predominantly involving docetaxel and mitoxantrone, following ^{223}Ra was feasible and appeared to be well tolerated (34). Furthermore, the results of a prospective, single-arm phase 3b study, which was part of an early access programme, showed that it is safe to combine ^{223}Ra with abiraterone or enzalutamide in patients with mCRPC, including those with asymptomatic bone metastases (35). Although the study had a relatively short follow-up, it additionally showed that the concomitant use of ^{223}Ra and abiraterone and/or enzalutamide, or denosumab compared to ^{223}Ra alone prolonged the median OS. Clinical studies are currently assessing if these promising results can be confirmed in a randomised setting. Interim results of the phase 2 eRADicAte trial, presented at the 2016 ASCO Genitourinary Cancers Symposium, indicated that ^{223}Ra combined with abiraterone plus prednisone improved the QOL of patients with CRPC and symptomatic bone metastases (36). In addition, patients reported less bone pain and had stabilised performance status scores following the combination treatment.

Financial aspects

Although the treatment landscape of mCRPC has changed greatly with the recent introduction of a number of effective therapies, little is known about their cost-effectiveness. Therefore, studies have been undertaken to evaluate this aspect of the current clinical care in mCRPC. For instance, in the Netherlands a study has been conducted to assess the cost-effectiveness of ^{223}Ra compared with abiraterone, enzalutamide and cabazitaxel in a population of Dutch mCRPC patients previously treated with docetaxel. The cost-effectiveness was evaluated using a Markov model, which combined efficacy, the frequency of SSEs and safety data with Dutch-specific resource use and costs for mCRPC treatment from a societal perspective. The total quality-adjusted life years (QALYs) and costs were calculated over a period of five years. The model showed that the effectiveness expressed in QALYs and life years gained were comparable between ^{223}Ra, abiraterone, enzalutamide and cabazitaxel (Peters et al., manuscript submitted for publication). However, due to lower drug and SSE-related costs, the lifetime costs were lower following ^{223}Ra treatment than after the other therapies. Thus, while ^{223}Ra offers similar gains in

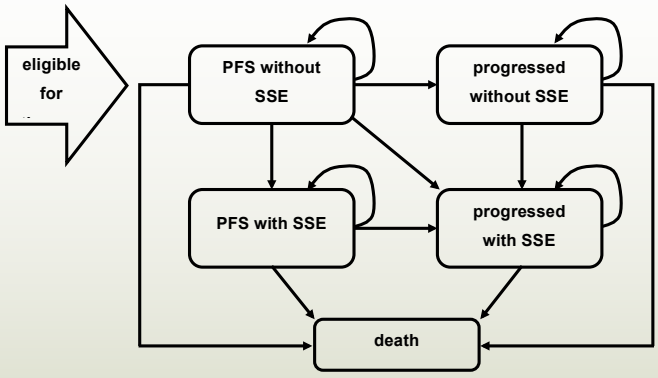

PFS = progression free survival; SSE = symptomatic skeletal-related event

Markov model structure.

Costs and health benefits of ^{223}Ra compared to cabazitaxel, abiraterone and enzalutamide.

outcome	^{223}Ra	CA	increm. ^{223}Ra-CA	^{223}Ra	AA	increm. ^{223}Ra-AA	^{223}Ra	EN	increm. ^{223}Ra-EN
discounted costs (€)	76,014	80,347	-4,333	76,014	81,926	-5,912	76,014	83,186	-7,172
discounted QALYs	0.80	0.79	0.01	0.80	0.78	0.02	0.80	0.86	-0.06
discounted LYs	1.39	1.38	0.01	1.39	1.36	0.03	1.39	1.50	-0.11
incremental cost per QALY	*Ra-223 dominates*			*Ra-223 dominates*			*Ra-223 slightly less effective and less costly*		
incremental cost per LY	*Ra-223 dominates*			*Ra-223 dominates*			*Ra-223 slightly less effective and less costly*		

AA = abiraterone acetate; CA = cabazitaxel; EN = enzalutamide; increm. = incremental; LY = life-year; QALY = quality-adjusted life year; ^{223}Ra = radium-223 dichloride

Table adapted from Peters et al., manuscript submitted for publication

health benefits compared to abiraterone, enzalutamide and cabazitaxel, it is relatively cost-saving in Dutch mCRPC patients previously treated with docetaxel.

Conclusions and perspectives

Due to intense (pre)clinical research and the continuous development of effective agents the treatment of metastatic prostate cancer has greatly improved over the last decade. Following the introduction of novel chemotherapeutics, hormonal therapies and ^{223}Ra the OS of patients with mCRPC has almost been doubled since 2004. Moreover, the establishment of ^{223}Ra for the treatment of bone metastases has significantly improved their quality of life. Hence, the nuclear medicine physician is increasingly involved in the management of metastatic prostate cancer.

Clearly, unresolved issues remain, and include the determination of the optimal timing, sequencing and combination of the treatments involved. In addition, the absence of adequate biomarkers hampers the selection of patients who may benefit more from one therapy than from another. Future studies are expected to clarify these issues and further improve the treatment of advanced prostate cancer.

Acknowledgements

This publication was financially supported by Bayer Pharma and inspired by a recent masterclass on multidisciplinary decision making in mCRPC organised by the Dutch Society of Nuclear Medicine.

dirk.wyndaele@catharinaziekenhuis.nl

References

1. GLOBOCAN: Prostate cancer. Estimated incidence, mortality and prevalence worldwide in 2012. http://globocan.iarc.fr/old/FactSheets/cancers/prostate-new.asp (September 13th, 2016)
2. Hague C and Logue JP. Clinical experience with radium-223 in the treatment of patients with advanced castrate-resistant prostate cancer and symptomatic bone metastases. Ther Adv Urol. 2016;8:175-80
3. Schellhammer PF. Combined androgen blockade for the treatment of metastatic cancer of the prostate. Urology. 1996;47:622-8
4. Gartrell BA, Coleman R, Efstathiou E, et al. Metastatic Prostate Cancer and the Bone: Significance and Therapeutic Options. Eur Urol. 2015;68:850-8
5. Madan RA, Gulley JL and Dahut WL. Radium-223 in prostate cancer: emitting the right signals. Lancet Oncol. 2016;17:1186-
6. Tannock IF, de Wit R, Berry WR, et al. Docetaxel plus prednisone or mitoxantrone plus prednisone for advanced prostate cancer. N Engl J Med. 2004;351:1502-12
7. van Soest RJ, de Morrée ES, Shen L, et al. Initial biopsy Gleason score as a predictive marker for survival benefit in patients with castration-resistant prostate cancer treated with docetaxel: data from the TAX327 study. Eur Urol. 2014;66:330-6
8. Petrylak DP, Tangen CM, Hussain MH, et al. Docetaxel and estramustine compared with mitoxantrone and prednisone for advanced refractory prostate cancer. N Engl J Med. 2004;351:1513-20
9. de Bono JS, Oudard S, Ozguroglu M, et al. Prednisone plus cabazitaxel or mitoxantrone for metastatic castration-resistant prostate cancer progressing after docetaxel treatment: a randomised open-label trial. Lancet. 2010;376:1147-54

10. Sartor AO, Oudard S, Sengelov L, et al. Cabazitaxel vs docetaxel in chemotherapy-naive (CN) patients with metastatic castration-resistant prostate cancer (mCRPC): A three-arm phase III study (FIRSTANA). J Clin Oncol. 2016:34 (suppl):abstr 5006
11. Franke RM, Carducci MA, Rudek MA, et al. Castration-dependent pharmacokinetics of docetaxel in patients with prostate cancer. J Clin Oncol. 2010;28:4562-7
12. Sweeney CJ, Chen YH, Carducci M, et al. Chemohormonal Therapy in Metastatic Hormone-Sensitive Prostate Cancer. N Engl J Med. 2015;373:737-46
13. James ND, Sydes MR, Clarke NW, et al. Addition of docetaxel, zoledronic acid, or both to first-line long-term hormone therapy in prostate cancer (STAMPEDE): survival results from an adaptive, multiarm, multistage, platform randomised controlled trial. Lancet. 2016;387:1163-77
14. Gravis G, Fizazi K, Joly F, et al. Androgen-deprivation therapy alone or with docetaxel in non-castrate metastatic prostate cancer (GETUG-AFU 15): a randomised, open-label, phase 3 trial. Lancet Oncol. 2013;14:149-58
15. Tucci M, Bertaglia V, Vignani F, et al. Addition of Docetaxel to Androgen Deprivation Therapy for Patients with Hormone-sensitive Metastatic Prostate Cancer: A Systematic Review and Meta-analysis. Eur Urol. 2016;69:563-73
16. Vale CL, Burdett S, Rydzewska LH, et al. Addition of docetaxel or bisphosphonates to standard of care in men with localised or metastatic, hormone-sensitive prostate cancer: a systematic review and meta-analyses of aggregate data. Lancet Oncol. 2016;17:243-56
17. Cornford P, Bellmunt J, Bolla M, et al. EAU-ESTRO-SIOG Guidelines on Prostate Cancer. Part II: Treatment of Relapsing, Metastatic, and Castration-Resistant Prostate Cancer. Eur Urol. 2016 Aug 31. [Epub ahead of print]
18. de Bono JS, Logothetis CJ, Molina A, et al. Abiraterone and increased survival in metastatic prostate cancer. N Engl J Med. 2011;364:1995-2005
19. Fizazi K, Scher HI, Molina A, et al. Abiraterone acetate for treatment of metastatic castration-resistant prostate cancer: final overall survival analysis of the COU-AA-301 randomised, double-blind, placebo-controlled phase 3 study. Lancet Oncol. 2012;13:983-92
20. Scher HI, Fizazi K, Saad F, et al. Increased survival with enzalutamide in prostate cancer after chemotherapy. N Engl J Med. 2012;367:1187-97
21. Ryan CJ, Smith MR, de Bono JS, et al. Abiraterone in metastatic prostate cancer without previous chemotherapy. N Engl J Med. 2013;368:138-48
22. Ryan CJ, Smith MR, Fizazi K, et al. Abiraterone acetate plus prednisone versus placebo plus prednisone in chemotherapy-naive men with metastatic castration-resistant prostate cancer (COU-AA-302): final overall survival analysis of a randomised, double-blind, placebo-controlled phase 3 study. Lancet Oncol. 2015;16:152-60
23. Beer TM, Armstrong AJ, Rathkopf DE, et al. Enzalutamide in metastatic prostate cancer before chemotherapy. N Engl J Med. 2014;371:424-33
24. Antonarakis ES, Lu C, Wang H, et al. AR-V7 and resistance to enzalutamide and abiraterone in prostate cancer. N Engl J Med. 2014;371:1028-38
25. Bernemann C, Schnoeller TJ, Luedeke M, et al. Expression of AR-V7 in Circulating Tumour Cells Does Not Preclude Response to Next Generation Androgen Deprivation Therapy in Patients with Castration Resistant Prostate Cancer. Eur Urol. 2016 Jul 25. [Epub ahead of print]
26. Takeuchi T, Okuno Y, Hattori-Kato M, et al. Detection of AR-V7 mRNA in whole blood may not predict the effectiveness of novel endocrine drugs for castration-resistant prostate cancer. Res Rep Urol. 2016;8:21-5
27. Coleman RE. Clinical features of metastatic bone disease and risk of skeletal morbidity. Clin Cancer Res. 2006;12:6243s-6249s
28. Parker C, Nilsson S, Heinrich D, et al. Alpha emitter radium-223 and survival in metastatic prostate cancer. N Engl J Med. 2013;369:213-23
29. Hoskin P, Sartor O, O'Sullivan JM, et al. Efficacy and safety of radium-223 dichloride in patients with castration-resistant prostate cancer and symptomatic bone metastases, with or without previous docetaxel use: a prespecified subgroup analysis from the randomised, double-blind, phase 3 ALSYMPCA trial. Lancet Oncol. 2014;15:1397-406
30. Parker C, Finkelstein SE, Michalski JM, et al. Efficacy and Safety of Radium-223 Dichloride in Symptomatic Castration-resistant Prostate Cancer Patients With or Without Baseline Opioid Use From the Phase 3 ALSYMPCA Trial. Eur Urol. 2016 Jun 22. [Epub ahead of print]
31. Nilsson S, Cislo P, Sartor O, et al. Patient-reported quality-of-life analysis of radium-223 dichloride from the phase III ALSYMPCA study. Ann Oncol. 2016;27:868-74
32. FDA: approval radium-223 dichloride. http://www.fda.gov/Drugs/InformationOnDrugs/ApprovedDrugs/ucm352393.htm (September 13th, 2016)
33. EMA: approval radium-223 dichloride. http://www.ema.europa.eu/ema/index.jsp?curl=pages/medicines/human/medicines/002653/human_med_001692.jsp&mid=WC0b01ac058001d124 (September 13th, 2016)
34. Sartor O, Hoskin P, Coleman RE, et al. Chemotherapy following radium-223 dichloride treatment in ALSYMPCA. Prostate. 2016;76:905-16
35. Saad F, Carles J, Gillessen S, et al. Radium-223 and concomitant therapies in patients with metastatic castration-resistant prostate cancer: an international, early access, open-label, single-arm phase 3b trial. Lancet Oncol. 2016;17:1306-16
36. Shore ND. Open-label phase II study evaluating the efficacy of concurrent administration of radium Ra 223 dichloride (Ra-223) and abiraterone acetate (AA) in men with castration-resistant prostate cancer (CRPC) patients with symptomatic bone metastases. J Clin Oncol. 2016;34 (suppl 2S): abstr 177

^{188}Re-HEDP in the treatment of patients with bone metastatic castration-resistant prostate cancer, a review

E.W. Bouman-Wammes, MD[1]; A.J.M. van den Eertwegh, MD, PhD[1]; H.J. Bloemendal, MD, PhD[2,7]; R. ter Heine MD, PhD[6]; R. Lange, MD[3]; J.M. van Dodewaard-de Jong, MD[1,2]; A. Kooistra, MD, PhD[4]; Prof. H.M.W. Verheul, MD[1]; J.M.H. de Klerk, MD, PhD[5]

[1]Department of Medical Oncology, VU University Medical Centre, Amsterdam, the Netherlands
Departments of [2]Oncology, [3]Hospital Pharmacy, [4]Urology and [5]Nuclear Medicine, Meander Medical Centre, Amersfoort, the Netherlands
[6]Department of Hospital Pharmacy, RadboudUMC, Nijmegen, the Netherlands
[7]Department of Oncology, UMC Utrecht, the Netherlands

Abstract

Bouman-Wammes EW, Van den Eertwegh AJM, Bloemendal HJ, ter Heine R, Lange R, Van Dodewaard-de Jong JM, Kooistra A, Verheul HMW, De Klerk JMH. ^{188}Re-HEDP in the treatment of patients with bone metastatic castration-resistant prostate cancer, a review. In patients with prostate cancer, bone is the most common site for metastases. These lesions can cause severe pain, thereby seriously affecting quality of life. For patients with multiple bone metastases, treatment with radiopharmaceuticals such as ^{188}Re-HEDP is a promising option as it results in a quick pain relief without major side-effects. ^{188}Re-HEDP is easily produced, and is suitable for repeated injections. Combination with chemotherapy is feasible and save, and results of the first phase II study are promising.**Tijdschr Nucl Geneesk 2016; 38(4):1660-1665**

Introduction

Prostate cancer is the most common cancer in elderly men and in patients with castration-resistant prostate cancer (CRPC), bone is the most common site for metastases (1). These metastases are frequently located in the lumbar spine, vertebrae and pelvis and can cause severe bone pain, thereby seriously affecting quality of life (2). Larger metastases cause pain due to stretch of the periosteum, whereas the smaller lesions cause severe pain due to stimulation of nerve endings by several mediators in the endosteum (3).
Skeletal metastases from prostate cancer are mostly osteoblastic and therefore clearly visualised by bone scintigraphy.
There is a variety of treatment options for patients with CRPC, including hormonal therapy, chemotherapy and immunotherapy. All these treatments can result in a decrease of pain, skeletal related events and improvement of overall survival (4). However, especially in patients with advanced disease, these therapies might not be tolerated, or insufficient for optimal pain palliation (5).
Another option is external beam radiation therapy (EBRT), which can generate a major pain relief in patients with a limited number of painful metastases (6). However, for patients with multiple or diffuse metastases, EBRT is not feasible due to the high toxicity of radiation of all metastases. In these cases treatment with bone seeking radiopharmaceuticals is a good alternative. Due to the systemic administration and very specific bone targeting, all osteoblastic bone lesions are treated simultaneously.

One of these radiopharmaceuticals is rhenium-188 hydroxyethylidene diphosphonate (^{188}Re-HEDP), which is a complex of the β-emitting radionuclide ^{188}Re and the bone targeting bisphosphonate hydroxyethylidene diphosphonate (HEDP). ^{188}Re-HEDP accumulates in osteoblastic bone lesions, similar to nuclear diagnostic agents used for bone scintigraphy. Therefore, pre-therapeutic technetium-99m-HDP bone scintigraphy must show skeletal metastatic uptake (osteoblastic activity).

Pain relief is putatively accomplished by destruction of the malignant cells and immune cells which causes reduction of pressure in the periosteum, and decreases the secretion of cytokines (7,8). Prostatic bone metastases are mostly osteoblastic, unlike the mix of osteoblastic and osteoclastic components in the metastases accompanying other tumour types. Henceforth, the quantitative uptake in skeletal metastases from prostate cancer is higher, leading to an increased absorbed dose. This makes this patient group suitable for treatment with bone targeting therapeutic radiopharmaceuticals (9). However, bone seeking radiopharmaceuticals can be used in patients with bone metastases from any cancer, provided that there is osteoblastic activity.

^{188}Re-HEDP: characteristics and production

Characteristics

The isotope ^{188}Re has a half-life of approximately 17 hours, and decays to stable osmium-188 by β-(2.1 MeV) and γ (155 KeV) decay (10). Liepe et al. found a mean effective half-life of 15.9±3.5h in bone metastases, 10.9±2.1h in the bone marrow, 11.6±2.1h in the whole body and 7.4±3.4h in the bladder. They assessed a rapid urinary excretion, in which 41% of the administered rhenium was excreted in the first 8 hours, with an excretion rate of 61%±12% after 48 hours (11). The maximum penetration depth of the electrons in soft tissue is 11mm, with an average of 3.8mm (12).

Production

^{188}Re-HEDP (as perrhenate) can be eluted from commercially available tungsten-188 (^{188}W)/^{188}Re generators, which allows on demand production in the hospital. These generators can be used up to six months due to the long half-life of the ^{188}W of 69 days. ^{188}Re-HEDP can easily be synthesised by heating a mixture of radioactive ^{188}Re (as sodium perrhenate), non-radioactive perrhenate, stannous chloride, HEDP, hydrochloric and gentisic acid. Complexation of ^{188}Re with HEDP is facilitated by the stannous ion which is a reducer for the perrhenate ion. Gentisic acid acts as an anti-oxidant and is used as a stabiliser. After the labelling, the pH of the acidic solution should be adjusted to a more physiological pH, for example with sodium acetate. Although several groups have reported the synthesis of ^{188}Re-HEDP (13-15), production under GMP circumstances is a prerequisite for its application. A compliant method has been described by Ter Heine et al (16).

Clinical results

Several clinical trials have shown the beneficial effect of ^{188}Re-HEDP in the treatment of patients with painful bone metastases from CRPC, in terms of pain relief, quality of life and survival. The results of these trials are quite similar, and are summarised in table 1 (8,17-22). Pain relief is mostly defined as a decline of at least two steps on the Visual Analogue Scale (VAS) lasting at least for two consecutive weeks without increased analgesics intake, but a major problem in literature is the use of different definitions.

Pain relief

A single injection of ^{188}Re-HEDP results in pain relief in 60-89.5% of the patients. Pain relief is achieved in 92-94% of patients when two or three injections are administered (8,17-22). The maximum effect is seen between four to eight weeks after start of treatment. Palmedo et al. reported a duration of pain relief of 2.6 months after a single injection, and a median response duration of 5.6 months for patients treated with two injections (20).

Three articles reported the mean VAS scores pre-treatment and twelve weeks after treatment, and all showed a decrease (44±18% pre-treatment to 31±25% in week 12, p=0.009 (19), 4.9±1.7 versus 2.8±1.5, p=0.0001(20), and 4±2 versus 3±2, p=0.06 (21)). Lange et al. reported a significant decrease of mean VAS scores in week 4 and 8 after treatment (5.7±0.4 pre-treatment versus 3.2±0.4 in week 4, p<0.05 and 4.0±0.6 in week 8, p<0.05 (8)).

Liepe et al. used the Karnofsky score (a 0-100 scale to classify patients based on their functional impairment), and reported an increase in Karnofsky score in two separate studies. In their article published in 2000 (15 patients included in a prospective study), the Karnofsky score increased from 74±8% before therapy to 84±11%, 12 weeks after injection (p=<0.05), with a maximal increase of 27%. Later, this group reported a similar result in a prospective study with 27 included patients from 74±7% before therapy to 85±9% in week 12 after therapy (p<0.05)(17,20).

Lange et al. reported a significant increase on the Quality of Life scale (using the European Organisation of Research for the Treatment of Cancer (EORTC) Quality of Life (QoL) Questionnaire C30 version 3) from mean 40 ±2.8 pre-treatment to 54±3.3 (P<0.05) in week 4, and 47±4.0 in week 8 (p=0.14).

Single versus repeated administration of ^{188}Re-HEDP

Two studies compared the outcome of patients receiving a single versus two or more injections of ^{188}Re-HEDP. Palmedo et al. randomised 64 (6 not eligible for follow-up) patients between one (n=30) or two (n=28) cycles of ^{188}Re-HEDP 40 MBq/kg, and showed an overall survival benefit for the repeated treatment arm. The median overall survival in the single dose arm was 7.0 months (range 1.3-36.7) versus 12.7 months (range 4.1-32.2, p<0.05) for patients in the repeated treatment arm. The response rate in terms of pain relief was also better in the repeated treatment group with a response of 92% versus 60% in group A (p<0.05)(20).

Biersack et al. published a retrospective study, in which patients were divided in three cohorts (group A consisted of patients who received a single injection ^{188}Re-HEDP, group B of patients who received two injections and group C consisted of patients treated with 3 or more doses of ^{188}Re-HEDP). The mean survival was 4.5 months in group A, 10.0 months in group B and 15.7 months in group C (P<0.05). In contrast to Palmedo et al. this study could not find any significant difference in pain response between the groups. Although this was a retrospective study, with selection bias as a possible confounder, the results are remarkable. Especially because the baseline characteristics as well as the prognostic factor according to Helpap (including the modified Gleason system, grade, stage, tumour extent and serum PSA) were comparable between the three groups.

Side effects

All mentioned studies reported the observed side effects of ^{188}Re-HEDP. The most common haematological side effect was a thrombopenia, with grade I thrombopenia occurring in 4.5-8.6% of the patients, grade II in 4-7.5% of the patients and grade III in 5.3% of the patients (grade III was only observed in the study of Lange et al). Clinical problems related to

Table 1. Summary of clinical trials investigating treatment of mCRPC with ^{188}Re-HEDP.

	sample size	methods	dose	results	side effects / safety
Liepe et al. 2000	15 (14 pts prostate cancer, 1 pt breast cancer)	observational intervention, prospective	1600-3459 MBq (13 pts 2700-3459MBq) single dose	pain relief∞:80% Karnofsky index 74 ->84 (p=0.0001) PSA decrease; NS	lowest leukocyte count 3.0*10^3/µl lowest platelet count 86*10^3/µl
Palmedo 2000	22	dose escalating observational, prospective	escalating (1.3-2.6-3.3-4.4GBq) single dose	pain relief; 64% (dose 3.3: 66%; dose 4.4: 75%) duration of response;:7.5 weeks start effect: 12.5 days safe dose: 3.3 GBq	dose 2.6 GBq; thrombopenia grade I (1 patient) dose 3.3 GBq; thrombopenia grade I (1) and grade II (1), leukopenia grade I (3) dose 4.4; thrombopenia grade III(1) and IV (2), leukopenia grade I (3), grade II (3) grade IV (1)
Liepe 2003	27	phase II, prospective	2700-3587 MBq (mean 3245MBq) single dose	pain relief: 76% (5 pts pain free) VAS: 44->31* (p=0.009) Karnofsky index: 74 ->85*(p=0.001) maximum effect week 3-8	thrombopenia grade I (2) and II (1) leukopenia grade I (1) pain flare in 16% of patient no significant PSA level changes
Palmedo 2003	58 (group A n=30, group B n=28)	randomised, prospective phase II	group A one dose group B; two doses (8 week interval) both groups 40.7 Mbq/kg/dose	pain relief: group A 60%, median duration 2.55 months group B 92%, median duration 5.66 months PSA response: 10% group A and 40% group B† median overall survival: 7.0 versus 12.7 months (p=0.043)	thrombopenia grade I (5) and II (3) leukopenia grade I (6) and II (2) pain flare in 8.6% of patients
Liepe 2005	25	observational, intervention, prospective	3300 MBq	pain relief 80%	thrombopenia grade I (2) and II (1) leukopenia grade I (1)
Biersack 2011	60, (group A n=19, group B n=19, group C n=22)	retrospective	2960-3300MBq/dose group A; 1 dose group B; 2 doses group C; 3 doses	pain relief group A/B/C of 89.5%/94.8%/ 90.9% no significant PSA response mean survival A/B/C of 4.5/10.0/15.7 months	only reversible thrombopenia grade I and II, and leukopenia grade I
Lange 2016	34 (56 included, 34 evaluable)	observational, prospective	40MBq/kg (max 3300MBq)	pain response 68.7% QoL response 67.6% VAS 5.7->3.2(week 4)->4.0 (week 8) QoL 40-> 54 (week 4)->47 (week 8)	thrombopenia grade III in 5.3% leukopenia grade III in 3.6%

∞ pain relief of two steps on the VAS at least in two consecutive weeks without increase in analgesics intake
*at week 12
† reduction of >50% compared to baseline values, maintained for at least 8 weeks

thrombopenia in the form of bleeding or need of transfusion were not observed (in the 240 patients included in the different studies). Leukopenia grade I was seen in 4-13.6% of the patients, grade II in 3.4% and grade III in 3.6% of the patients (grade II and III only reported in one article with 58 and 34 patients respectively). There were no reports of neutropenic fever and all patients recovered to normal values during follow up. The used dose of ^{188}Re-HEDP in the studies is explicated in table 1.
Only in the dose finding study of Palmedo et al., in the dose group of 4.4 GBq (a higher dose than used in other studies) thrombopenia grade IV was observed, in 2 patients (25%), as well as one episode of a grade III thrombopenia (12.5%). Also the incidence of leukopenia was higher in this group, with a grade I in 3 patients (37.5%), grade II in 3 patients (37.5%) and grade IV in 1 patient (12.5%). The conclusion of this study was that 3.3 GBq was the maximum tolerated dose, and all later performed studies used this as the maximum dose.
Two studies reported about a pain flare in 8.6% (5 of 58 patients) and 16% (4 of 27 patients) of the included patients, within 14 days after infusion of ^{188}Re-HEDP (19,20).

^{188}Re-HEDP and other radiopharmaceuticals

The most commonly used bone seeking radiopharmaceuticals besides ^{188}Re-HEDP are the β-emitting radiopharmaceuticals like strontium-89-chloride (^{89}Sr-Cl), samarium-153-EDTMP (^{153}Sm-EDTMP) and rhenium-186-HEDP (^{186}Re-HEDP), as well as the α-emitter radium-223-chloride (^{223}Ra-Cl). There are two ways for reaching the bone metastases; ^{153}Sm-EDTMP and $^{186/188}$Re-HEDP are bisphosphonate based radiopharmaceuticals, unlike the calcimimetic agents ^{89}Sr-Cl and ^{223}Ra-Cl.
In terms of physical characteristics, ^{188}Re-HEDP has the

shortest half-life, the highest β-energy and the largest range, as shown in table 2. In theory, a shorter physical half-life allows for higher administered activities and higher dose rates at the tumour. However, a head-to-head comparison between the different radiopharmaceuticals has not been performed, so evidence about superiority of one of these pharmaceuticals does not exist.
Van Dodewaard et al. recently provided a systematic review, including 36 studies, in which they compared the efficacy of the radiopharmaceuticals in terms of pain relief in patients with prostate cancer metastatic to the bone. Pain response following treatment with ^{153}Sm-EDTMP, ^{186}Re-HEDP and ^{188}Re-HEDP were comparable to each other (responses of 70%, range 38-89%), with a slightly lower response to ^{89}Sr-Cl with 50-60% (range 35-92%) pain response rates. Median overall survival ranged from 4.0-21.0 months, without any difference between the trials reporting this outcome. Also for haematological toxicity, no serious differences could be found between the different radionuclides. A pain flare was reported in 24 trials, with the following incidences per radionuclide; ^{89}SrCl 0-39% of the patients, ^{153}Sm-EDTMP 0-12%, ^{186}Re-HEDP 0-63% and ^{188}Re-HEDP 6-17% of the patients. One study with ^{223}RaCl reported an incidence of pain flair, in 11% of the patients (9).

^{223}Ra-Cl is a calcimimetic bone seeking radiopharmaceutical with a proven survival benefit in a large randomised trial (23), when used as a single agent. The ALSYMPCA study randomised 921 patients in a 2:1 ratio between 6 injections of ^{223}Ra-Cl (50kBq per kilogram per injection) or placebo, with overall survival as primary endpoint. There was a significant improvement of overall survival in the group receiving ^{223}Ra-Cl, with an overall survival of 14.9 months versus 11.3 months in the control group (hazard ratio 0.70, 95% CI 0.58-0.83, p<0.001). Pain and quality of life were no endpoints in this study.

Combination of ^{188}Re-HEDP and other radiopharmaceuticals with chemotherapy

Several studies have investigated the combination of radiopharmaceuticals and chemotherapy. Tu and colleagues were the first study group who combined these forms of treatment; they combined doxorubicin with ^{89}Sr-Cl in a randomised phase II study, including 72 patients (24). Median overall survival in the group of patients treated with the combination therapy was significantly longer than in the control group (receiving doxorubicin monotherapy): 27.7 months versus 16.8 months.

Later studies combined docetaxel (which is the standard first-line chemotherapy for prostate cancer) with ^{153}Sm-EDTMP (25,26). Two phase I trials combined docetaxel and ^{153}Sm-Cl in a weekly and a three weekly schedule. Tu et al. treated 18 patients in a conventional 3+3 dose escalating design, with a maximum of docetaxel 35mg/m^2 weekly in combination with ^{153}Sm-EDTMP 37MBq/kg monthly, in two cycles. Combination treatment at these dosages was feasible and well tolerated, with five patients (28%) experiencing transient grade 3 hematologic toxicity, without any grade IV hematologic or non-haematological toxicity (25).
In the same year, Morris et al. published a phase I trial of 28 patients treated with the same combination of climbing dosages docetaxel and ^{153}Sm-EDTMP, but in a different schedule (26). The maximum dose was docetaxel 75mg/m2 three weekly and ^{153}Sm-EDTMP 37MBq/kg six weekly. Also in this trial, the maximum-tolerated dose was not reached. Patients received an average of 5.6 docetaxel doses and 2.9 doses of ^{153}Sm-EDTMP. Fifteen patients (54%) achieved a more than 50% decline of PSA and treatment significantly reduced indices of bone deposition and resorption.
Fizazi et al. performed a phase II trial of consolidation docetaxel and ^{153}Sm-EDTMP (27). Forty-three patients, who achieved a response or stabilisation after four cycles of docetaxel, were given consolidation docetaxel 20mg/m2 weekly for six weeks in combination with ^{153}Sm-EDTMP 37MBq/kg in week 1. A PSA response was obtained in 77% (95% CI 61%-82%) of the patients, and a pain response in 69% (95% CI 49%-85%). There were no major side effects, with only 2 episodes (5%) of thrombopenia grade III. This regimen resulted in a long term pain response, a median PSA-PFS of 6.4 months (95% CI 6-7 months) and a median overall survival of 29 months (95% CI 22-31 months). The authors concluded that this combination was well tolerated, and yielded major pain relief which persisted after treatment. The overall survival was favourable compared to what was expected in this population.

Table 2. Summary of the physical characteristics of the most common radionuclides.

radionuclide	half-life (days)	energy (meV)	emission	range (mm)
strontium-89	50.57	1.46	β	6.6
samarium-153	1.90	0.71	B/γ	3.1
rhenium-186	3.75	1.07	B/γ	4.5
rhenium-188	0.70	2.12	B/γ	10.2
radium-223	11.43	5.72	α	<0.1

As far as we know, the Taxium II and the ReCab study are the only studies investigating ^{188}Re-HEDP in combination with the current standard-lines of chemotherapy. The Taxium I study, a dose finding trial, proved that combined therapy with docetaxel, prednisolone and repeated ^{186}Re-HEDP is safe and generally well tolerated in patients with metastatic CRPC (mCRPC) (28). Because of production problems in the Netherlands and the fact that ^{188}Re-HEDP has an identical radiopharmaceutical profile as ^{186}Re-HEDP, ^{186}Re-HEDP was replaced by ^{188}Re-HEDP in the Taxium II trial. Eighty-eight patients were randomised between an experimental arm (46 patients, three cycles of docetaxel 75 mg/m^2 three weekly, followed by ^{188}Re-HEDP 40MBq/kg, followed by another three cycles of docetaxel and a second dose of ^{188}Re-HEDP 20MBq/kg) and a control group (42 patients, docetaxel 75mg/m^2 monotherapy). All patients received prednisolone 10mg daily. Results of this trial were presented at the ASCO 2016 annual meeting, and showed no difference in progression free survival (PFS), survival or PSA response in the intention to treat analysis (29). However, the incidence of new musculoskeletal pain was lower in the experimental arm. Results of the per protocol analysis are very promising in terms of overall survival; these results are submitted and under review at this moment.
Although neutropenia grade 3/4 was seen more often in the combined treatment group (16% versus 5%) the incidence of neutropenic fever was comparable between both groups (14% versus 16%). Publication of these results is expected soon.

In the ReCab study ^{188}Re-HEDP will be combined with cabazitaxel; the standard second line in chemotherapy for patients with mCRPC. After completing the phase I part of the study, in June 2016 the ReCab trial continued as a phase II randomised trial. The results of the phase I part of this study are awaited this year.

Discussion

^{188}Re-HEDP is a powerful β-emitting bone targeting radiopharmaceutical, which has the great advantage over other radiopharmaceuticals that it can easily be prepared on demand in a hospital setting at relatively low costs. The clinical benefit in terms of pain relief has been proven in several studies. Pain relief is achieved in 60-89.5% of the patients treated with a single injection, increasing to 92-94.8% in the patients receiving two or more injections. Data on the effect on QoL are scarce, but in studies, which report the QoL or Karnofsky score, a significant improvement has been observed.
As shown, there is a rapid pain relief within 24 to 48 hours with a duration of several weeks (mostly >8 weeks). Furthermore, due to its short half-life, ^{188}Re-HEDP is an excellent agent for repeated administration, as it has only mild and transient side effects.
Pain palliation by ^{188}Re-HEDP, as well as other radiopharmaceuticals, is comparable to the efficacy of EBRT, which is only suitable for patients carrying a limited number of metastases. However, pain relief is more rapid compared to EBRT (24-48 hours for ^{188}Re-HEDP versus 2-3 weeks for EBRT), which is especially meaningful in patients with severe bone pain. All published studies show a very acceptable toxicity profile, with thrombopenia and leukopenia (transient and without clinical complications) as the most common side effects.
A survival benefit of ^{188}Re-HEDP has not yet been proven, nor for the other β-emitting radionuclides, as there have been no large randomised trials with overall survival as primary outcome. However, two small trials (one retrospective study and one small randomised trial) suggest a benefit in median overall survival following repeated injections of ^{188}Re-HEDP compared to a single injection. These promising results warrant confirmation by an adequately powered randomised trial. A survival benefit has been shown for the α–emitter ^{223}Ra-Cl (11.3 months versus 14.9 months) in a large randomised trial, which raises the question whether this can also be achieved with repeated treatment with β-emitting radionuclides. In addition, a direct comparison between the less costly β-emitting radionuclides and the α-emitter ^{223}Ra-Cl would be of great interest.

Several studies have shown that the combination of radiopharmaceuticals with chemotherapy is feasible and save, and suggest that this combination might be preferable above monotherapy in terms of pain relief, quality of life and overall survival.
Studies with the combination of ^{188}Re-HEDP and chemotherapy have been performed, are recruiting or are being planned. As mentioned, the results of the Taxium II (docetaxel in combination with ^{188}Re-HEDP) as well as the ReCab phase I (cabazitaxel with ^{188}Re-HEDP) are expected. At this moment, the ReCab II is open for inclusion. This phase II study aims to include 86 patients with mCRPC who progressed during or after treatment with docetaxel. Patients will be randomised between cabazitaxel 25mg/m^2 three weekly (control arm) or cabazitaxel 25mg/m^2 in combination with two cycles of ^{188}Re- HEDP 40MBq/kg (after the second and fourth cycle of cabazitaxel). Primary endpoint is PFS, with overall survival, pain relief (and duration of pain relief), QoL, PSA response and toxicity as secondary endpoints.

With these expected and ongoing studies, we hope to gain more insight in the possibilities of ^{188}Re-HEDP in terms of palliation as well as survival benefit.

Conclusion

^{188}Re-HEDP is a powerful β-emitting radionuclide with good results in pain palliation and quality of life in patients with symptomatic bone metastasis. It is easily produced, and is suitable for repeated injections. Future studies should clarify its role in improvement of survival with or without concurrent chemotherapy, and its place in reference to other radionuclides, especially ^{223}Ra-Cl.

e.bouman@vumc.nl

References

1. Arnold M, Karim-Kos HE, Coebergh JW, et al. Recent trends in incidence of five common cancers in 26 european countries since 1988: Analysis of the European cancer observatory. Eur J Cancer. 2015;51(9):1164-87
2. Saad F, Clarke N, Colombel M. Natural history and treatment of bone complications in prostate cancer. Eur Urol. 2006;49:429-40
3. Nielsen OS, Munro AJ, Tannock IF. Bone metastases; pathophysiology and management policy. J Clin Oncol. 1991;9:509-24
4. Van Dodewaard-De Jong JM, Verheul HM, Bloemendal HJ, et al. New treatment options for patients with metastatic prostate cancer: What is the optimal sequence? Clin Genitourin Cancer. 2015;13:271-9
5. Mercandente S. Malignant bone pain: pathophysiology and treatment. Pain. 1997;69:1-18
6. Van der Linden YM, Lok JJ, Steenland E, et al. Single fraction radiotherapy is efficious: a further analysis of the dutch bone metastases study controlling for the influence of retreatment. Int J Radiation Oncology Biol. Phys. 2004;59:528-37
7. Hoskin PJ. Bisphosphonates and radiation therapy for palliation of metastatic bone disease. Cancer Treat Rev. 2003;29:321-7
8. Lange R, Overbeek F, de Klerk JMH, et al. Treatment of painful bone metastases in prostate and breast cancer patients with the therapeutic radiopharmaceutical rhenium-188-HEDP.Clinical benefit in a real world study. Nuklearmedizin. 2016 ;56 (epub ahead of print)
9. Van Dodewaard- de Jong JM, Oprea-Lager DE, Hooft L, et al. Radiopharmaceuticals for palliation of bone pain in patients with castration resistant prostate cancer metastatic to bone: a systematic review, Eur Urol. 2016;70:416-26 (http://dx/doi.org/10.1016/j.eururo.2015.09.005)
10. Pillai MR, Dash A, Knapp FF. Rhenium-188: availability from the (188)W/(188)Re generator and status of current applications. Curr. Radiopharm. 2012;5:228-24
11. Liepe K, Hliscs R, Kropp J, et al. Dosimetry of 188Re-hydroxyethylidene diphosphonate in human prostate cancer skeletal metastases. J Nucl Med. 2003;44:953-60
12. Knapp FF, Mirzade S. Beets AL, et al. Reactor-produced radioisotopes from ORNL for bone pain palliation. Appl radiat Isot. 1998;49:309-15
13. Hashimoto K. Synthesis of a 188Re-HEDP complex using carrier-free 188Re and a study of its stability. Appl. Radiot. Isot. 1998;49:351-356
14. Hsieh BT, Hsieh JF, Tsai SC, et al. Comparison of various rhenium-188-labeled diphsphonates for the treatment of bone metastases. Nucl. Med. Biol. 1999;26:973-6
15. Lin WY, Hsieh JF, Lin CP, et al. Effect of reaction conditions of preparations of rhenium-188 hydorxyethylidene diphosphonate complexes. Nucl Med. Biol. 1999;26:455-9
16. Ter Heine R, Lange R, Breukels O, et al. Bench to bedside development of GMP grade Rhenium-188-HEDP, a radiopharmaceutical for targeted treatment of painful bone metastases. Int J Pharm. 2014;465:317-24
17. Liepe K, Hliscs R, Kropp J, et al. Rhenium-188-HEDP in the Palliative Treatment of Bone Metastases. Cancer Biother Radiopharm. 2000 ;15(3):261-5
18. Palmedo H, Guhlke S, Bender H, et al. Dose escalation study with rhenium-188 hydroxyethylidene diphosphonate in prostate cancer patients with osseous metastases. Eur J Nucl Med. 2000;27:123-30
19. Liepe K, Kropp J, Runge and Kotzerke J. Therapeutic efficiency of rhenium-188-HEDP in human prostate cancer skeletal metastases. Br J Cancer. 2003;89(4):625-9
20. Palmedo H, Manka-Waluch A, Albers P, et al. Repeated Bone-Targeted Therapy for Hormone-Refractory Prostate Carcinoma: Randomised Phase II Trial With the New, High-Energy Radiopharmaceutical Rhenium-188-Hydroxyethylidenediphosphate. J Clin Oncol. 2003;21(15):2869-75
21. Liepe K, Runge R, Kotzerke J. The benefit of bone-seeking radiopharmaceuticals in the treatment of metastatic bone pain. J Cancer Res Clin Oncol. 2005;131(1):60-6
22. Biersack H, Palmedo H, Andris A, et al. Palliation and Survival After Repeated 188Re-HEDP Therapy of Hormone-Refractory Bone Metastases of Prostate Cancer: A Retrospective Analysis. J Nucl Med. 2011;52(11):1721-6
23. Parker C, Nilsson S, Heinrich D et al. Alpha emitter radium-113 and survival in metastatic prostate cancer. N Engl J Med. 2013;369:213-23
24. Tu SM, Millikan RE, Mengistu B, et al. Bone-targeted therapy for advanced androgen-independent carcinoma of the prostate: a randomised phase II trial. Lancet. 2001;357:336-41
25. Tu SM, Mathew P, Wong FC, et al. Phase I study of concurrent weekly docetaxel and repeated samarium-153 lexidronam in patients with castration-resistant metastatic prostate cancer. J Clin Oncol. 2009;27:3319-24
26. Morris MJ, Pandit-Taskar N, Carasquillo J, et al. Phase I study of samarium-153 lexidronam with docetaxel in castration-resistant metastatic prostate cancer. J Clin Oncol. 2009;27:2436-42
27. Fizazi K, Beuzeboc P, Lumbroso J, et al. Phase II trial of consolidation docetaxel and samarium-153 in patients with bone metastases from castration-resistant prostate cancer. J Clin Oncol. 2009;27:2429-35
28. Van Dodewaard- de Jong JM, De Klerk JMH, Bloemendal HJ, et al. A phase I study of combined docetaxel and repeated high activity 186Re-HEDP in castration-resistant prostate cancer (CRPC) metastatic to bone (the TAXIUM trial). Eur J Nucl Med Mol Imaging. 2011;38:1990-8
29. Van Dodewaard-de Jong JM, Bloemendal HJ, De Klerk HJM, et al. A randomized phase II study of repeated rhenium-188-HEDP (rhenium) combined with docetaxel versus docetaxel alone in castration resistant prostate cancer (CRPC) metastatic to bone. The Taxium II trial. J Clin Oncol. 2016;34 (suppl; abstract 5081)

Advances in image guidance of therapy in nuclear medicine

C. Beijst, PhD[1,2]; B. Kunnen, MSc[1,2]; Prof. M.G.E.H. Lam, MD[1]; H.W.A.M. de Jong, PhD[1]

[1]Department of Radiology and Nuclear Medicine, UMC Utrecht, Utrecht, the Netherlands
[2] Image Sciences Institute, UMC Utrecht, Utrecht, the Netherlands

Abstract

Beijst C, Kunnen B, Lam MGEH, de Jong HWAM. Advances in image guidance of therapy in nuclear medicine. Internal radiation therapy with radionuclides (i.e. radionuclide therapy) owes its success to the many advantages over other, more conventional treatment options. One distinct advantage of radionuclide therapies is the potential to use (part of) the emitted radiation for imaging of the radionuclide distribution. Imaging can help in treatment planning, dosimetry and assessment of treatment response. This paper focuses on a selection of advances in imaging technology relevant for image guidance of therapy in nuclear medicine. This involves developments in nuclear imaging modalities, as well as other anatomical and functional imaging modalities. The quality and quantitative accuracy of images used for guidance therapy in nuclear medicine is continuously being improved, which in turn may improve the therapeutic outcome and efficiency of therapies in nuclear medicine.
Tijdschr Nucl Geneesk 2016; 38(4):1666-1675

Background

Radionuclide therapy combines the specificity of cancer cell targeting (like chemotherapy) with targeted ionizing radiation (like external beam therapy and/or brachytherapy). An advantage of using radionuclide therapy over radiotherapy and/or brachytherapy is that radionuclide therapy has the potential to not only eliminate the primary tumour but also metastasized and/or undetected tumours. Strategies for targeted delivery of radionuclides include:

1. binding of radionuclides to a cell targeting molecule, for example the treatment of neuroendocrine tumours with ^{177}Lu-DOTA^{0},Tyr^{3}-octreotate (DOTATATE) (1);
2. employing the ability of the radionuclide to target specific cells on its own, such as the treatment of thyroid carcinoma with ^{131}I (2);
3. intra-arterial injection, for example radioembolisation with ^{90}Y microspheres for liver malignancies (3).

Another advantage of radionuclide therapies is the potential to use the emitted radiation for imaging of the radionuclide distribution. This may aid in optimized targeting, treatment planning, dosimetry and assessment of treatment response.

This paper focuses on a selection of advances in imaging technology relevant for image guidance of therapy in nuclear medicine. First, developments in the field of the traditional nuclear imaging modalities (i.e. SPECT and PET) are discussed. Then advances in other anatomical and functional imaging modalities that are used for the guidance of therapy in nuclear medicine are discussed. Note that the image guidance of radionuclide therapies often imposes additional challenges on imaging modalities. For example, dosimetry requires quantitative images and real-time guidance of procedures often means that dedicated hardware is needed.

SPECT

The type of decay of radionuclides used for (guidance of) therapy in nuclear medicine determines what modality is used for imaging. Planar scintigraphy and single photon emission computed tomography (SPECT) are used for imaging of the majority of radionuclides, especially for pre- and posttherapeutic dosimetry. A large variety of radioisotopes with varying emitted (photon) energies can be imaged with SPECT.

Current status

Planning and dosimetry require quantitative images to convert the reconstructed activity concentration (in Bq) into absorbed dose (in Gy). SPECT/CT images are not inherently quantitative due to effects like photon attenuation, scatter and blurring. Therefore, attenuation correction is commonly incorporated in the projection operators of the iterative reconstruction method by using attenuation maps from co-registered CT images. Scatter correction is also routinely implemented into clinical practice and is often performed using the triple energy window (TEW) method (4). Further improvement of the image quality can be achieved by applying resolution recovery. This is done by accurately characterizing the shape of the point spread function (PSF) and incorporating it into the reconstruction algorithm.

Advances in SPECT

This section discusses the advances in SPECT that concern an improvement of image quality in general, as well as developments specifically aimed at improving the guidance of radionuclide therapy.

Instrumentation: collimators and detectors

Tumour dosimetry requires the accurate quantification of small

structures. This is severely hampered by the partial volume effects that reduce contrast due to limited image resolution. As image resolution is for a large part determined by the resolution of the collimator, the development of collimators that reduce collimator penetration is one of the strategies able to reduce partial volume effects. Many of the isotopes used for radionuclide therapies (e.g. ^{131}I and ^{90}Y) emit high-energy photons that easily penetrate the collimator, and cause lower image resolution, so optimizing the collimator may be crucial to achieve quantitative accuracy. The strategy used to optimize parallel hole collimators for high-energy applications is to increase septal thickness and length to limit septal penetration. However, optimizing the design of a parallel hole collimator involves a trade-off between septal penetration, spatial resolution and sensitivity. Alternatively, pinhole collimators are used that can be designed in such a way that collimator penetration is limited (5). Moreover, multiple pinholes can be used to overcome the problem of limited sensitivity (6,7). An example of a commercially available multi-pinhole system is the G-SPECT (MiLabs, Utrecht, the Netherlands), which achieves high resolution and sensitivity, although the narrow bore of the scanner only allows use in applications with a small field-of-view such as brain and paediatric SPECT. The image quality may also be improved by using a collimator consisting of cone-shaped holes (the parallel cone collimator, figure 1), that limits collimator penetration while preserving resolution and sensitivity (8).

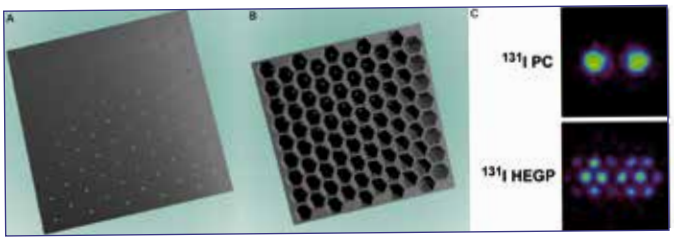

Figure 1. Rendering of the parallel cone collimator from different perspectives: from the face of the collimator (A), and back of collimator (B). Double point source Monte Carlo simulations of the PC collimator and HEGP collimator for ^{131}I are shown in (C). The simulations show that the PC collimator is able to detect the two sources separately, whereas the HEGP collimator is not able to. This research was originally published by Beijst et al.(8) © by the Society of Nuclear Medicine and Molecular Imaging, Inc.

Most commercial diagnostic hybrid systems are designed to perform a large variety of examinations. However, systems can also be designed for a specific purpose. Dedicated systems may significantly reduce acquisition times or radiation dose while maintaining high image quality, resulting in increased patient comfort and efficiency of scanning.

Detectors can be optimized for high-energy photons (emitted by the isotopes used for radionuclide therapies) by using thicker crystal (5/8" instead of the standard 3/8") or by employing scintillation crystals with high stopping power, which increases the detection efficiency. Walrand et al. have designed a camera dedicated for Bremsstrahlung imaging of ^{90}Y (5,9). They describe a dedicated system with a 30 mm thick BGO crystal and a 8 mm high-energy pinhole with extra shielding to prevent penetration of high-energy photons. Additionally, it is suggested that the camera can be mounted on a robotic gantry for use in the intervention room, as shown in figure 2.

Advances in detector technology also include the development of solid-state detectors (10). Cadmium zinc telluride (CZT) detectors directly convert the energy of incident gamma photons into an electric signal, in contrast to indirect scintillation-based detector systems that require photomultiplier tubes. Advantages of CZT detectors are the high-energy resolution and the high count rate capability as compared with photomultiplier cameras with NaI crystals. Superior energy resolution results in a lower detection of scattered events due to a narrow energy window. This also paves the way for dual isotope applications, for which clear separation of photopeaks is essential (11). High count rate capabilities are an advantage of radionuclide therapies. However, CZT detectors have low stopping power which makes them less suitable for imaging of high-energy photons. CZT technology is more suitable for isotopes with low-energy photopeaks such as ^{99m}Tc, ^{166}Ho or ^{177}Lu (12). Clinical SPECT cameras equipped with CZT detectors such as the Valiance X12 (Molecular Dynamics, Caesarea, Israel) and the Discovery NM/CT 670 CZT (GE Healthcare, Milwaukee, United States) recently became commercially available (13).

Reconstruction algorithms

Specifically for the application of radionuclide therapy, quantitative results benefit dosimetry and assessment of treatment response. However, iterative reconstruction algorithms are able to obtain images with high SNR but do not necessarily generate (linearly) quantitative images. In general, SPECT images have long been regarded as solely qualitative images, in contrast to PET that allows the use of (semi-) quantitative measures such as the standardized uptake value (SUV). Despite the relatively low resolution of SPECT images (as compared with PET) quantitative SPECT images can now be obtained when image degrading effects are adequately corrected for. This includes corrections for attenuation, scatter, PSF and/or dead time. Although quantitative images can be obtained using easy-to-implement scatter correction techniques, the accuracy of quantitation can be improved by using Monte Carlo based scatter modelling (14). Monte Carlo simulated forward projections can be used in the reconstruction algorithm to accurately model object scatter and hence, correct for the image degrading effects of scatter. Over the years, several Monte Carlo codes have been incorporated into the reconstruction algorithm, such as GATE, SIMSET, MCNP, SIMIND, and UMCS (15,16). Commercial solutions

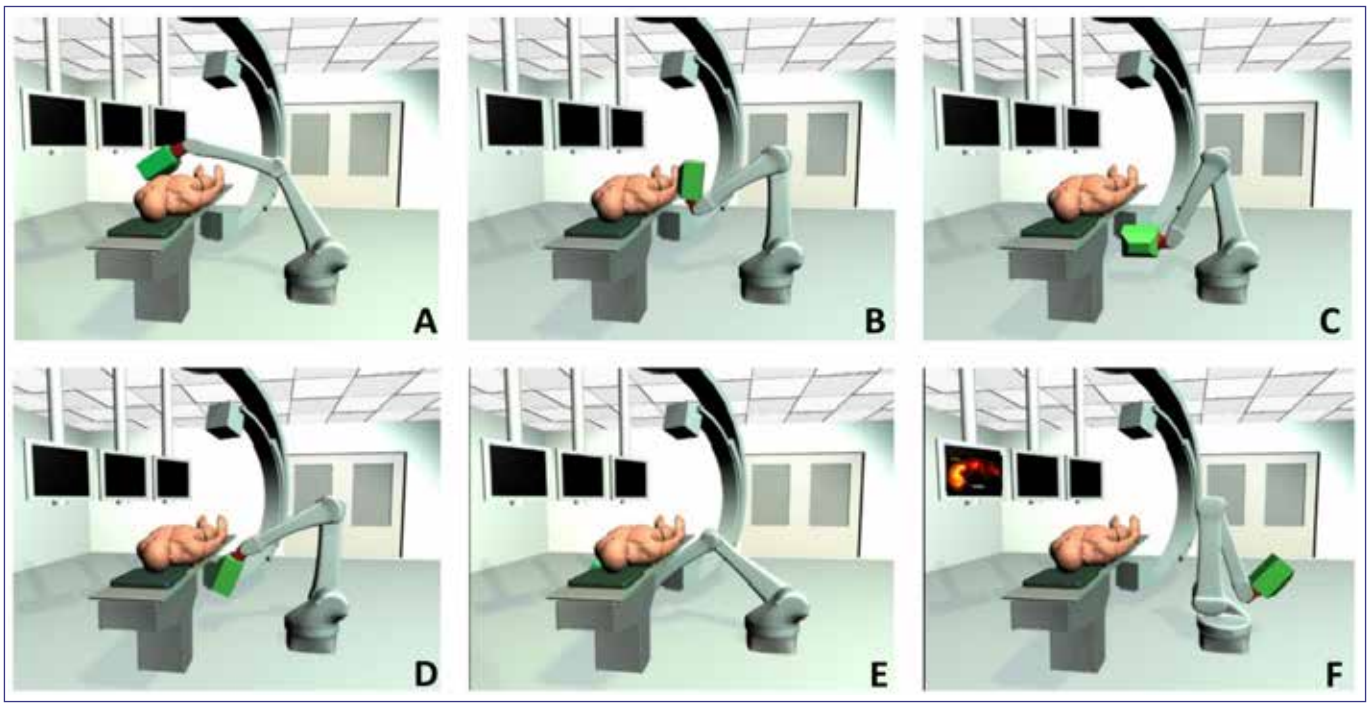

Figure 2. Rendering of an interventional pinhole SPECT camera mounted on a six-axis arm robot (9).

are also available (Hermes Medical Solutions AB, Stockholm, Sweden) (17). As Monte Carlo simulations are notoriously slow, acceleration is often performed using variance reduction techniques. One of the strategies is to use convolution forced detection (CFD), which forces particles towards the collimator by creating daughter particles at every interaction in the phantom with weighting to correct for the likelihood of detection (18,19). In spite of the challenges of quantitative SPECT, a quantitative accuracy of within 5% can be obtained, which is equivalent to the accuracy of PET/CT systems (20).

To obtain quantitative images for dosimetric applications, the images representing the activity concentration (in Bq per unit volume) are converted to images that represent patient dose (in Gy or Sv). For this purpose, an estimation of retention time and information about the spatial dose distribution (e.g. dose point kernels) is needed. The retention time may be estimated by assuming a theoretical effective half-life or by acquiring multiple scans over time to achieve a time integrated activity in a target volume (organ or tumour). Subsequently, the absorbed dose can be calculated by multiplying the activity concentration with a radionuclide specific constant (21) by convolving the activity distribution with a dose point kernel or by performing Monte Carlo simulations (22), depending on the required accuracy of the dose estimation.

Advances in the development of SPECT reconstruction algorithms also involve the use of anatomical priors. For example, maximum a posteriori (MAP) algorithms that incorporate smoothing within, but not across organ and/or lesion boundaries may improve the quality of images used for guidance of radionuclide therapy (23–25). The xSPECT algorithm (Siemens Healthcare, Erlangen, Germany) is a commercial example of a reconstruction method that uses anatomical information from the CT scanner to improve ^{99m}Tc methyl diphosphonate (MDP) images (26,27). A fundamental issue with the use of anatomical priors is that the resulting images are no longer purely molecular images, but they also include anatomical information.

Developments in SPECT reconstruction algorithms also include corrections for cardiac and/or respiratory motion (28–30). The correction for cardiac motion mostly benefits cardiac applications, whereas corrections for respiratory motion may improve lesion detection in general. Motion correction is discussed in more detail in the next section.

PET

^{18}F fluorodeoxyglucose (FDG) PET accounts for the vast majority of PET studies in clinical practice, and is often used for staging and follow-up after radionuclide therapy. However, PET is also used for imaging of other nuclides (e.g. ^{90}Y, ^{124}I, ^{64}Cu and ^{68}Ga) for treatment planning, dosimetry and assessment of treatment response in radionuclide therapies. In all cases, good quantitative accuracy is required, either for precise SUV-based therapy response monitoring or more detailed dosimetry for therapy planning.

Current status

As for SPECT, quantitative PET requires application of

correction techniques. Attenuation correction for PET can easily be performed by determining the attenuation correction sinogram, typically based on co-registered CT data. In addition, scatter correction is often implemented in clinical practice using the single scatter simulation (SSS) method (31). Correction for random counts is generally performed by applying delayed event subtraction (32). Random and scatter correction can either be incorporated by subtracting the randoms from the sinogram before reconstruction, or by adding the randoms to the measured sinogram during each iteration in the forward projection (33,34). The latter has proven to be beneficial for image quality.

The time difference of detection between annihilation photons contains information about the location of the annihilation event along the line of response. This time-of-flight (TOF) information can be incorporated in the reconstruction during the backprojection step to improve image quality. The availability of TOF has paved the way for imaging isotopes with very low positron abundance like ^{90}Y.

As the intrinsic resolution of PET detectors is limited, the shape of the PSF can be incorporated in the reconstruction method to improve the quality of reconstructed images. This is often referred to as resolution recovery.

Radiation detection systems suffer from dead time effects due to pulse pile-up when subjected to high count rates. Dead time losses are routinely corrected for, based on measurements of a large range of activities and knowledge of the true count rate model.

Advances in PET

Instrumentation

The quality of PET images is continuously being improved by advances in PET instrumentation aiming at the improvement of resolution and sensitivity. This may aid in optimized targeting, treatment planning, dosimetry and assessment of treatment response in radionuclide therapies.

PET scanners traditionally use photomultiplier tubes (PMTs) to convert the optical signal coming from the scintillation crystal into an electronic signal. However, semiconductor-based alternatives are also becoming commercially available for clinical systems. The most commonly used alternatives are avalanche photodiodes (APDs) and silicon photomultipliers (SiPMs). APDs essentially are semiconductor photodetectors that operate in avalanche mode, which means that the output is linear with the amount of scintillation light. SiPMs consist of a multipixel array of small APDs that operate in Geiger mode. Therefore, the output of a single pixel of an SiPM is not linear with the amount of scintillation light. However, the amount of SiPM pixels that produce an avalanche pulse is a measure of the energy of the incident gamma photon. The individual SiPM pixels have a size of 20 to 100 micrometers, as shown in figure 3. SiPMs can be fabricated to couple with smaller size crystals and therefore improve resolution (35). Another advantage of SiPMs is their good timing resolution, which improves the efficiency of PET images (35–37) through better

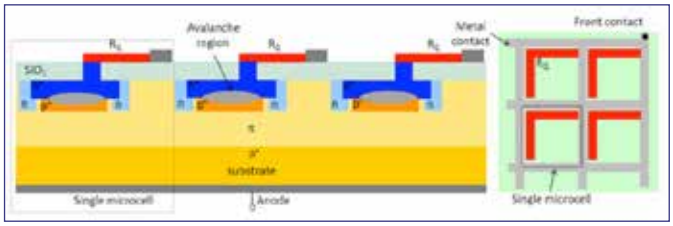

Figure 3. Schematic drawing of a SiPM.

Improving the TOF resolution results in an improved SNR, since noise is projected over a limited number of image voxels instead of an entire line of response. Therefore, improvement of the coincidence resolving time (CRT) is subject to research. TOF detectors typically use 4x4x22 mm^3 scintillation crystal elements, where photodetectors are placed on one of the small surfaces (top or bottom). Moses et al. developed a detector where the photodetector is mounted on the side of the crystal element (38). This reduces the mean path length of the scintillation photons to the photodetectors, which in turn improves timing resolution. Another approach to improve the timing resolution is by utilizing a double-sided readout, as described by Seifert and Schaart (39). They describe a setup in which photodetectors are mounted on the top and bottom of the crystal element, enabling correction of depth dependent effects to the timing uncertainty. An additional advantage of this approach is that depth of interaction (DOI) can be extracted.

Another method to improve the efficiency of PET images is by increasing axial detector length. The image quality of low-abundance isotopes such as ^{90}Y may benefit from this approach. Extending the axial field-of-view of a PET scanner from 16.2 cm (3 detector rings) to 21.8 cm (4 detector rings) already significantly increases system sensitivity (40). A whole body PET system with an axial detector length of approximately 2 m is currently under development at UC Davis, as shown in figure 4 (41). Although the increase of axial detector length increases sensitivity, it also increases the adverse effects of parallax errors as observed with traditional detectors. Parallax errors occur when an annihilation photon enters one crystal element, but is absorbed after penetrating into an adjacent crystal element. This generally occurs for high oblique angles of incidence. Parallax errors may be reduced if detectors are equipped with DOI information (42,43).

Reconstruction

Advances in image reconstruction include modelling of motion by incorporating the information of motion into the reconstruction algorithm (44,45). Motion correction can easily be performed by including counts only from a certain phase

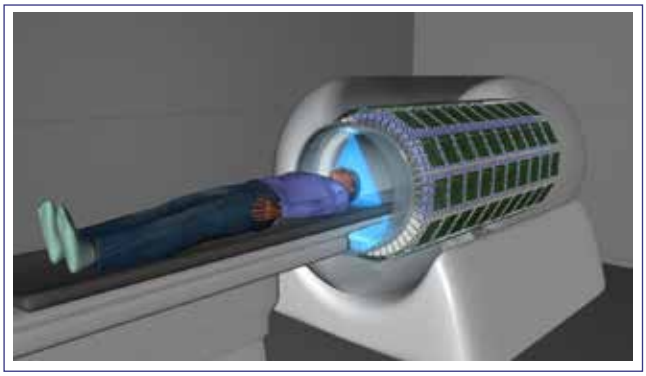

Figure 4. The 'EXPLORER' total-body PET scanner (Courtesy Dr. S.R Cherry and Dr. R.D. Badawi, UC Davis, United States).

of the respiratory cycle (e.g. end expiration). Such a phase gated approach suffers however from prolonged scan times (or increased noise) due to the loss of data that are discarded for reconstruction. Correction for respiratory motion may be implemented by using information of motion from additional hardware (e.g. a belt system). However, similar results can also be obtained with data-driven approaches (46), without the use of additional hardware. Event-by-event motion correction is an approach in which all data is used to reconstruct an image (47,48). This leads to less noise compared to phase gated motion correction. In general, list mode data is often used instead of binned sinograms for four-dimensional reconstruction algorithms to preserve temporal information of the counts.

As for SPECT, PET images may be improved by integrating anatomical information in the reconstruction algorithm by using anatomical priors (49–52). In addition to using anatomical priors, smoothing priors can be incorporated with a penalty term that suppresses noise (53,54). A penalized likelihood reconstruction algorithm for PET called Q.Clear (GE Healthcare, Milwaukee, United States) is commercially available (55).

For some isotopes, positrons are emitted in cascade with the emission of other gamma photons, so that additional photons are emitted together with the two annihilation photons (figure 5). Iodine-124 (^{124}I) and yttrium-86 (^{86}Y) are examples of isotopes that emit prompt gammas in cascade with the positron, and are often used for matched pairs dosimetry of the therapeutic isotopes ^{131}I and ^{90}Y, respectively (56). When these prompt gamma photons are detected, they may be mistaken for an annihilation photon, resulting in an erroneous line of response. The adverse effects of the prompt gamma photons can be corrected for by implementing a prompt gamma correction (PGC) in the reconstruction algorithm (57–59).

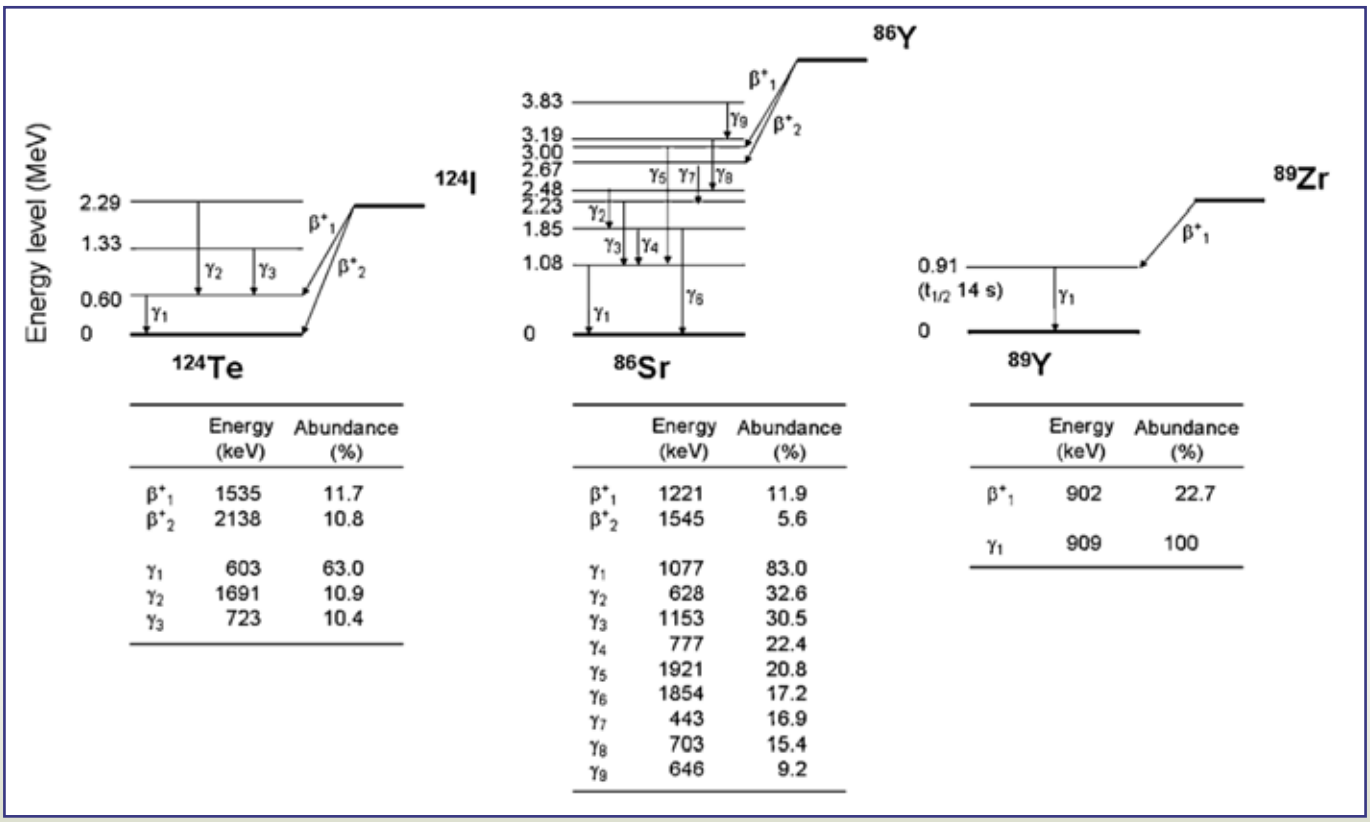

	Energy (keV)	Abundance (%)
β^+_1	1535	11.7
β^+_2	2138	10.8
γ_1	603	63.0
γ_2	1691	10.9
γ_3	723	10.4

	Energy (keV)	Abundance (%)
β^+_1	1221	11.9
β^+_2	1545	5.6
γ_1	1077	83.0
γ_2	628	32.6
γ_3	1153	30.5
γ_4	777	22.4
γ_5	1921	20.8
γ_6	1854	17.2
γ_7	443	16.9
γ_8	703	15.4
γ_9	646	9.2

	Energy (keV)	Abundance (%)
β^+_1	902	22.7
γ_1	909	100

Figure 5. The decay scheme of several isotopes that emit prompt gamma rays in cascade with the positron emission (60).

PET/MR

PET/MR has several advantages over PET/CT, of which higher soft-tissue contrast is probably most important for treatment planning, dosimetry and assessment of treatment response of radionuclide therapies. Additionally, the simultaneous acquisition of co-registered MRI images may benefit accurate dosimetry. Also, MRI can be used to identify organs at risk (or parts of one organ), which may be essential for determining the maximum tolerable radionuclide dosage. Moreover, the simultaneous acquisition of anatomical and molecular images enables accurate motion correction, for instance by making real-time MRI images of the lungs.

The integration of PET and MRI modalities does however bring about serious challenges, as mutual interference between modalities can occur. That is, photomultiplier tubes used in traditional PET detectors do not function in the strong magnetic fields used for MR imaging. Moreover, the radiofrequency signal used for MR imaging is affected by the PET modules (61). For this reason, the first generation of PET/MR systems acquired PET and MR images in sequence and the modalities were spatially separated. Integrated systems where the PET detectors are inserted into the bore of the MR scanner are now available so that PET and MR images can be acquired simultaneously. Integrated PET/MR systems employ detector systems based on either APDs or SiPMs that are insensitive to the magnetic field. The simultaneous measurement ensures a better spatial agreement of PET and MR data and provides a unique opportunity for 4D acquisitions for example to perform motion correction, without the need for respiratory motion sensors.

Disadvantages of PET/MR include the high costs and the fact that ferromagnetic metallic implants are contraindications for MR imaging. Moreover, one of the big challenges for PET/MR is attenuation correction. CT images are ideal for attenuation correction as they provide electron density images, whereas MR images give information about proton density, which makes them less suitable for attenuation correction. Moreover, MR images are often transaxially truncated. However, electron density information ('pseudo-CT') can still be extracted from the MR images with methods based on atlas information and machine learning techniques or segmentation-based approaches (62,63). Alternatively, the attenuation maps may be estimated by using algorithms that use the (time-of-flight) emission and/or transmission data (64).

Hand held gamma cameras and gamma probes

Hand held gamma cameras and gamma probes can be used to acquire intra-operative information about the distribution of activity (65–67). Gamma probes give acoustic feedback and/or display a count rate, whereas hand held gamma cameras provide the surgeon with a small field of view image. They are routinely used for the localization of sentinel lymph nodes during sentinel lymph nodes biopsies.

A wide range of different gamma probe designs is commercially available, optimized for different surgical applications. Advances in gamma probe technology include the use of a wireless gamma probe for open surgery (68) and a drop-in gamma probe for laparoscopic procedures that can be inserted via the trocar and positioned with laparoscopic tools (figure 6) (69). The one-dimensional information from the probe can be reconstructed to a three-dimensional estimate of the distribution using reconstruction algorithms to obtain freehand SPECT (fhSPECT) images (70,71). Interventional SPECT images can be acquired using a hand held gamma camera mounted on a robotic arm (72,73).

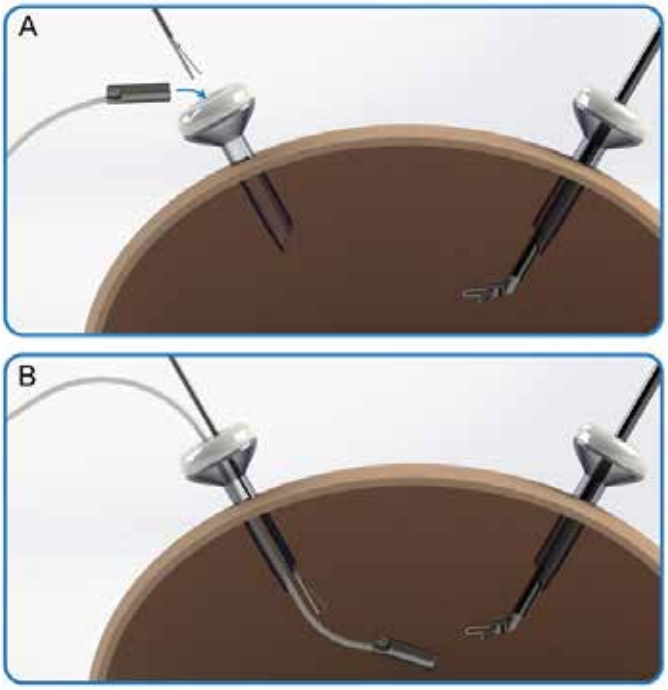

Figure 6. Schematic drawing of the insertion of the drop-in gamma probe through a trocar (A) after which the surgeon can grab the probe with the available surgical tool (B) (69).

In general, the interpretation of the information acquired by gamma probes and hand held gamma cameras may be difficult owing to the lack of co-registered anatomical information. This can be solved by registration of preoperative anatomical data to the interventionally acquired images (74). Nevertheless, non-rigid registration remains a challenge and the preoperative images may not represent the actual activity distribution. Therefore, fusion of freehand SPECT images with ultrasound images is a promising technique for hybrid image guidance (75).

Other modalities for guidance

Imaging modalities other than nuclear imaging are also used for the guidance of radionuclide therapy. For example,

fluoroscopic imaging is used for radionuclide therapies that require real-time image guidance, such as assisting in the positioning of catheters for liver radioembolisation (76). With the development of interventional MR scanners, these procedures may also be performed in the future under MR guidance for increased soft-tissue contrast and the absence of radiation dose. Intratumoral injection of radionuclides may also be performed under guidance of interventional CT images or using ultrasound (77,78).

Other ways of hybrid image guidance include the use of hybrid gamma emitting and fluorescent tracers for sentinel lymph node procedures that enable two-step navigation by preoperative imaging with SPECT/CT and intraoperative guidance by near-infrared fluorescence imaging (79).

Future perspectives

Simultaneous x-ray and nuclear imaging

To date, no real-time hybrid imaging modalities for interventional purposes have been developed that combine simultaneously acquired nuclear and anatomical images. Real-time functional imaging in conjunction with anatomical imaging would provide the physician with valuable information during the procedure, thereby improving therapeutic efficiency. We developed a prototype that relies on placing an x-ray tube, an x-ray detector and a gamma camera in one line enabling imaging of the same field-of-view (80). Since straightforward combination of these elements would block the line of views, a gamma camera geometry that looks around the x-ray tube was developed. A prototype was built using a mobile c-arm and a gamma camera with a four-pinhole collimator. Measurements with the hybrid imaging prototype device that combines simultaneous x-ray and nuclear imaging of the same field of view have demonstrated the feasibility of real-time simultaneous hybrid imaging in the intervention room (figure 7).

PET versus SPECT

Generally, PET outperforms SPECT with respect to sensitivity, resolution and quantitative capabilities. One approach to improve the quality of nuclear images is to replace SPECT tracers with positron emitting PET tracers. Examples include the use of diagnostic ^{124}I metaiodobenzylguanidine (MIBG) PET instead of ^{123}I MIBG SPECT (81) or the use of the low abundance internal pair production of ^{90}Y for ^{90}Y PET instead of Bremsstrahlung ^{90}Y SPECT (82). Matched pairs dosimetry exploits the characteristics of isotopes that are most suitable for imaging (^{124}I and ^{86}Y) and uses their beta emitting counterparts (^{131}I and ^{90}Y) for therapeutic purposes (56).

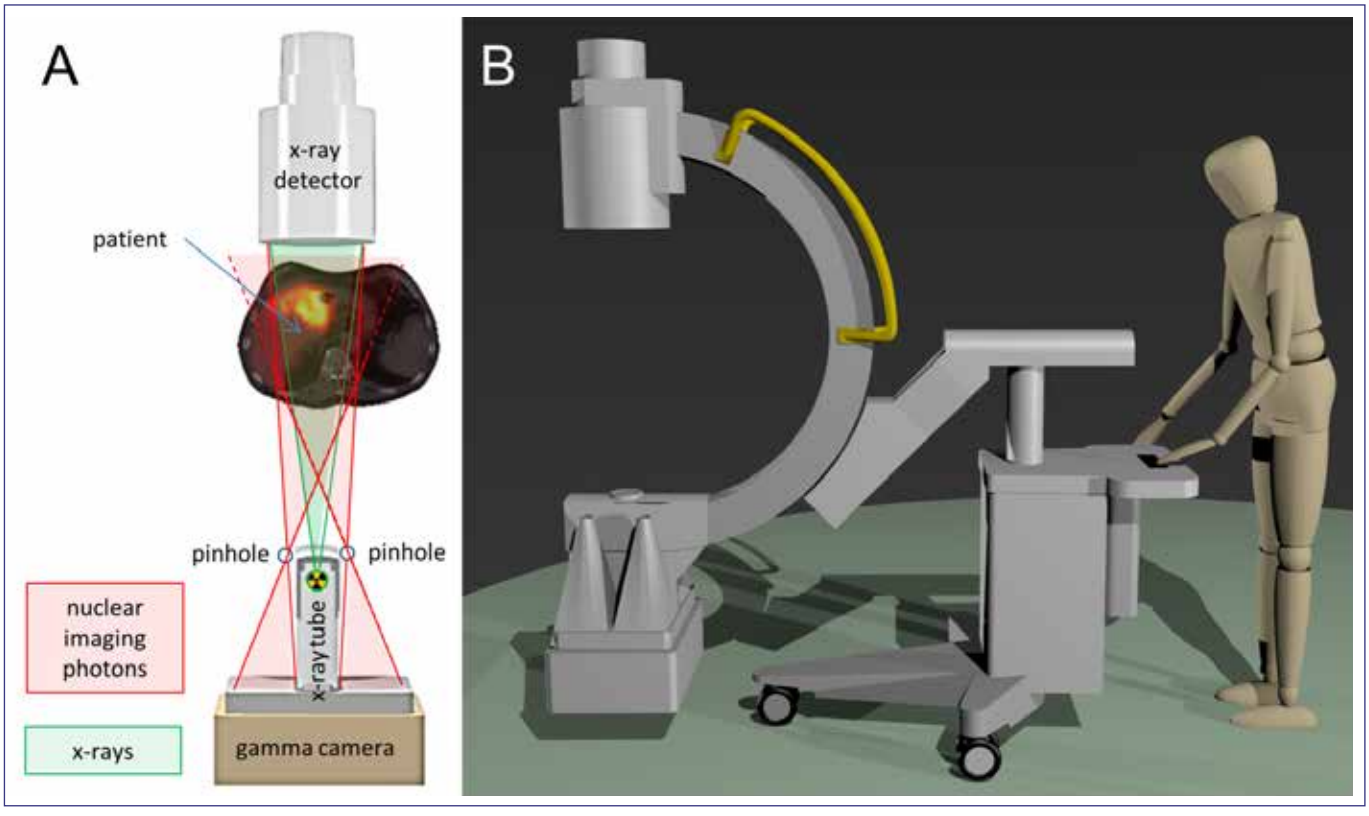

Figure 7. Schematic drawing of the hybrid C-arm showing the field of view of the pinhole collimator and the x-ray photons (A) and a rendering of the system (B) (80).

These advances spur the question of whether there is a future for SPECT systems in the nuclear medicine department (83–85). Some have argued that PET may completely replace scintigraphy and SPECT in the future (84). However, the type of decay determines whether SPECT or PET is used for imaging. Finding suitable and cost-effective positron-emitting alternatives remains a challenge for many SPECT radiopharmaceuticals.

Conclusion

The quality of images used for guidance therapy in nuclear medicine is continuously improving, which in turn improves the therapeutic outcome and efficiency. This includes advances in algorithms and instrumentation for traditional nuclear imaging modalities, as well as in the development of novel modalities.

cbeijst@umcutrecht.nl

References

1. Kwekkeboom DJ, de Herder WW, Kam BL, et al. Treatment with the radiolabeled somatostatin analog [177 Lu-DOTA 0,Tyr3]octreotate: toxicity, efficacy, and survival. J Clin Oncol. 2008;26(13):2124–30
2. Seidlin SM, Marinelli LD, Oshry E. Radioactive iodine therapy; effect on functioning metastases of adenocarcinoma of the thyroid. J Am Med Assoc. 1946;132(14):838–47
3. Smits MLJ, Prince JF, Rosenbaum CENM, et al. Intra-arterial radioembolization of breast cancer liver metastases: a structured review. Eur J Pharmacol. 2013;709(1–3):37–42
4. Ogawa K, Harata Y, Ichihara T, Kubo A, Hashimoto S. A practical method for position-dependent Compton-scatter correction in single photon emission CT. IEEE Trans Med Imaging. IEEE; 1991;10(3):408–12
5. Walrand S, Hesse M, Wojcik R, Lhommel R, Jamar F. Optimal design of anger camera for bremsstrahlung imaging: Monte Carlo evaluation. Front Oncol. 2014;4:149
6. Schramm NU, Ebel G, Engeland U, et al. High-resolution SPECT using multipinhole collimation. Nucl Sci IEEE Trans. 2003;50(3):315–20
7. Goorden MC, Beekman FJ. High-resolution tomography of positron emitters with clustered pinhole SPECT. Phys Med Biol. 2010;55(5):1265–77
8. Beijst C, Elschot M, Viergever MA, de Jong HWAM. A parallel-cone collimator for high-energy SPECT. J Nucl Med. 2015;56(3):476–82
9. Walrand S, Hesse M, Demonceau G, Pauwels S, Jamar F. Yttrium-90-labeled microsphere tracking during liver selective internal radiotherapy by bremsstrahlung pinhole SPECT: feasibility study and evaluation in an abdominal phantom. EJNMMI Res. 2011;1(1):32
10. Sharir T, Slomka PJ, Berman DS. Solid-state SPECT technology: fast and furious. J Nucl Cardiol. 2010;17(5):890–6
11. Melis M, de Swart J, de Visser M, et al. Dynamic and static small-animal SPECT in rats for monitoring renal function after 177Lu-labeled Tyr3-octreotate radionuclide therapy. J Nucl Med. Society of Nuclear Medicine; 2010;51(12):1962–8
12. Kojima A, Gotoh K, Shimamoto M, Hasegawa K, Okada S. Iodine-131 imaging using 284 keV photons with a small animal CZT-SPECT system dedicated to low-medium-energy photon detection. Ann Nucl Med. 2016;30(2):169–75
13. Esteves FP, Raggi P, Folks RD, et al. Novel solid-state-detector dedicated cardiac camera for fast myocardial perfusion imaging: multicenter comparison with standard dual detector cameras. J Nucl Cardiol. 2009;16(6):927–34
14. van Gils CAJ, Beijst C, van Rooij R, et al. Impact of reconstruction parameters on quantitative I-131 SPECT. Phys Med Biol.; 2016;61(14):5166–82
15. Elschot M, Smits MLJ, Nijsen JFW, et al. Quantitative Monte Carlo-based holmium-166 SPECT reconstruction. Med Phys. 2013;40(11):112502–12
16. Xiao J, de Wit TC, Staelens SG, Beekman FJ. Evaluation of 3D Monte Carlo-based scatter correction for 99mTc cardiac perfusion SPECT. J Nucl Med. 2006;47(10):1662–9
17. Willowson K, Bailey DL, Baldock C, et al. Quantitative SPECT reconstruction using CT-derived corrections. Phys Med Biol. IOP Publishing; 2008;53(12):3099–112
18. De Jong HWAM, Slijpen TP, Beekman FJ. Acceleration of Monte Carlo SPECT simulation using convolution-based forced detection. Nucl Sci IEEE Trans. 2001;48(1):58–64
19. Beekman FJ, De Jong HWAM, Van Geloven S. Efficient fully 3-D iterative SPECT reconstruction with Monte Carlo-based scatter compensation. IEEE Trans Med Imaging. 2002;21(8):867–77
20. Bailey DL, Willowson KP. Quantitative SPECT/CT: SPECT joins PET as a quantitative imaging modality. Eur J Nucl Med Mol Imaging. 2014;41 Suppl 1:S17-25
21. Dewaraja YK, Frey EC, Sgouros G, et al. MIRD pamphlet no. 23: Quantitative SPECT for patient-specific 3-dimensional dosimetry in internal radionuclide therapy. J Nucl Med. 2012;53(8):1310–25
22. Akabani G, Hawkins WG, Eckblade MB, Leichner PK. Patient-specific dosimetry using quantitative SPECT imaging and three-dimensional discrete Fourier transform convolution. J Nucl Med. 1997;38(2):308–14
23. Kulkarni S, Khurd P, Hsiao I, et al. A channelized Hotelling observer study of lesion detection in SPECT MAP reconstruction using anatomical priors. Phys Med Biol. IOP Publishing; 2007;52(12):3601–17
24. Lehovich A, Bruyant PP, Gifford HC, et al. Human-observer LROC study of lesion detection in Ga-67 SPECT images reconstructed using MAP with anatomical priors. IEEE Nucl Sci Symp Conf Rec (1997). NIH Public Access; 2006;3:1699–702
25. Lehovich A, Bruyant PP, Gifford HS, et al. Impact on reader performance for lesion-detection/ localization tasks of anatomical priors in SPECT reconstruction. IEEE Trans Med Imaging. NIH Public Access; 2009;28(9):1459–67
26. Ma J, Vija AH. Noise and resolution characteristics for xSPECT reconstruction method. J Nucl Med. Society of Nuclear Medicine; 2014;55(supplement 1):2129
27. Ma J, Vija AH, Bartenstein P, et al. Generation and validation of a surrogate truth model for xSPECT Bone concordance analysis.

J Nucl Med. Society of Nuclear Medicine; 2015;56(supplement 3):1280
28. Reader AJ, Verhaeghe J. 4D image reconstruction for emission tomography. Phys Med Biol. 2014;59(22):R371-418
29. Li G, Citrin D, Camphausen K, et al. Advances in 4D medical imaging and 4D radiation therapy. Technol Cancer Res Treat. 2008;7(1):67–81
30. Shrestha UM, Seo Y, Botvinick EH, Gullberg GT. Image reconstruction in higher dimensions: myocardial perfusion imaging of tracer dynamics with cardiac motion due to deformation and respiration. Phys Med Biol. 2015;60(21):8275–301
31. Zaidi H, Montandon M-L. Scatter Compensation Techniques in PET. PET Clin. 2007;2(2):219–34
32. Casey ME, Hoffman EJ. Quantitation in positron emission computed tomography: 7. A technique to reduce noise in accidental coincidence measurements and coincidence efficiency calibration. J Comput Assist Tomogr. 1986;10(5):845–50
33. Willowson KP, Tapner M, Team, QUESTI, Bailey DL. A multicentre comparison of quantitative (90)Y PET/CT for dosimetric purposes after radioembolization with resin microspheres : The QUEST Phantom Study. Eur J Nucl Med Mol Imaging. 2015;42(8):1202–22
34. Brasse D, Kinahan PE, Lartizien C, et al. Correction methods for random coincidences in fully 3D whole-body PET: impact on data and image quality. J Nucl Med. 2005;46(5):859–67
35. Slomka PJ, Pan T, Germano G. Recent Advances and Future Progress in PET Instrumentation. Semin Nucl Med. 2016;46(1):5–19
36. Surti S. Update on time-of-flight PET imaging. J Nucl Med. 2015;56(1):98–105
37. Conti M. Improving time resolution in time-of-flight PET. Nucl Instruments Methods Phys Res Sect A Accel Spectrometers, Detect Assoc Equip. 2011;648:S194–8
38. Moses WW, Janecek M, Spurrier MA, et al. Optimization of a LSO-Based Detector Module for Time-of-Flight PET. IEEE Trans Nucl Sci. 2010;57(3):1570–6
39. Seifert S, Schaart DR. Improving the Time Resolution of TOF-PET Detectors by Double-Sided Readout. IEEE Trans Nucl Sci. 2015;62(1):3–11
40. Jakoby BW, Bercier Y, Watson CC, Bendriem B, Townsend DW. Performance Characteristics of a New LSO PET/CT Scanner With Extended Axial Field-of-View and PSF Reconstruction. IEEE Trans Nucl Sci. 2009;56(3):633–9
41. Poon JK, Dahlbom ML, Moses WW, et al. Optimal whole-body PET scanner configurations for different volumes of LSO scintillator: a simulation study. Phys Med Biol. 2012;57(13):4077–94
42. Ito M, Hong SJ, Lee JS. Positron emission tomography (PET) detectors with depth-of- interaction (DOI) capability. Biomed Eng Lett. 2011;1(2):70–81
43. Schmall JP, Karp JS, Werner M, Surti S. Parallax error in long-axial field-of-view PET scanners-a simulation study. Phys Med Biol. 2016;61(14):5443–55
44. Rahmim A, Rousset O, Zaidi H. Strategies for Motion Tracking and Correction in PET. PET Clin. 2007;2(2):251–66
45. Rahmim A, Tang J, Zaidi H. Four-dimensional (4D) image reconstruction strategies in dynamic PET: Beyond conventional independent frame reconstruction. Med Phys. American Association of Physicists in Medicine; 2009;36(8):3654
46. Büther F, Vehren T, Schäfers KP, Schäfers M. Impact of Data-driven Respiratory Gating in Clinical PET. Radiology. 2016;152067
47. Liu C, Alessio AM, Kinahan PE. Respiratory motion correction for quantitative PET/CT using all detected events with internal-external motion correlation. Med Phys. 2011;38(5):2715–23
48. Chan C, Jin X, Fung EK, et al. Event-by-event respiratory motion correction for PET with 3D internal-1D external motion correlation. Med Phys. 2013;40(11):112507
49. Cheng-Liao J, Qi J. PET image reconstruction with anatomical edge guided level set prior. Phys Med Biol. IOP Publishing; 2011;56(21):6899–918
50. Somayajula S, Panagiotou C, Rangarajan A, et al. PET image reconstruction using information theoretic anatomical priors. IEEE Trans Med Imaging. 2011;30(3):537–49
51. Gindi G, Lee M, Rangarajan A, Zubal IG. Bayesian reconstruction of functional images using registered anatomical images as priors. In: Information Processing in Medical Imaging. Berlin/ Heidelberg: Springer-Verlag; 1991. 121–31
52. Bowsher JE, Johnson VE, Turkington TG, et al. Bayesian reconstruction and use of anatomical a priori information for emission tomography. IEEE Trans Med Imaging. 1996;15(5):673–86
53. Fessler JA, Hero AO. Penalized maximum-likelihood image reconstruction using space-alternating generalized EM algorithms. IEEE Trans Image Process. 1995;4(10):1417–29
54. Hebert T, Leahy R. A generalized EM algorithm for 3-D Bayesian reconstruction from Poisson data using Gibbs priors. IEEE Trans Med Imaging. IEEE; 1989;8(2):194–202
55. Teoh EJ, McGowan DR, Macpherson RE, Bradley KM, Gleeson F V. Phantom and Clinical Evaluation of the Bayesian Penalized Likelihood Reconstruction Algorithm Q.Clear on an LYSO PET/CT System. J Nucl Med. Society of Nuclear Medicine; 2015;56(9):1447–52
56. Lopci E, Chiti A, Castellani MR, et al. Matched pairs dosimetry: 124I/131I metaiodobenzylguanidine and 124I/131I and 86Y/90Y antibodies. Eur J Nucl Med Mol Imaging. 2011;38 Suppl 1:S28-40
57. Beattie BJ, Finn RD, Rowland DJ, Pentlow KS. Quantitative imaging of bromine-76 and yttrium-86 with PET: a method for the removal of spurious activity introduced by cascade gamma rays. Med Phys. 2003;30(9):2410–23
58. Preylowski V, Schlögl S, Schoenahl F, et al. Is the image quality of I-124-PET impaired by an automatic correction of prompt gammas? PLoS One. 2013;8(8):1–8
59. Surti S, Scheuermann R, Karp JS. Correction technique for cascade gammas in I-124 imaging on a fully-3D, Time-of-Flight PET Scanner. IEEE Trans Nucl Sci. NIH Public Access; 2009;56(3):653–60
60. Lubberink M, Herzog H. Quantitative imaging of 124I and 86Y

with PET. Eur J Nucl Med Mol Imaging. Springer; 2011;38 Suppl 1(Suppl 1):S10-8
61. Torigian DA, Zaidi H, Kwee TC, et al. PET/MR Imaging: Technical Aspects and Potential Clinical Applications. Radiology. 2013;267(1):26–44
62. Mehranian A, Arabi H, Zaidi H. Vision 20/20: Magnetic resonance imaging-guided attenuation correction in PET/MRI: Challenges, solutions, and opportunities. Med Phys. American Association of Physicists in Medicine; 2016;43(3):1130–55
63. Wagenknecht G, Kaiser H-J, Mottaghy FM, Herzog H. MRI for attenuation correction in PET: methods and challenges. MAGMA. Springer; 2013;26(1):99–113
64. Nuyts J, Dupont P, Stroobants S, et al. Simultaneous maximum a posteriori reconstruction of attenuation and activity distributions from emission sinograms. IEEE Trans Med Imaging. IEEE; 1999;18(5):393–403
65. Schneebaum S, Even-Sapir E, Cohen M, et al. Clinical applications of gamma-detection probes - Radioguided surgery. Eur J Nucl Med. 1999;26(SUPPL.):26–35
66. Hoffman EJ, Tornai MP, Levin CS, MacDonald LR, Siegel S. Gamma and beta intra-operative imaging probes. Nucl Instruments Methods Phys Res Sect A Accel Spectrometers, Detect Assoc Equip. 1997;392(1–3):324–9
67. Heller S, Zanzonico P. Nuclear probes and intraoperative gamma cameras. Semin Nucl Med. Elsevier Inc.; 2011;41(3):166–81
68. Park HM, Joo KS. Feasibility of a wireless gamma probe in radioguided surgery. Phys Med Biol. IOP Publishing; 2016;61(12):N311–21
69. Oosterom M van, Simon H, Mengus L, et al. Revolutionizing (robot-assisted) laparoscopic gamma tracing using a drop-in gamma probe technology. Am J Nucl Med Mol Imaging. 2016;6(1):1
70. Wendler T, Hartl A, Lasser T, et al. Towards intra-operative 3D nuclear imaging: reconstruction of 3D radioactive distributions using tracked gamma probes. Med Image Comput Comput Assist Interv. 2007;10(Pt 2):909–17
71. Bluemel C, Schnelzer A, Okur A, et al. Freehand SPECT for image-guided sentinel lymph node biopsy in breast cancer. Eur J Nucl Med Mol Imaging. 2013;40(11):1656–61
72. Fuerst B, Sprung J, Pinto F, et al. First Robotic SPECT for Minimally Invasive Sentinel Lymph Node Mapping. IEEE Trans Med Imaging. 2015;PP(99):1
73. Matthies P, Sharma K, Okur A, et al. First Use of Mini Gamma Cameras for Intra-operative Robotic SPECT Reconstruction. In Springer Berlin Heidelberg; 2013. p. 163–70
74. Wood BJ, Locklin JK, Viswanathan A, et al. Technologies for guidance of radiofrequency ablation in the multimodality interventional suite of the future. J Vasc Interv Radiol. 2007;18(1):9–24
75. Freesmeyer M, Opfermann T, Winkens T. Hybrid integration of real-time US and freehand SPECT: proof of concept in patients with thyroid diseases. Radiology. 2014;271(3):856–61
76. Kennedy AS, Salem R. Radioembolization (yttrium-90 microspheres) for primary and metastatic hepatic malignancies. Cancer J. 2010;16(2):163–75
77. Tian JH, Xu BX, Zhang JM, et al. Ultrasound-guided internal radiotherapy using yttrium-90-glass microspheres for liver malignancies. J Nucl Med. 1996;37(6):958–63
78. Phillips WT, Bao A, Brenner AJ, Goins BA. Image-guided interventional therapy for cancer with radiotherapeutic nanoparticles. Adv Drug Deliv Rev. 2014;76:39–59
79. van den Berg NS, Valdés-Olmos RA, van der Poel HG, van Leeuwen FWB. Sentinel lymph node biopsy for prostate cancer: a hybrid approach. J Nucl Med. 2013;54(4):493–6
80. Beijst C, Elschot M, Viergever MA, de Jong HWAM. Toward Simultaneous Real-Time Fluoroscopic and Nuclear Imaging in the Intervention Room. Radiology. 2016;278(1):232–8
81. Cistaro A, Quartuccio N, Caobelli F, et al. 124I-MIBG: a new promising positron-emitting radiopharmaceutical for the evaluation of neuroblastoma. Nucl Med Rev Cent East Eur. 2015;18(2):102–6
82. Kao Y-H, Steinberg JD, Tay Y-S, et al. Post-radioembolization yttrium-90 PET/CT - part 1: diagnostic reporting. EJNMMI Res. 2013;3(1):56
83. Gholamrezanejhad A, Mirpour S, Mariani G. Future of nuclear medicine: SPECT versus PET. J Nucl Med. 2009;50(7):16N–18N
84. Alavi A, Basu S. Planar and SPECT imaging in the era of PET and PET-CT: can it survive the test of time? Eur J Nucl Med Mol Imaging. 2008;35(8):1554–9
85. Mariani G, Bruselli L, Duatti A. Is PET always an advantage versus planar and SPECT imaging? Eur J Nucl Med Mol Imaging. 2008;35(8):1560–5

new

Nu te bestellen bij: bol.com

ISBN:	ISBN 978-90-78876-09-0
Uitgever:	Kloosterhof Neer B.V.
Omvang:	780 pagina's
Uitvoering:	garengenaaid
Prijs:	€ 53 (leden NVNG excl. verzendkosten)
	€ 79,50 (excl. verzendkosten)

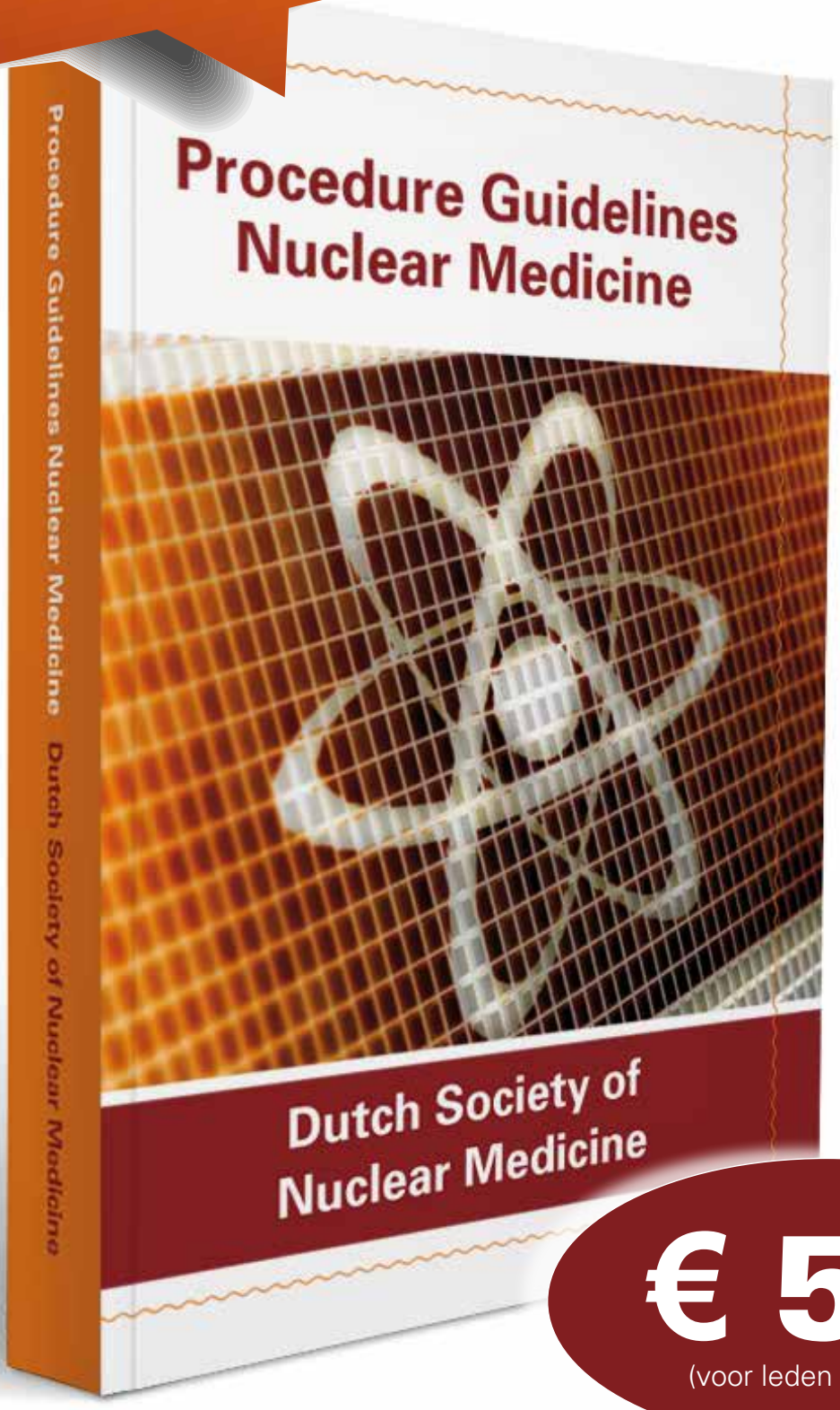

€ 53

(voor leden NVNG)

In Memoriam dr. G. de Haas

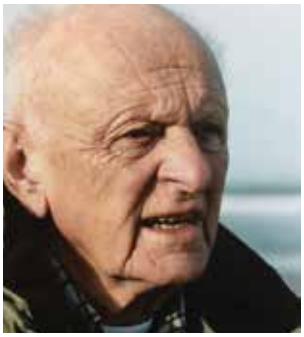

Dr. Gerrit de Haas, een der pioniers van de nucleaire geneeskunde in Nederland, is op 1 oktober in de leeftijd van 88 jaar overleden. Een nestor is niet meer.

Dr. de Haas, van origine huisarts – samen met zijn echtgenote – en later radioloog, was met generatiegenoten van diverse disciplines betrokken bij de oprichting van de NVNG, de totstandkoming en erkenning van het specialisme nucleaire geneeskunde in Nederland en de vormgeving van onze specialistenopleiding. Hij hechtte groot belang aan de opleiding van (toen zogeheten) arts-assistenten en laboranten. Een tastbaar testimonium is het Leerboek Nucleaire Geneeskunde, dat onder zijn redactie in 1984 werd gepubliceerd.
Minstens zo betekenisvol is wat dr. de Haas als opleider en als docent met al zijn charisma heeft overgedragen. Over sommige zaken was hij buitengewoon uitgesproken, en hij stond niet klakkeloos voor alles open. Zijn diep menselijke en humoristische aard, gekoppeld aan een grote nieuwsgierigheid, een open geest en tomeloze geestdrift hebben vele van zijn medewerkers en leerlingen positief beïnvloed. Het besef dat de mens op de eerste plaats komt, heeft generaties aios in Utrecht gevormd tot nucleair geneeskundigen met toewijding voor wie zich aan hen toevertrouwen, onderwijl de hoogste eisen stellend aan de eigen vakkennis – kritisch en collegiaal.
Dr. de Haas was een belezen man en een bevlogen arts, die zich ook op hoge leeftijd nog flink kon opwinden over misstanden in de medische wereld, en een enorme belangstelling behield voor geschiedenis, filosofie en kunst. Na zijn werk als arts was de hedendaagse kunst zijn voornaamste passie, één van de grote liefdes die hij deelde met zijn vrouw Rie. Samen hebben zij ontelbare musea en tentoonstellingen bezocht in binnen- en buitenland. Gerrit was daarbij vooral geïnteresseerd in de modernen en post-modernen. Hij was een groot bewonderaar van Armando, en de persoonlijke ontmoetingen met deze kunstenaar betekenden voor hem een absoluut hoogtepunt.
Toen Gerrit de Haas meer en meer aan huis gekluisterd raakte, is hij zelf als kunstenaar actief geworden. Hij vervaardigde kunstobjecten veelal uit tegelfragmenten, half doorgeslepen vazen en acrylverf. De verzamelaar van oud-hollandse tegels en de liefhebber van moderne kunst kwamen in zijn oeuvre bijeen. Inspiratie vond hij onveranderlijk in existentiële levensvragen. Terugkerende thema's waren de teloorgang van christelijke waarden in de samenleving en dilemma's rond het onherroepelijke levenseinde. Dat einde is nu gekomen.

Gerrit, rust in vrede. Moge het verlies voor je dierbaren draaglijker zijn in de wetenschap dat je mooiste tradities voortleven in velen van ons.
Dag prachtmens.

Dr. Hans van Isselt

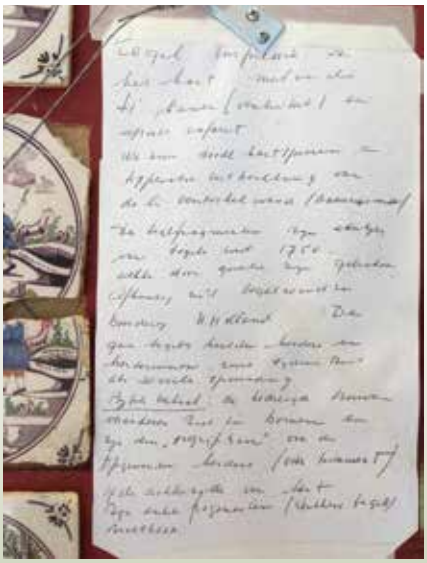

Tijdschrift voor Nucleaire Geneeskunde
ISSN 1381-4842, nr. 3, september 2016
Uitgever

KLOOSTERHOF
ACQUISITIE SERVICES - UITGEVERIJ
Kloosterhof acquisitie services - uitgeverij
Napoleonsweg 128a
6086 AJ Neer
T 0475 59 71 51
F 0475 59 71 53
E info@kloosterhof.nl
I www.kloosterhof.nl

Hoofdredacteur
prof. dr. J. Booij
j.booij@amc.uva.nl

Redactie
dr. M. Bauwens
mw. drs. B. Bosveld
dr. B.F. Bulten
dr. J. van Dalen
drs. J. Emmering
dr. A.W.J.M. Glaudemans
A. Reniers
dr. H.J. Verberne
dr. O. de Winter

Adviesraad
prof.dr. F.J. Beekman
prof.dr. O.C. Boerman
prof.dr. E.F.I. Comans
prof.dr. R.A.J.O. Dierckx
prof.dr. A.A.M.S. van Dongen
prof.dr. B.L.F. van Eck-Smit
prof.dr. P.H. Elsinga
prof.dr.ir. M.de Jong
prof.dr. L.F. de Geus-Oei
prof.dr.I. Goethals
prof.dr. N.H. Hendrikse
prof.dr. O.S. Hoekstra
prof.dr. A.A. Lammertsma
prof.dr. W.J.G. Oyen
prof.dr. J. Pruim
prof.dr. J.F. Verzijlbergen
prof.dr. A.D. Windhorst

Bureauredactie
Yvonne van Pol-Houben
T 0475 60 09 44
E nucleaire@kloosterhof.nl

Advertentie-exploitatie
Kloosterhof Neer B.V.
acquisitie services – uitgeverij
Eric Vullers
T 0475 597151
E. eric@kloosterhof.nl

Vormgeving
Kloosterhof Vormgeving
Marie-José Verstappen
Annemieke Peeters

Abonnementen
Leden en donateurs van de aangesloten Leden en donateurs van de aangesloten beroepsverenigingen ontvangen het Tijdschrift voor Nucleaire Geneeskunde kosteloos. Voor anderen geldt een abonnementsprijs van € 45,00 per jaar; studenten betalen € 29,00 per jaar (incl. BTW en verzendkosten).
Voor buitenlandse abonnementen gelden andere tarieven. Opgave en informatie over (buitenlandse) abonnementen en losse nummers (€ 13,50) bij Kloosterhof acquisitie services - uitgeverij, telefoon 0475 59 71 51.
www.tijdschriftvoornucleairegeneeskunde.nl

Verschijningsdata, jaargang 39
Nummer 1: 28 maart 2017
Nummer 2: 27 juni 2017
Nummer 3: 26 september 2017
Nummer 4: 29 december 2017

Verschijningsdata, jaargang 40
Nummer 1: 26 maart 2018

Aanleveren kopij, jaargang 39
Nummer 1: 1 januari 2017
Nummer 2: 1 april 2017
Nummer 3: 1 juli 2017
Nummer 4: 1 oktober 2017

Aanleveren kopij, jaargang 40
Nummer 1: 1 januari 2018

Kloosterhof acquisitie services - uitgeverij

Cursus- en congresagenda

2017

SNMMI 2017 Mid-Winter Meeting
19 – 22 January, 2017. Phoenix, USA. www.snmmi.org/mwm

International Symposium: Molecular Imaging agents in medicine
13 - 15 February 2017. UMCG, Groningen, the Netherlands. http://www.bnms.org.uk/images/Molecular_Imaging_Agents_in_Medicine_13-15_Feb.pdf

6th Balkan Congress of 2017 Nuclear Medicine
20 – 22 April, 2017. Sofia, Bulgaria. http://bcnm2017.com/

ECR 2017 - European Congress of Radiology Annual Meeting
1 - 5 March, 2017. Vienna, Austria. https://www.myesr.org/cms/website.php?id=/en/ecr_2017.htm

BELNUC 18th Symposium 2017
5 – 7 May, 2017. Gent, Belgium. http://belnuc.be/event/belnuc-18th-symposium-2017

ICNC 2017, Nuclear Cardiology & Cardiac CT
7 – 9 May, 2017. Vienna, Austria. https://www.escardio.org/Congresses-&-Events/ICNC/ICNC-Nuclear-Cardiology-and-Cardiac-CT

Radiologendagen 2017
11 - 12 May, 2017. Rotterdam, the Netherlands. www.radiologen.nl

BNMS Spring Meeting 2017
20 – 22 May, 2017. Birmingham, U.K. http://www.bnms.org.uk/

SNMMI 2017 Annual Meeting
10 – 14 June, 2017. Denver, USA. http://www.snmmi.org/AM/

Symposium Oncologie in Perspectief
15 June, 2017. Amsterdam, the Netherlands. https://www.oncologieinperspectief.avl.nl/

EANM 2017 - 30th Annual Congress of the European Association of Nuclear Medicine
21 – 25 October, 2017. Vienna, Austria. http://www.eanm.org/congresses_events/future_congresses.php?navId=343

Adreswijzigingen

Regelmatig komt het voor dat wijzigingen in het bezorgadres voor het Tijdschrift voor Nucleaire Geneeskunde op de verkeerde plaats terechtkomen. Adreswijzigingen moeten altijd aan de betreffende verenigingssecretariaten worden doorgegeven. Dus voor de medisch nucleair werkers bij de NVMBR, en voor de leden van de NVNG en het Belgisch Genootschap voor Nucleaire Geneeskunde aan hun respectievelijke secretariaten.
De verenigingssecretariaten zorgen dan voor het doorgeven van de wijzigingen aan de Tijdschrift adresadministratie.
Alleen adreswijzigingen van betaalde abonnementen moeten met ingang van 1 januari 2011 rechtstreeks aan de abonnementenadministratie van Kloosterhof Neer B.V. worden doorgegeven: Kloosterhof Neer B.V., t.a.v. administratie TvNG, Napoleonsweg 128a | 6086 AJ Neer of per E-mail: nucleaire@kloosterhof.nl

Overweeg start met kuur Xofigo® bij patiënten progressief op 2e generatie hormoontherapie[1,2]

L.NL.MKTSM.10.2016.1335

XOFIGO® is geïndiceerd voor de behandeling van volwassenen met castratieresistent prostaatcarcinoom, symptomatische botmetastasen en geen bekende viscerale metastasen[3]

* De mediane overlevingswinst van Xofigo® vs placebo in de ALSYMPCA bedraagt 3.6 maanden

Zie voor referenties en productinformatie elders in dit blad.

Xofigo®
radium Ra 223 dichloride

AANBEVOLEN IN DE LANDELIJKE RICHTLIJN PROSTAATCARCINOOM 2016[4]

Xofigo® wordt aanbevolen als behandeloptie in:

- 1e lijn (chemo-fit & niet chemo-fit)
- 2e lijn (post-docetaxel)

bij mCRPC-patiënten met symptomatische bot-metastasen en geen bekende viscerale metastasen[4]

gehealthcare.com

Open the door to freedom from chronic diarrhoea

How a diagnosis of bile acid malabsorption (BAM) with SeHCAT™ can help patients with irritable bowel syndrome[1]

- SeHCAT, Tauroselcholic [75Se] acid, is an accurate diagnostic test for identifying patients with bile acid malabsorption (BAM)[1-3]
- BAM may be the underlying cause of chronic diarrhoea in 1/3 of patients previously diagnosed with diarrhoea predominant irritable bowel syndrome (D-IBS)[1,3,4]
- Accurate diagnosis and effective treatment of chronic diarrhoea can lead to improvements in patients' symptoms and quality of life[1]

Imagination at work

SeHCAT™
Tauroselcholic [^{75}Se] acid

VERKORTE BIJSLUITER SeHCAT 370 kBq capsules
Voor volledig informatie raadpleeg de samenvatting van de productkenmerken (SPC).
Samenstelling: [^{75}Se]Tauroselcholzuur wordt geleverd in de vorm van capsules met 370 kBq op de referentiedatum voor de activiteit. **Indicaties:** Uitsluitend voor diagnostisch gebruik. [^{75}Se]Tauroselcholzuur wordt toegepast voor het onderzoek naar de malabsorptie van galzuren en ter bepaling van het totale verlies aan galzuren. Het kan worden gebruikt ter beoordeling van de ileumfunctie, voor onderzoek naar "Inflammatory Bowel Disease" en chronische diarree en ter bestudering van de enterohepatische kringloop. **Dosering en wijze van toediening:** De normale dosis voor volwassenen en ouderen is één capsule, oraal toegediend. Er is geen pediatrische toedieningsvorm en evenmin is er klinische ervaring met het gebruik van dit product bij kinderen. Alvorens het product bij kinderen wordt toegepast, moeten de voor- en nadelen zorgvuldig worden afgewogen, met name omdat het gebruik van een vaste dosis een verhoogd EDE bij kinderen tot gevolg heeft (zie SPC). Indien het product aan kinderen wordt toegediend, wordt dezelfde dosering als voor volwassenen aangehouden. Ter verzekering van een goede passage van de capsule naar de maag wordt de patiënt aangeraden voor, tijdens en na het doorslikken van de capsule telkens 15 ml water te drinken. Tijdens het innemen dient de patiënt te zitten of te staan. **Procedure voor gebruik:** Bepaling van de vermindering van de galzuur-pool: De bepaling van het tempo waarin het galzuur van de endogene pool verminderd kan -indien gebruik wordt gemaakt van SeHCAT-worden uitgevoerd ófwel door de retentie van de activiteit in het lichaam over een periode van een aantal dagen te meten, ófwel door de excretie van de activiteit in de faeces te bepalen. Het resultaat kan worden uitgedrukt als een afnametempo indien meerdere metingen zijn gedaan, of eenvoudiger als een retentie-percentage na een vaste periode (7 dagen is gebruikelijk). Bij dit onderzoek kunnen zowel een "whole body counter" als andere teltechnieken worden gebruikt. Voor sommige onderzoeken kunnen scintigrafische studies geschikter zijn. Bepaling van de retentie van de radioactiviteit: *Whole body counter*: Een 370 kBq (10 µCi) capsule wordt samen met een slok water aan de patiënt toegediend. Gebruikmakend van de conventionele "whole body" teltechnieken kan een initiële telling van de patiënt worden uitgevoerd. Deze telling geeft, na substractie van de achtergrond, de "zero-time" of 100% waarde. Na 7 dagen vindt opnieuw een telling plaats. De achtergebleven radioactiviteit wordt als percentage van de 100% waarde uitgedrukt. Indien geen "*whole body counter*" beschikbaar is, kunnen andere teltechnieken worden toegepast. Omdat de radioactiviteit beperkt blijft tot de abdominale regio, zal een teller die deze regio bestrijkt, volstaan. Ook kan het onderzoek worden uitgevoerd met een gammacamera zonder collimator of zelfs met een enkel scintillatiekristal. Bepaling van de excretie van de radioactiviteit: De alternatieve methode om het verlies van galzuur te bepalen is het tellen van de radioactiviteit in faecale monsters die worden genomen gedurende een bepaalde periode (bijvoorbeeld 7 dagen). Een dosis van 370 kBq (10 µCi, oranje/gele capsule) wordt hiervoor aanbevolen. Het is belangrijk dat de standaard geometrie gehandhaafd blijft en dat alle faeces verzameld wordt. Monsters van patiënten die gelijktijdig andere radionuclidische onderzoeken ondergaan, dienen slechts geteld te worden indien de faecale excretie van het andere radionuclide verwaarloosbaar klein is of indien de signaalverwerkingsapparatuur van het telapparaat selectief de ^{75}Se-gammalijnen kan tellen. **Contra-indicaties:** Overgevoeligheid voor het werkzame bestanddeel of voor één van de hulpstoffen. **Waarschuwingen:** Er moet altijd rekening worden gehouden met het optreden van overgevoeligheidsreacties. Adequate reanimatievoorzieningen moeten onmiddellijk beschikbaar zijn. Voorzichtigheid is geboden bij de toediening van [^{75}Se]Tauroselcholzuur aan patiënten met een ernstige leveraandoening of obstructie van de galwegen, want bij deze aandoeningen wordt de stralingsdosis voor de lever aanzienlijk vergroot. Dit geneesmiddel bevat 71,04 mg natriurn per capsule. Dit moet in aanmerking worden genomen bij patiënten op een natriumarm dieet. **Bijwerkingen:** Immuunsysteemaandoeningen: Niet bekend: Overgevoeligheid. **Farmacotherapeutische groep:** Technetium (^{99m}Tc) Macrosalb, deeltjes voor injectie, ATC Code: V09EB01. **Nummer van de vergunning voor het in handel brengen:** RVG 16191. **Afleverstatus:** Geneesmiddel op medisch voorschrift (U.R). Beroepsbeoefenaren in de gezondheidszorg worden verzocht alle vermoedelijke bijwerkingen te melden. Neem voor het melden van bijwerkingen en/of voor medische informatie contact op met MAH in NL: GE Healthcare B.V., De Rondom 8, 5612 AP, Eindhoven (040-299 1000). **Datum:** Januari 2012

References: 1. Smith MJ *et al.* J R Coll Physicians Lond 2000; 34 (5): 448–51. **2.** Galatola G *et al.* Eur J Gastroenterol Hepatol 1992; 4: 533-7. **3.** Fernández-Bañares F et al. Am J Gastroenterol 2007; 102: 2520–8. **4.** Basumani P *et al.* Gut 2008; 57 (Suppl I): A1-A172.

07-2015 JB32650NL/OS THE NETHERLANDS